The PHILOSOPHICAL MAGAZINE

FIRST PUBLISHED IN 1798

Vol. 1 Eighth Series No. 10 October 1956

A Journal of Theoretical Experimental and Applied Physics

PRICE £1 0s. 0d.
Annual Subscription £10 10s. 0d. payable in advance

ALERE FLAMMAM.
Printed and Published by
TAYLOR & FRANCIS LTD.
RED LION COURT, FLEET STREET, LONDON, E.C.4

CONTENTS OF No. 10.

*** All communications for the Philosophical Magazine should be addressed, post-paid, to the Editors, c/o Messrs. Taylor and Francis, Ltd., Red Lion Court, Fleet Street, London, England.

XCI. *The Self-Energy and Interaction Energy of Stacking Faults in Metals*

By R. W. Attree† and J. S. Plaskett‡
H. H. Wills Physical Laboratory, University of Bristol§

[Received August 1955 ; and in revised form January 10, 1956]

Abstract

A model is considered of a crystal lattice having slip of less than a lattice vector on two close packed planes. The effect of this slip on the eigenvalues of one electron wave functions extending throughout the crystal is calculated, using first order perturbation theory to give the wave functions in a perfect crystal. The self-energy of a fault in a monovalent metal is found to be about 20 ergs/cm^2. The interaction energy is found to be about 0·4 ergs/cm^2 when the faults are one lattice plane apart and negligible when they are further apart. An unsuccessful attempt is made to calculate the effect of electrons with wave vectors near zone faces. The theory involved a clarification of the Bloch–Floquet theory and the use of a contour integral to sum the zeros of an exponential sum.

§ 1. Introduction

In 1950 Barrett reported that few stacking faults were to be found in cold worked aluminium, but that many faults could be found in certain copper–silicon alloys (cf. review article by Barrett in Shockley 1952, p. 112). Mott suggested at that time that the difference should be explained in terms of a higher surface energy for faults in Al than in Cu, this difference in surface energy being due in its turn to strong Bragg reflections of electrons at faults in the case of Al and only slight reflection in Cu (because there are no electrons near zone faces in Cu).

Of course no measurements have been made on the energies of stacking faults, but there have recently been measurements of the energies of (111) twins in Cu and Al by Fullman (1951) (and quoted by Fisher and Dunn in Shockley 1952, p. 336). Fullman finds that the ratio of twin energy to grain boundary energy in Cu is 0·045 while in Al it is 0·21. In the first case the average grain boundary energy is known to be 550 ergs/cm^2, giving 25 ergs/cm^2 for the surface energy of a twin in Cu. Presumably

† Now at the Research Chemistry Branch, Atomic Energy of Canada, Chalk River.
‡ Now at the Physics Department, University of Virginia, Charlottesville.
§ Communicated by the Authors.

the energy is about five times this in Al. Mott's explanation of the difference in surface energy is expected to be as valid for twins as for stacking faults.

This paper fills in the details of Mott's explanation for surface energies of faults, with some precision for monovalent metals and very imprecisely for aluminium. The results are as expected.

Of course, the experimental determination of the surface energy of a stacking fault is difficult so that it would be nice to know the relation between the energy of a fault and of a twin. On the basis of Lennard–Jones forces between atoms it is found that the energy of a fault is roughly twice the energy of a twin. On the same basis Heidenreich and Shockley (1948) deduce that the energy of a fault in cobalt is 7 ergs/cm^2 using the known difference in energy between hexagonal and cubic cobalt (and forgetting that this has the wrong sign). The reasonableness of this figure should not be taken as an indication that the energy of a fault is really twice that of a twin, for the same theory (Lennard–Jones forces) shows that the energy of two faults separated by one layer (ABC|B|ABC Frank's fault of the second kind (1951)) is roughly the same as a single fault. Whereas our calculation shows that two faults have almost exactly twice the energy of one, even though they are only one layer apart.

Unfortunately, the energy of a twin is a more difficult calculation, and we have not attempted it. We have only calculated the energy of two faults M layers apart. It would clearly be possible to extend the calculation to more than two faults, but not many more. The energy difference between hexagonal and cubic would again be easy.

A Brief Summary of §§ 2 *to* 5 *Follows*

§ 2 : An electron in a Bloch function, which has a real wave vector $\mathbf{k}$, is unfortunately not entirely scattered into other Bloch functions. Some of the scattered waves look like Bloch functions but have a complex $\mathbf{k}$. The proper development of these functions is through Floquet's theory. We attempt to explain this theory, its differences from Bloch's theory, and the method of using it when there is one direction in the cyrstal that is not completely periodic.

§ 3 : It is not enough merely to consider scattering of electrons at the fault surface. An energy difference is required and this can only be obtained by working out eigenvalues that are forced on the problem by suitable boundary conditions. The surfaces of the crystal are therefore introduced and a determinant for the eigenvalues obtained. The individual eigenvalues do very peculiar things when a fault is introduced into the cystal, but by a contour integration we are able to calculate the average behaviour of a great many eigenvaules.

§ 4 : The general theory so far developed is applied to a metal in which it is supposed that the wave functions are given by the 'nearly free electron approximation' (generalized for complex $\mathbf{k}$), i.e., first order

non-degenerate perturbation theory. This confines our attention to monovalent metals. The theory for two faults is completely worked out in terms of the Fourier coefficients of the potential of the perfect crystal. The energy change is of the second order in these coefficients and the interation energy decreases exponentially with M. The special potential $Ze^2 \exp(-q'r)/r$ is used round each atom, some approximations are made, and an easily understood answer is found.

§ 5 : Some early work (1950) on aluminium is briefly reviewed and the difficulties of obtaining any answer are discussed.

§ 2. Solutions of the Schrödinger Equation in which the Potential is Periodic only in Limited Regions

A crystal with one or two parallel stacking faults in it, only has periodicity in planes parallel to the faults. The periodicity is interrupted in a direction that goes through a fault. Thus the potential in the Schrödinger equation

$$-\frac{\hbar^2}{2m}\nabla^2\psi+V(\mathbf{r})\psi=E\psi(\mathbf{r}) \quad . \quad . \quad . \quad . \quad . \quad (2.1)$$

has the property

$$V(\mathbf{r}+\tau_1)=V(\mathbf{r}+\tau_2)=V(\mathbf{r}) \qquad \text{for all } \mathbf{r}, \quad . \quad . \quad . \quad (2.2)$$

where τ_1 and τ_2 are two fundamental periods that are parallel to the plane of the fault. Owing to the limited periodicity in any third direction, it is only possible to apply Bloch's theorem to the τ_1 and τ_2 directions. In order to make this possible we apply periodic boundary conditions in these directions

$$\psi(\mathbf{r}+N_1\tau_1)=\psi(\mathbf{r}+N_2\tau_2)=\psi(\mathbf{r}) \qquad \text{for all } \mathbf{r}. \quad . \quad . \quad (2.3)$$

A simplification of the statement of Bloch's theorem and also of the subsequent mathematics is obtained if we introduce a unit vector $\mathbf{i}$ not in the τ_1, τ_2 plane and call ρ the projection of $\mathbf{r}$ into the τ_1, τ_2 plane parallel to $\mathbf{i}$, so that

$$\mathbf{r}=\rho+x\mathbf{i}. \quad . \quad . \quad . \quad . \quad . \quad . \quad . \quad . \quad . \quad (2.4)$$

Bloch's theorem now shows that any solution of (2.1) in which the potential has the property (2.2), that satisfies the boundary condition (2.3) can be written as a sum of *solutions* each of which has the form

$$\exp(i\kappa \,.\, \rho)u(\rho, x) \quad . \quad . \quad . \quad . \quad . \quad . \quad . \quad . \quad (2.5)$$

where $u(\rho+\tau_i, x)=u(\rho, x)$ and κ must satisfy the equation $\kappa \,.\, N_i\tau_i=2n_i\pi$ (cf. e.g. Shockley 1950, pp. 399–404). The periodic function $u(\rho, x)$ depends on κ but we omit explicit reference to this fact in (2.5). It is possible to confine κ to a definite plane defined by the vectors α_1 and α_2 that satisfy the relations

$$\alpha_i \,.\, \tau_j=2\pi\delta_{ij}. \quad . \quad . \quad . \quad . \quad . \quad . \quad . \quad (2.6)$$

Clearly α_1 and α_2 are subject to considerable ambiguity for we could add to them any vectors perpendicular to both τ_1 and τ_2. However, having

fixed them in some way, we can write

$$\kappa = n_1\alpha_1/N_1 + n_2\alpha_2/N_2 \qquad n_1, n_2 \text{ integers.} \quad . \quad . \quad . \quad . \quad (2.7)$$

n_1 and n_2 are the quantum numbers of the Bloch function. It makes no difference how we choose the α_i—the solution 2.5) is only determined by the integers n_1 and n_2.

We must now determine how $u(\rho, x)$ varies with x. By hypotheses we can expand $V(\mathbf{r}) = V(\rho, x)$ and $u(\rho, x)$ in Fourier series with respect to ρ, i.e.

$$V(\rho, x) = \Sigma V_\alpha(x) \exp(-i\alpha \cdot \rho), \qquad u(\rho, x) = \Sigma A_\alpha(x) \exp(-i\alpha \cdot \rho) \quad (2.8)$$

where the coefficients are functions of x and the sum is over all α of the form $m_1\alpha_1 + m_2\alpha_2$ (m_1 and m_2 integers and α_1 and α_2 can be the same α's as were previously chosen—the particular choice is again of no importance, since only the invariant $\alpha \cdot \rho$ occurs in (2.8). We now insert the expansion (2.8) in the eqn. (2.1) and assume that term by term differentiation is permissible. The $A_\alpha(x)$ must satisfy a doubly infinite set of second order simultaneous equations ; when the κ plane is chosen to be parallel to the ρ plane these equations are

$$-\sec^2\theta \frac{\hbar^2}{2m}[A_\alpha'' + 2iA_\alpha'(\kappa-\alpha) \cdot \mathbf{i} + A_\alpha\{\cos^2\theta(\kappa-\alpha)^2 + [(\kappa-\alpha) \cdot \mathbf{i}]^2\}] + \Sigma V_{\alpha-\alpha'} A_{\alpha'} = EA_\alpha, \quad . \quad . \quad . \quad . \quad . \quad . \quad (2.9)$$

where θ is the angle between $\mathbf{i}$ and the normal to the ρ plane.

Now let us suppose that $V(\rho, x)$ is periodic in x for some range of x, e.g. between faults, then

$$V_\alpha(x+\tau) = V_\alpha(x), \qquad \text{for all } \alpha. \quad . \quad . \quad . \quad . \quad (2.10)$$

Then the $A_\alpha(x)$ satisfy a set of ordinary differential equations with periodic coefficients. In our subsequent work we require a complete set of independent solutions to these equations. The Bloch theory is of no use since it only gives the form of the solutions that are subject to periodic boundary conditions, but the Floquet theory can be applied. Strictly speaking the Floquet theory only applies to a finite system of simultaneous equations but that it should still be true for our infinite system (2.9) seems very reasonable physically in that it should make only a small error if we cut off the expansion (2.8) for $|\alpha|$ beyond some large value.

The Floquet theory (see e.g. Ince 1927, § 15.7. Notice that there is no need to assume that the coefficients of the differential equations are analytic functions of x, i.e. $V(\mathbf{r})$ need not be analytic ; furthermore the theory can obviously be generalized to a finite set of simultaneous equations) states that in general a complete set of solutions of (2.9) can be found, all of which have the form

$$A_\alpha(x) = \exp(i\mu x) v_\alpha(x), \quad . \quad . \quad . \quad . \quad . \quad . \quad . \quad (2.11)$$

where $v_\alpha(x+\tau) = v_\alpha(x)$. The μ's for these different solutions are the roots of a ' secular ' equation of the form

$$\det[a_{ij}(E) - \exp(i\mu\tau)\delta_{ij}] = 0. \quad . \quad . \quad . \quad . \quad . \quad (2.12)$$

If the roots of (2.12) are distinct, i.e. all the exp $(i\mu\tau)$ are different, then a complete set of solutions is of the form (2.11). If, on the other hand, there is a repeated root, then there will only, in general, be one solution of the form (2.11) for that root, the other solutions being of a more complicated form. This, however, does not affect our problem since we may take limits of the solutions as E tends to an awkward value for which there are coincident roots.

There is no difficulty in showing that the a_{ij} are integral functions of E, i.e. expressible as power series in E with an infinite radius of convergence (see Ince 1927, § 3.31 and Kramers 1935). All the μ's are therefore the various branches of an analytic function of E ; the branches that differ by $2\pi/\tau$ clearly do not give different Floquet functions.

We now give some of the properties of the μ's, which we shall temporarily write μ_i. These properties are essential for our later work.

2.1. *Properties of the real* μ_i

If one μ_i is real then E must be real. This can be proved by inserting (2.11) in (2.9), multiplying through by $A_\alpha{}^*$ summing over α, and integrating with respect to x from 0 to τ.

If $\mu_k(E')=\mu'$ is real and $\mu_i(E')\neq\mu'$ for any $i\neq k$ then $d\mu_k(E')/dE\neq 0$. Suppose that the first derivative that was not zero was the nth then

$$\mu_k(E)=\mu'+(E-E')^n A_n+\ldots,$$

but then

$$E=E'+A_n{}^{-1/n}(\mu_k-\mu')^{1/n}+\ldots$$

(Copson 1935, § 6.22, p. 121). We could therefore choose a complex E that gave a real $\mu_k(E)$ unless $n=1$.

If $\mu_k(E')=\mu'$ is real and $\mu_i(E')\neq\mu'$ for any $i\neq k$ then $\mu_k(E)$ is real for real E in a neighbourhood of E'. Since

$$\mu_k(E)=\mu'+(E-E')A_1+(E-E')^2A_2+\ldots$$

we have

$$E=E'+(\mu_k-\mu')B_1+(\mu_k-\mu')^2B_2+\ldots.$$

It follows that $B_1, B_2, \ldots$ must be real, since if we choose $\mu_k(E)$ real E must be real. The reality of $A_1, A_2, \ldots$ follows from that of $B_1, B_2, \ldots$ and proves the statement.

2.2. *Properties of the complex* μ_i

If the potential $V(\mathbf{r})$ has a centre of inversion then the complex $\mu_i(E)$, for real E, are present in conjugate pairs. It is easy to show that if $\exp(i\mu_i x)v_{\alpha i}(x)$ is a solution of (2.9) then so is $[\exp(-i\mu_i x)v_{\alpha i}(-x)]^*$ so proving the assertion.

These properties suggest the following classification of the μ_i: (*a*) complex μ's with positive imaginary part and real μ's with positive derivative, (*b*) complex μ's with negative imaginary part and real μ's with negative derivative. A μ of class (*a*) herinafter called μ^+, cannot

possibly become a μ of class (b) hereinafter called μ^-, and *vice versa*, except at a branch point ; in the neighbourhood of such a point

$$\mu(E)=\mu'+A_1(E-E')^{1/p}+A_2(E-E')^{2/p}+\ldots$$

with p an integer. It is easy to show that the arg $A_1=n\pi/p$ (n integral) and that therefore the p different branches of $\mu(E)$ occur in conjugate pairs both for $E<E'$ and for $E>E'$. If p is even there are two real μ's (one a μ^+ and one a μ^-) for $E<E'(>E')$ and as E increases (decreases) they approach μ' and turn into two complex μ's (one a μ^+ and one a μ^-) for $E>E'$ ($<E'$). If p is odd there is only one real μ (either μ^+ or μ^-) and as E goes through E' this real μ goes through μ' without changing its classification.

There are a ' doubly infinite ' set of μ^+'s and μ^-'s which we can label by the generic symbols α, α', ... that mean the sets

$$m_1\alpha_1+m_2\alpha_2,\quad m_1'\alpha_1+m_2'\alpha_2,\ldots\quad m_i, m_i',\ldots\quad \text{integers.} \qquad (2.13)$$

All out independent solutions of (2.9) can therefore be written

$$(a)\ \exp(i\mu_{\alpha'}{}^+x)v_{\alpha\alpha'}{}^+(x),\qquad (b)\ \exp(i\mu_{\alpha'}{}^-x)v_{\alpha\alpha'}(x), \qquad (2.14)$$

where different values of α' give different solutions.

Incidentially, the group velocity of a wave that is a linear combination of Floquet functions (with fixed κ) with values of μ that are centred round μ_0 is $i\hbar(d\mu/dE)^{-1}$ evaluated at $\mu=\mu_0$. So that ' μ^+ waves ' move from left to right while ' μ^- waves ' move from right to left if μ is real. If μ is complex, the ' μ^+ waves ' decrease exponentially towards the right while the ' μ^- waves ' decrease exponentially towards the left. This, then, is the physical significance of the $\pm$ classification.

§ 3. The Determinant for the Energy Levels of Two Stacking Faults

In this section we shall apply the results obtained in § 2 from Bloch's and Floquet's theorems to the physical situation of two parallel faults in a face-centred cubic crystal. We shall eventually obtain an equation for the eigenvalues of this problem in the form of an infinite determinant, and we shall show how this determinant may be simplified—although the new determinant is still infinite—and yet still lead to a determination, not of individual eigenvalues, but of sums of eigenvalues in a given range of energy.

First of all, however, we must specify the vectors τ_1, τ_2, $\mathbf{i}$, α_1, and α_2. which were left so arbitrary in § 2. It is immediately clear how we should choose the first three of these vectors : τ_1 and τ_2 must obviously lie in the plane of the stacking fault and $\mathbf{i}$ in the direction of the third period vector of the face-centred cubic lattice. In other words, τ_1, τ_2, and $\mathbf{i}\tau$ must be three fundamental periods for this lattice. If we assume that the faulted planes are (111) planes of the crystal, as we shall from now on (for reasons that will become clear from an examination of

eqn. (3.9) and the related discussion), then in a certain set of rectangular coordinates

$$\tau_1=\frac{\tau}{\sqrt{2}}(110), \qquad \tau_2=\frac{\tau}{\sqrt{2}}(101), \qquad \mathbf{i}\tau=\frac{\tau}{\sqrt{2}}(011), \tag{3.1}$$

where $\tau\sqrt{2}$ is the length of an edge of the fundamental cube. α_1 and α_2 must now be (in order to satisfy (2.6))

$$\alpha_1=\frac{\pi\sqrt{2}}{\tau}[(11\bar{1})+a_1(\bar{1}11)], \qquad \alpha_2=\frac{\pi\sqrt{2}}{\tau}[(1\bar{1}1)-a_2(\bar{1}11)], \tag{3.2}$$

where a_1 and a_2 are arbitrary. If we take a_1 and a_2 zero, the α_1 and α_2 are just two of the ordinary reciprocal vectors of the face-centred cubic lattice. If, on the other hand, we choose a_1 and a equal to $\frac{1}{3}$, then α_1 and α_2 lie in the $\tau_1\tau_2$ plane, and they are, explicitly,

$$\alpha_1=\frac{2\pi\sqrt{2}}{3\tau}(12\bar{1}), \quad . \quad \alpha_2=\frac{2\pi\sqrt{2}}{3\tau}(1\bar{1}2). \quad . \quad . \quad . \tag{3.3}$$

These vectors make an angle of arc cos $(-\frac{1}{2})$ with each other, that is to say, they are the obvious reciprocal vectors of τ_1 and τ_2 in the $\tau_1\tau_2$ plane and form a triangular net reciprocal to the triangular net formed by τ_1 and τ_2. Both these choices of $\alpha_1\alpha_2$ are useful to us. The first gives us an obvious correlation between $\kappa\mu$ of § 2 and the $\mathbf{k}$ vector of the three dimensional Bloch theorem for the eqn. (2.1), where we have

$$V(\mathbf{r}+\mathbf{i}\tau)=V(\mathbf{r})$$

besides (2.2) : The Bloch–Floquet function that we found in § 2 defined by eqns. (2.5), (2.8), and (2.11) is

$$\exp(i\kappa\,.\,\rho+\mu x)\Sigma v_\alpha(x)\exp(-i\alpha\,.\,\rho) \quad . \quad . \quad . \tag{3.4}$$

and is to be compared with $\exp(i\mathbf{k}\,.\,\mathbf{r})u(\mathbf{r})$, so that

$$\mathbf{k}\,.\,\rho+\mu x\equiv\mathbf{k}\,.\,\mathbf{r}\equiv\mathbf{k}\,.\,(\rho+\mathbf{i}x) \quad . \quad . \quad . \quad . \quad . \quad . \tag{3.5}$$

(from (2.4)) for all ρ and x. If κ is chosen perpendicular to $\mathbf{i}(a_1=a_2=0)$, we can write the left hand side of (2.5) as $\mathbf{k}\,.\,\mathbf{r}$ with

$$\mathbf{k}=\kappa+\mu(\bar{1}11)/\sqrt{2}. \quad . \quad . \quad . \quad . \quad . \quad . \quad . \quad . \tag{3.6}$$

If, on the other hand, $a_1=a_2=\frac{1}{3}$ then the relation between κ, μ and $\mathbf{k}$ is not so simple, but the mathematics of § 4, for example, is easier. So we shall still leave the choice of a_1, a_2 in (3.2) until a choice is necessary.

Since we have used *Floquet's* theorem for the $\mathbf{i}$ direction, we can consider crystals in which periodicity in the $\mathbf{i}$ direction does not persist indefinitely. Let us then lay down L layers of face-centred cubic material with the fundamental translation periods given by (3.1). We fix the origin of the x coordinate so that the lattice planes are given by

$$x=(m+\tfrac{1}{2})\tau \text{ or } \mathbf{r}=\rho+(m+\tfrac{1}{2})\mathbf{i}\tau, \quad m=-L,\,-L+1,\,\ldots-2,\,-1. \tag{3.7}$$

We shall only consider lattices with one atom per unit cell, and we shall take the nuclei to be at the positions

$$\mathbf{r}=m_1\tau_1+m_2\tau_2+(m+\tfrac{1}{2})\mathbf{i}\tau, \quad m_1m_2 \text{ integers.} \quad . \quad . \quad . \tag{3.8}$$

The potential inside this block will be taken as periodic so that

$$V(\rho+\tau_i, x)=V(\rho, x)=V(\rho, x+\tau), \quad -L\tau<x<-\tau. \qquad (3.9)$$

This is the crucial approximation that enables us to solve the problem: we have assumed that the potential right up to $x=0$ is unaffected by what happens for positive x (and similarly to the left of $x=-L$). The mathematical statement (3.9) carries the following physical implications :

(*a*) The nuclei remain in their normal positions given by (3.8) despite the disturbing influence of whatever is present for $x>0$ (even if this is nothing).

(*b*) The potential $V(\rho, x)$ contains the potential of the valence electrons, so the charge density of these electrons is supposed to be unchanged by the presence of the boundary. This precludes the possibility of a self-consistent solution.

(*c*) The potential due to any ions we may place in the region $x>0$ is not supposed to extend into the region $x<0$.

If we were to attempt to take account of any of these points, we would be forced to solve a ' boundary layer ' problem rather than a ' boundary surface ' problem, a practical impossibility.

Of cource all these difficulties are at their smallest when we choose to make the plane τ_1, τ_2 the closest packed plane. This is the reason for choosing to consider faults on (111) planes.

Suppose we grow on our substrate ($x<0$) more of the same crystal displaced by an amount $\mathbf{t}$ (lying in the $\tau_1\tau_2$ plane) with respect to the substrate. That is to say, we grow M layers of atoms whose nuclei are at the positions

$$\mathbf{r}=m_1\tau_1+m_2\tau_2+\mathbf{t}+(m+\tfrac{1}{2})\mathbf{i}\tau, \quad m=0, 1, \ldots M-1 \qquad (3.10)$$

so producing what, if we may extend Frank's (1951) definition a little, we may call a translation twin. If $\mathbf{t}$ happens to be an integer multiple of τ_1 and τ_2, the crystal is perfect through $x=0$. If however,

$$\mathbf{t}=(\tau_1+\tau_2)/3, \qquad (3.11)$$

then the crystal is not perfect but is still close packed. This is most easily seen by projecting the position of the nuclei (3.8) and (3.10) on the τ_1, τ_2 plane (in the direction $(\bar{1}11)$ not $\mathbf{i}$)

$$[m_1+(m+\tfrac{1}{2})\tfrac{1}{3}]\tau_1+[m_2+(m+\tfrac{1}{2})\tfrac{1}{3}]\tau_2, \quad m=-L, \ldots, -2, -1, \qquad (3.8')$$

$$[m_1+(m+\tfrac{3}{2})\tfrac{1}{3}]\tau_1+[m_2+(m+\tfrac{3}{2})\tfrac{1}{3}]\tau_2, \quad m=0, 1, \ldots, M. \qquad (3.10')$$

Clearly we have just removed one plane of atoms from the perfect crystal actually $m=0$ in (3.8′) or $m=-1$ in (3.10′). Such a crystal is said to have a stacking fault of the first kind in it. There are clearly only three types of layers, on projection on the τ_1, τ_2 plane : In (3.8′) we can call them $m=-3$, -2, and -1 or A, B, and C. Then $m=0, 1, 2, 3 \ldots$ in (3.10′) are B, C, A, B, ... There is no translation, other than that

given by (3.11), which leads to a close packed arrangement different from the perfect crystal. The potential for $x>0$ clearly has the periodicity $\mathbf{i}\tau$

$$V(\rho, x+\tau)=V(\rho, x) \quad \text{for} \quad 0<x<(M-1)\tau, \qquad . \; . \; . \; (3.12)$$

and is related to the potential for $x<0$ by

$$V(\rho+\mathbf{t}, x+\tau)=V(\rho, x) \quad \text{for} \quad -\tau<x<0. \qquad . \; . \; . \; . \; (3.13)$$

In other words (from (2.8))

$$V_\alpha(x+\tau)\exp(i\alpha \,.\, \mathbf{t})=V_\alpha(x) \quad \text{for} \quad -\tau<x<0. \qquad . \; (3.14)$$

Furthermore, we see that, if $A_\alpha(x)=\exp(i\mu x)v_\alpha(x)$ is a solution of the differential eqn. (2.9) for $x<0$, then $\exp(i\mu x)v_\alpha(x)\exp(i\alpha \,.\, \mathbf{t})$ is a solution of the equation for $x>0$ where $v_\alpha(x)$ is then defined as being periodic from $-L\tau$ to $(M-1)\tau$. Of course, these two solutions of the differential equation, one valid for $x<0$ and the other for $x>0$, do not fit together at $x=0$.

On the plane $x=M\tau$ we now introduce another translation twin and continue the crystal to $N\tau$. So that to (3.9) and (3.12) we must now add

$$V(\rho, x+\tau)=V(\rho, x) \qquad M\tau<x<(N-1)\tau \qquad . \; . \; . \; (3.15)$$

and to (3.13) we must add

$$V(\rho+\mathbf{t}', x+\tau)=V(\rho, x) \qquad (M-1)\tau<x<M\tau. \qquad . \; . \; (3.16)$$

We do not write $\mathbf{t}'=\mathbf{t}$ because we wish to regard $\mathbf{t}$ and $\mathbf{t}'$ as variables. This will enable us to follow the variation of the eigenvalues as slip occurs and also to put $\mathbf{t}'=0$ and so obtain the energy of a single fault.

In the same way as before, if $\exp(i\mu x)v_\alpha(x)$ is a solution of the differential eqn. (2.9) for $x<0$, then $\exp(i\mu x)v_\alpha(x)\exp[i\alpha \,.\, (\mathbf{t}+\mathbf{t}')]$ is a solution of the equation for $x>M\tau$, where $v_\alpha(x)$ is now periodic for all x from $-L\tau$ to $(N-1)\tau$ if the crystal extends from $-L\tau$ to $N\tau>M\tau$.

If we make $M=1$, then we obtain a single stacking fault of the second kind, in which the sequence of the lattice planes is $\ldots ABC|B|ABCA\ldots$ In other words, an additional plane of atoms has been inserted into the perfect lattice. From the calculation of the energy as a function of the integer M we shall be able to deduce the interaction energy of faults of the first kind and in particular the self-energy of a fault of the second kind (cf. the similar results for a simple solid given in § 1).

In each of the three regions of the crystal—to the left of $x=0$, between $x=0$ and $M\tau$, and to the right of $x=M\tau$—the solution of the Schrödinger equation (with given E) can be expanded in terms of the fundamental Floquet functions (2.5), (2.8), and (2.11):

$$A_\alpha(x)=\begin{cases} \sum_{\alpha'} a_{\alpha'}{}^{+}\exp(i\mu_{\alpha'}{}^{+}x)v_{\alpha\alpha'}{}^{+}(x)+\sum_{\alpha'} a_{\alpha'}{}^{-}\exp(i\mu_{\alpha'}{}^{-}x)v_{\alpha\alpha'}{}^{-}(x) \\ \qquad\qquad -L\tau<x<0 \\ \sum_{\alpha'} b_{\alpha'}{}^{+}\exp(i\mu_{\alpha'}{}^{+}x)v_{\alpha\alpha'}{}^{+}(x)\exp(i\alpha \,.\, \mathbf{t})+ \\ \qquad +\sum_{\alpha'} b_{\alpha'}{}^{-}\exp(i\mu_{\alpha'}{}^{-}x)v_{\alpha\alpha'}{}^{-}(x)\exp(i\alpha \,.\, \mathbf{t}) \\ \qquad\qquad 0<x<M\tau, \end{cases} \qquad (3.17)$$

and similarly with $c_{\alpha'}{}^{+}$ and $c_{\alpha'}{}^{-}$ for the coefficients in the region $M\tau<x<N\tau$. In order that the $A_\alpha(x)$ defined in this way for all relevant x should be a solution of the Schrödinger equation for all x, the coefficients must be chosen so that $A_\alpha(x)$ and $A_{\alpha'}(x)$ are continuous functions of x at $x=0$ and $x=M\tau$. Since $v_{\alpha\alpha'}(x)$ is a periodic function of x for all x, we have $v_{\alpha\alpha'}(0)=v_{\alpha\alpha'}(M\tau)$, and we shall write this as just $v_{\alpha\alpha'}$. Similarly we shall write $dv_{\alpha\alpha'}(0)/dx=v_{\alpha\alpha''}$. Furthermore, we shall omit the $+$ and $-$ when $+$ and $-$ expressions occur symmetrically. The equations of continuity at $x=0$ are

$$\left.\begin{aligned} &\sum_{\alpha'} a_{\alpha'} v_{\alpha\alpha'} = \sum_{\alpha'} b_{\alpha'} v_{\alpha\alpha'} \exp(i\boldsymbol{\alpha}\,.\,\mathbf{t}) \\ \text{and}\quad &\sum_{\alpha'} a_{\alpha'}(i\mu_{\alpha'} v_{\alpha\alpha'} + v_{\alpha\alpha''}) = \sum_{\alpha'} b_{\alpha'}(i\mu_{\alpha'} v_{\alpha\alpha'} + v_{\alpha\alpha''}) \exp(i\boldsymbol{\alpha}\,.\,\mathbf{t}). \end{aligned}\right\} \quad (3.18)$$

Similar equations are obtained for $x=M\tau$. We note here for future reference that $\mu_{\alpha'}$, $v_{\alpha\alpha'}$, and $v_{\alpha\alpha''}$ are analytic functions of E and also of course functions of the discrete variable κ that can have N_1N_2 different possible values given by (2.7).

If we had one Floquet wave 'incident' on the left of $x=0$; i.e., only one $a_{\alpha'}{}^{+}$ not equal to zero, then the eqns. (3.18) would suffice to determine uniquely the $a_{\alpha'}{}^{-}$ and the $b_{\alpha'}{}^{+}$, i.e. reflected and transmitted waves (it being assumed that $b_{\alpha'}{}^{-}=0$). The eqns. (3.18) are in fact the mathematical expression of the so-called 'dynamic theory' of electron diffraction. These equations contain the rule for finding the wave vectors of the reflected or transmitted waves: If $\exp i[\kappa-\alpha+\mu_\alpha{}^{+}(E)(\bar{1}11)/\sqrt{2}]\,.\,\mathbf{r}$ is the incident wave, then $\exp i[\kappa-\alpha'+\mu_{\alpha'}{}^{-}(E)(\bar{1}11)/\sqrt{2}]\,.\,\mathbf{r}$ is a possible reflected wave, where α' can take any value of the form (2.13), but E is the same as for the incident wave (see (3.6) and discussion of eqn. (4.4)). The amplitude of this reflected wave is $|a_{\alpha'}{}^{-}|^2$ and will not in general be zero for any α'. This gives all the reflected waves that would be expected from a two-dimensional 'cross grating' with fundamental periods τ_1 and τ_2. Of course, there will only be a finite number of α''s that make $\mu_{\alpha'}{}^{-}(E)$ real (the more the bigger E is), viz. give undamped reflected waves.

We are not directly interested in the waves scattered by a fault, as we would be if we wanted to calculate the electrical resistance due to it; rather we want the allowed energy levels of the electrons. That is to say, we must now impose some boundary conditions at $x=-L\tau$ and $N\tau$. If we imposed periodic boundary conditions, we would introduce the interaction energy between a periodic array of faults separated by a distance $(L+N)\tau$, in order to avoid introducing all these spurious interactions, we impose zero boundary conditions. This certainly corresponds more precisely to the actual physics of a bounded crystal and is, in any event, no more difficult to handle. Of course there is an interaction energy between a fault and the surface of the crystal; however, the mathematics shows that, if we make L and N tend to infinity, the *sum* of the changes in the eigenvalues due to introducing the two faults tends

to a definte limit. This limit is presumably the energy of two ' isolated ' faults a distance $M\tau$ apart.

The boundary conditions imply

$$\Sigma a_{\alpha'} v_{\alpha\alpha'} \exp(-i\mu_{\alpha'} L\tau)=0 \quad \text{and} \quad \Sigma c_{\alpha'} v_{\alpha\alpha'} \exp[i\alpha \cdot (\mathbf{t}+\mathbf{t}')] \exp(i\mu_{\alpha'} N\tau)=0. \qquad (3.19)$$

The eqn. (3.18) (and the corresponding ones for $x=M\tau$) and (3.19) are a set of homogeneous equations for the coefficients a, b, and c that only have a non-trivial solution if the determinant of the equations is zero. The elements of this determinant are functions of E, and so this gives us an equation for the eigenvalues of E (a different one for each value of κ). The problem has two simple quantum numbers κ corresponding to the perfect periodicity in the τ_1, τ_2 planes, but the usual third Bloch quantum number (eqn. (3.6)) is no longer a constant of the motion, and our eigenvalues cannot be classified by μ. The determinant is

$$\begin{vmatrix} v_{\alpha\alpha'} e^{-i\mu\alpha' L\tau} & 0 & 0 \\ 0 & 0 & v_{\alpha\alpha'} e^{i\alpha\cdot(\mathbf{t}+\mathbf{t}')} e^{i\mu\alpha' N\tau} \\ v_{\alpha\alpha'} & v_{\alpha\alpha'} e^{i\alpha\cdot\mathbf{t}} & 0 \\ w_{\alpha\alpha'} & w_{\alpha\alpha'} e^{i\alpha\cdot\mathbf{t}} & 0 \\ 0 & v_{\alpha\alpha'} e^{i\alpha\cdot\mathbf{t}} e^{i\mu\alpha' M\tau} & v_{\alpha\alpha'} e^{i\alpha\cdot(\mathbf{t}+\mathbf{t}')} e^{i\mu\alpha' M\tau} \\ 0 & w_{\alpha\alpha'} e^{i\alpha\cdot\mathbf{t}} e^{i\mu\alpha' M\tau} & w_{\alpha\alpha'} e^{i\alpha\cdot(\mathbf{t}+\mathbf{t}')} e^{i\mu\alpha' M\tau} \end{vmatrix} \qquad (3.20)$$

where $w_{\alpha\alpha'}=i\mu_{\alpha'} v_{\alpha\alpha'}+v_{\alpha\alpha''}$.

This appears to have six rows but only three columns, but actually each element should be split in two so doubling the number of columns, e.g. the top left hand element should really consist of the two elements

$$v_{\alpha\alpha'}{}^{+} \exp(-i\mu_{\alpha'}{}^{+} L\tau) \quad \text{and} \quad v_{\alpha\alpha'}{}^{-} \exp(-i\mu_{\alpha'}{}^{-} L\tau).$$

Furthermore, each element is really an $\infty \times \infty$ matrix with rows and columns specified by the vectors α and α' respectively (α and α' can only take discreet values (2.13)).

This determinant looks somewhat less formidable if we imagine $\mathbf{t}'=0$; i.e. only one fault present. We can then subtract the third column from the second column (as written in (3.20)) and factorize the resulting determinant to give

$$\begin{vmatrix} v_{\alpha\alpha'} e^{-i\mu\alpha' L\mathbf{t}} & 0 \\ 0 & v_{\alpha\alpha'} e^{i\alpha\cdot\mathbf{t}} e^{i\mu\alpha' N\tau} \\ v_{\alpha\alpha'} & v_{\alpha\alpha'} e^{i\alpha\cdot\mathbf{t}} \\ w_{\alpha\alpha'} & w_{\alpha\alpha'} e^{i\alpha\cdot\mathbf{t}} \end{vmatrix} \cdot \begin{vmatrix} v_{\alpha\alpha'} e^{i\alpha\cdot\mathbf{t}} e^{i\mu\alpha' M\tau} \\ w_{\alpha\alpha'} e^{i\alpha\cdot\mathbf{t}} e^{i\mu\alpha' M\tau} \end{vmatrix} \qquad (3.21)$$

The non-zero factors $\exp(i\alpha \cdot \mathbf{t})$ and $\exp(i\mu_{\alpha'} M\tau)$ can be removed from the rows and columns of the second determinant, and we see that what is left cannot possibly be zero for any E. It is the Wronskian of the

independent set of solutions of the eqns. (2.9) that we have labelled by an α' and a + or −. This means that eigenvalues for only one fault are given by the zeros of the first determinant in (3.21); a result we could have obtained directly by not introducing the slip $\mathbf{t}'$ on $x=M\tau$ in the first place. Similarly, if we put $M=0$, subtract the last column from the middle column of (3.20), and factorize, we again obtain the first determinant of (3.21) only with $\mathbf{t}+\mathbf{t}'$ instead of $\mathbf{t}$; as we should expect.

Returning to the general case, we see that the elements of the first two rows of the determinant (3.20) contain the factors $\exp(i\mu_{\alpha'}L\tau)$ and $\exp(i\mu_{\alpha'}N\tau)$. Since we are going to make the boundaries of the crystal very distant from the faults, L and N will be very large (of order 10^8). On the other hand, M—the number of lattice planes between the faults—will be quite small (not more than of order 10^2). This largeness of L and N will mean that the elements in the first two rows will oscillate, or exponentially vary, with the energy, so producing a very dense set of eigenvalues. We shall, therefore, isolate these first two rows by performing a Laplace development of the determinant in terms of them. In order to justify this and all the succeeding steps, we shall have to imagine that the determinant (3.20) is really finite; this we accomplish, as in § 2, by supposing that the $v_{\alpha\alpha'}$ are all zero for α and α' bigger than some number. When we have completed all our calculations, we shall take the limit as this number tends to infinity. As we have said before, we have no mathematical justification for this step; but we believe that it is physically justified to neglect the higher harmonics in the expansion of the wave function (2.8). It is convenient to introduce a symbol to represent the finite number of α's or α''s that we are dealing with; the symbol we introduce is ∞. So that the determinant (3.20) has 6∞ rows and columns. To obtain the Laplace development of (3.20) in terms of the first 2∞ rows, we must select 2∞ columns (out of the first 2∞ and the last 2∞ columns of (3.20)) to make a $2\infty\times 2\infty$ determinant, which we then multiply by its cofactor in (3.20) and sum over all possible selections $((4\infty)!/(2\infty)!$ of them). For example one term in the Laplace development of (3.20)—and a very important one, as we shall see—is

$$\begin{vmatrix} & v_{\alpha\alpha'}{}^{+}\,e^{-i\mu_{\alpha'}{}^{+}L\tau} & 0 \\ & 0 & v_{\alpha\alpha'}{}^{-}\,e^{i\alpha\,.\,(\mathbf{t}+\mathbf{t}')}\,e^{i\mu_{\alpha'}{}^{-}N\tau} \end{vmatrix} \cdot$$

$$\begin{vmatrix} v_{\alpha\alpha'}{}^{-} & v_{\alpha\alpha'}\,e^{i\alpha\,.\,\mathbf{t}} & 0 \\ w_{\alpha\alpha'}{}^{-} & w_{\alpha\alpha'}\,e^{i\alpha\,.\,\mathbf{t}} & 0 \\ 0 & v_{\alpha\alpha'}\,e^{i\alpha\,.\,\mathbf{t}}\,e^{i\mu\alpha' M\tau} & v_{\alpha\alpha'}{}^{+}\,e^{i\alpha\,.\,(\mathbf{t}+\mathbf{t}')}\,e^{i\mu_{\alpha'}{}^{+}M\tau} \\ 0 & w_{\alpha\alpha'}\,e^{i\alpha\,.\,\mathbf{t}}\,e^{i\mu\alpha' M\tau} & w_{\alpha\alpha'}{}^{+}\,e^{i\alpha\,.\,(\mathbf{t}+\mathbf{t}')}\,e^{i\mu_{\alpha'}{}^{+}M\tau} \end{vmatrix}, \quad . \quad (3.22)$$

where the middle column of the second determinant contains 2∞ columns while all the other columns of both determinants contain just 1∞ columns. Obviously the first determinant can be factorized:

$$\exp i\tau\left(\sum_{\alpha'}^{\infty}-\mu_{\alpha'}{}^{+}L+\sum_{\alpha'}^{\infty}\mu_{\alpha'}{}^{-}N\right)\cdot \begin{vmatrix} v_{\alpha\alpha'} & 0 \\ 0 & v_{\alpha\alpha'}{}^{-}\,e^{i\alpha\,.\,(\mathbf{t}+\mathbf{t}')} \end{vmatrix} . \quad (3.23)$$

Similarly the general term in the Laplace development will contain the factor

$$\exp i\tau\left(\sum_{\alpha'}^{\infty_1}-\mu_{\alpha'}L+\sum_{\alpha'}^{\infty_2}\mu_{\alpha'}N\right), \quad . \quad . \quad . \quad . \quad (3.24)$$

where the first sum means : select any $\infty_1 \leqslant \infty\alpha'$'s and choose in any way a $+$ or $-$ to go with each one. Similarly with the second sum, with $\infty_1+\infty_2=\infty$.

The procedure from now on depends on the number of real $\mu_{\alpha'}$ that exist for the particular E we are considering. We remind the reader that it is possible to read off the *real* $\mu_{\alpha'}$ for any given κ and E from the energy contours of the perfect face-centred cubic crystal. If we draw a line (cf. eqn. (3.6) and fig. 1) through the point $\mathbf{k}=\kappa$ in reciprocal space that is perpendicular to the plane of the fault then each intersection of this line with the energy surface E gives a real $\mu_{\alpha'}$ for the given κ and E. μ's that differ by $2\pi/\tau$ are not counted as different, and the $+$ or $-$ is decided by seeing whether μ increases or decreases with increasing E. Now it is perfectly possible for there to be ranges of E in which there are no real μ's. These are, so to speak, energy gaps ; but notice that these energy gaps are dependent on κ, i.e. the component of the wave vector $\mathbf{k}$ parallel to the surface of the fault. In the event that we are in an energy gap, so that there are no real μ's, it is immediately obvious that the term (3.23) in the Laplace expansion of (3.20) completely dominates all the other terms (3.24) for large L and N(μ^+ has a positive and μ^- a negative imaginary part). As a consequence the zeros of (3.20) are determined asymptotically by the zeros of (3.22). (This is a well-known theorem in the theory of exponential sums, cf. e.g. Langer (1931).) All this is very clear from the physical standpoint : any zero of (3.22) in an energy gap will give the eigenvalue of a ' bound ' eigenfunction, i.e. a function that decreases exponentially on going away from the faults, but such eigenvalues could be obtained by using only the $\mu_{\alpha'}{}^+$ solutions in (3.17) for $x<0$ and only the $\mu_{\alpha'}{}^-$ solutions for $x>M\tau$ and neglecting the boundary conditions (3.19) on $x=-L\tau$ and $x=N\tau$, so giving the second determinant in (3.22) directly. Zeros of the first determinant in (3.22) are of no interest to us ; they must either be zeros of

$$|\, v_{\alpha\alpha'}{}^+ \exp(-i\mu_{\alpha'}{}^+L\tau)\,| \quad \text{or} \quad |\, v_{\alpha\alpha'}{}^- \exp(i\mu_{\alpha'}{}^-N\tau\,|\,. \quad . \quad (3.25)$$

These zeros are the eigenvalues of ' surface states ' on the surface $x=-L\tau$ or $x=N\tau$. Mathematically it is clear that this first determinant is irrelevant to the calculation of the energy of the faults, because it is independent of $\mathbf{t}$ and $\mathbf{t}'$.

Now let us consider a range of E for which there are two real μ's, say for $\alpha'=\beta$, i.e. μ_β are real. Then there are four terms of the form (3.24) that have equal modulus ; namely :

$$\begin{aligned} &\exp i\tau(-\mu_\beta{}^+L+\mu_\beta{}^+N), \qquad \exp i\tau(-\mu_\beta{}^+L+\mu_\beta{}^-N), \\ &\exp i\tau(-\mu_\beta{}^-L+\mu_\beta{}^+N), \qquad \exp i\tau(-\mu_\beta{}^-L+\mu_\beta{}^-N), \end{aligned} \quad (3.26)$$

where we have neglected the common factor

$$\exp i\tau\left(\sum_{\alpha'\neq\beta}^{\infty} -\mu_{\alpha'}{}^{+}L+\sum_{\alpha'\neq\beta}^{\infty}\mu_{\alpha'}{}^{-}N\right) \quad . \quad . \quad . \quad . \quad . \quad (3.27)$$

All the remaining terms in the Laplace development can be neglected for the asymptotic determination of the zeros of (3.20) for large L and N. (The mathematical justification is as before, Langer (1931).) Similarly if there are four real μ's. then there are $16=2^4$ dominant terms ; if there are six real μ's, there are $64=2^6$ dominant terms. Thus for large L and N the eigenvalues are given by the zeros of a function of the following form

$$\Delta(E, \mathbf{t}, \mathbf{t}', N)=\sum_{l} h_l(E, \mathbf{t}, \mathbf{t}') \exp (i\xi_l(E)N),$$

where the sum is over $2^2, 2^4, \ldots$ values of l for 2, 4, . . . real μ's. The conditions on the h_l and ξ_l required for the proof of Theorem 2 in the Appendix are satisfied provided we take

$$\xi_1(E)=\tau(-\mu_\beta{}^{+}L/N+\mu_\beta{}^{-}), \qquad \xi_2(E)=\tau(-\mu_\beta{}^{-}L/N+\mu_\beta{}^{+})$$

in the case of two real μ_ls for example (cf. (3.26)). h_1 is always given by (3.22) with the exponential part factored out. Theorem 2 shows that if $E_p(\mathbf{t}, \mathbf{t}')$ are the zeros of Δ then

$$\frac{d}{dt}\sum_{\epsilon_1<E_p<\epsilon_2} E_p(\mathbf{t}, \mathbf{t}')= \frac{1}{2\pi i}\frac{d}{dt}\int_{\epsilon_1}^{\epsilon_2}\log h_1/h_2\, dE$$

where d/dt means differentiation with respect to one of the scalar components of $\mathbf{t}$ or $\mathbf{t}'$ and $L=O(N)$. In order, therefore, to evaluate the rate of change of the sum of the eigenvalues in (ϵ_1, ϵ_2) we need only evaluate two determinants, namely h_1 and h_2 neither of which contain N or L and so are rather smoothly varying functions of E. Notice that Theorem 1 of the Appendix shows that the density of states is unaffected by the presence of the faults.

§ 4. The Energy of Two Stacking Faults in a Monovalent Crystal

In § 3 we have shown how to evaluate the change of the sum of the one electron energy levels when two faults are introduced into a crystal. The calculation depends on determining the two functions $h_1(E)$ and $h_2(E)$, h_1 for example being given by (3.22). These determinants, h_1 and h_2, involve the wave functions of a perfect crystal (including those that have complex wave vectors, $\mathbf{k}$) and we must therefore decide on what wave functions to use. In this section we shall use the wave functions obtained by perturbation theory, i.e. regarding the periodic potential as a small perturbation, and we shall only go as far as the first order in the expansion in powers of the potential (neglect V^2 compared with V). This is usually called the ' nearly free electron approximation ' (cf. Mott and Jones 1936, p. 60). We shall imagine that there are sufficiently few electrons per atom that we do not have to worry about degeneracies between different energy bands. The effect of this degeneracy is discussed in § 5 where we consider aluminium.

We have then to solve the equation (2.9) to the first order. The solution is of the form (2.14) where $v_{\alpha\alpha'}(x)$ is periodic with period τ. We expand $v_{\alpha\alpha'}(x)$ and $V_\alpha(x)$ in Fourier series :

$$\left.\begin{aligned} V_\alpha(x)&=\sum_n V_{\alpha n}\exp(-ni\gamma x)\\ v_{\alpha\alpha'}(x)&=\sum_n v_{\alpha\alpha' n}\exp(-ni\gamma x)\end{aligned}\right\}\quad \gamma=\frac{2\pi}{\tau}\quad . \quad . \quad . \quad (4.1)$$

This implies that the potential [$V(\mathbf{r})$ of (2.1)] is

$$V(\rho, x)=\sum_{\alpha n} V_{\alpha n}\exp[-i(\alpha\,.\,\rho+n\gamma x)] \quad . \quad . \quad . \quad (4.2)$$

and the wave functions [$\psi(\mathbf{r})$ of (2.1)] are [(2.5), (2.8), (2.11) and (4.1)]

$$\psi(\rho, x)=\exp[i(\kappa\,.\,\rho+\mu_{\alpha'}x)]\sum_{\alpha p} v_{\alpha\alpha' p}\exp[-i(\alpha\,.\,\rho+n\gamma x)]\,. \quad (4.3)$$

The expansion (4.1) with (2.8) and (2.9) give

$$\sec^2\theta\frac{\hbar^2}{2m}\{(\mu_{\alpha'}-p\gamma)^2-2(\kappa-\alpha)\,.\,\mathbf{i}(\mu_{\alpha'}-p\gamma)+(\kappa-\alpha)^2\cos^2\theta$$
$$+[(\kappa-\alpha)\,.\,\mathbf{i}]^2\}v_{\alpha\alpha' p}+\sum_{\alpha'' m} V_{\alpha-\alpha'' p-m}v_{\alpha''\alpha' m}=Ev_{\alpha\alpha' p} \quad . \quad . \quad (4.4)$$

as a set of homogeneous simultaneous equations for $v_{\alpha\alpha' p}$, α and p specifying the equation, α' being fixed. In this equation, E is known while $\mu_{\alpha'}$ is the eigenvalue. The zero order solutions of (4.3) are plane waves that may be taken to be $\exp i[\mu_\alpha x+(\kappa-\alpha')\,.\,\rho]$ where

$$\mu_{\alpha'}=(\kappa-\alpha')\,.\,\mathbf{i}\pm\left\{\frac{2mE}{\hbar^2}-(\kappa-\alpha')^2\right\}^{1/2}\cos\theta \quad . \quad . \quad (4.5)$$

if $V_{00}=0$, i.e. $v_{\alpha\alpha' 0}=1$ and $v_{\alpha\alpha' p}=0$ if $p\neq 0$ and $\alpha\neq\alpha'$. The wave function to the first order is (4.3) with $v_{\alpha'\alpha' 0}=1$ and the other $v_{\alpha\alpha' p}$'s given by

$$v_{\alpha\alpha' p}\sec^2\theta\frac{\hbar^2}{2m}\left\{(\mu_{\alpha'}-p\gamma)^2-2(\kappa-\alpha)\,.\,\mathbf{i}(\mu_{\alpha'}-p\gamma)+(\kappa-\alpha)^2\cos^2\theta\right.$$
$$\left.+[(\kappa-\alpha)\,.\,\mathbf{i}]^2-\frac{2mE}{\hbar^2}\right\}=V_{\alpha-\alpha' p}. \quad . \quad . \quad . \quad . \quad . \quad (4.6)$$

The part in curly brackets can easily be factorized to give

$$v_{\alpha\alpha' p}\sec^2\theta\frac{\hbar^2}{2m}\{\mu_{\alpha'}-\mu_\alpha{}^+-p\gamma\}\{\mu_{\alpha'}-\mu_\alpha{}^--p\gamma\}=V_{\alpha-\alpha' p}. \quad . \quad (4.7)$$

The expressions that occur in the determinant h_1, (3.22), that we have to evaluate are

$$v_{\alpha\alpha'}(0)=\sum_p v_{\alpha\alpha' p}$$

and

$$w_{\alpha\alpha'}(0)=i\mu_{\alpha'}v_{\alpha\alpha'}(0)+v'_{\alpha\alpha'}(0)=\sum_p v_{\alpha\alpha' p}i(\mu_{\alpha'}-p\gamma). \quad . \quad . \quad (4.9)$$

If $\alpha=\alpha'$ these contain a zero order term, namely 1 and $i\mu_\alpha$ so that each of the sub-matrices, in (3.22) has zero order terms in the diagonal and first order terms elsewhere.

We now expand the determinant $h_1=A+B+C+$, where A, B, and C are the zero, first, and second order terms, respectively. (It is simplest to diagonalize the matrix to the zero order first and then expand.) Then

$$\log h_1=\log A+B/A+(C/A+B^2/2A^2)+\ldots \quad . \quad . \quad . \quad (4.10)$$

to the second order. It turns out that A and B do not contain $\mathbf{t}$ or $\mathbf{t}'$, so, for our purposes (3.28) $\log h_1=C/A$.

After some tedious algebra we find

$$\log (h_1/h_2)=I_0+I_1(\mathbf{t})+I_1(\mathbf{t}')+I_2(\mathbf{t}, \mathbf{t}'|M) \quad . \quad . \quad . \quad (4.11)$$

where I_0 is independent of $\mathbf{t}$ and $\mathbf{t}'$ and

$$I_1(\mathbf{t})=-\left(\frac{2m}{\hbar^2}\right)^2 \cos^4\theta \sum_{\alpha n m} \exp(\mathbf{i}\,\alpha\,.\,\mathbf{t}) V_{\alpha n} V_{-\alpha-m}$$
$$\times[K^+(\alpha, n, m|0)+K^-(\alpha, n, m|0)]-\text{cc}, \quad . \quad . \quad (4.12)$$

$$I_2(\mathbf{t}, \mathbf{t}'|M)=\left(\frac{2m}{\hbar^2}\right)^2 \cos^4\theta \sum_{\alpha n m} [\exp(i\alpha\,.\,\mathbf{t})+\exp(i\alpha\,.\,\mathbf{t}')-\exp\{i\alpha\,.\,(\mathbf{t}+\mathbf{t}')\}]$$
$$\times V_{\alpha n} V_{-\alpha-m}[K^+(\alpha, n, m|M)+K^-(\alpha, n, m|M)-\text{cc} \quad . \quad . \quad (4.13)$$

with

$$K(\alpha, n, m|M)=\exp[i(\mu_0-\mu_\alpha^-)M\tau][(\mu_0^+-\mu_0^-)(\mu_\alpha^+-\mu_\alpha^-)$$
$$\times(\mu_0-\mu_\alpha^--n\gamma)(\mu_0-\mu_\alpha^--m\gamma)]^{-1}. \quad . \quad . \quad . \quad (4.14)$$

$I_1(\mathbf{t})$ gives the self energy of a fault while $I_2(\mathbf{t}, \mathbf{t}'|M)$ gives the interaction energy. h_2 is obtained from h_1 by merely interchanging μ_0^+ and μ_0^-, these being the only real μ's.

The reader's attention is drawn to two facts: first, the energy can be split into self and interaction energies; secondly,

$$I_1(\mathbf{t})+I_1(\mathbf{t}')+I_2(\mathbf{t}, \mathbf{t}'|0)=I_1(\mathbf{t}+\mathbf{t}').$$

We now imagine that all states are occupied up to some energy E' so that we must integrate (4.12) and (4.13) with respect to E from $\hbar^2\kappa^2/2m$ (μ_0 must be real, (4.5)) to E'; these are the ϵ_1 and ϵ_2 of eqn. (3.28). Then we must sum over all κ's given by eqn. (2.7) inside a circle of radius $(2mE'/\hbar^2)^{1/2}$. κ and E occur in K only, so replacing the sum over κ by an integral, we find

$$\sum_\kappa \int K\,dE=\frac{N_1 N_2}{|\alpha_1 \wedge \alpha_2|}\iint K\,dE\,d\kappa=L(\alpha, n, m|M). \quad . \quad . \quad (4.15)$$

New variables of integration, ξ, η, and ζ are more convenient. ξ and η are rectangular coordinates in the κ plane chosen so that

$$\alpha(\hbar^2/2mE')^{1/2}=(c, 0, 0), \qquad \kappa(\hbar^2/2mE')^{1/2}=(\xi, \eta, 0), \quad . \quad (4.16)$$

while ζ is chosen so that

$$E=E'(\xi^2+\eta^2+\zeta^2). \quad . \quad . \quad . \quad . \quad . \quad . \quad (4.17)$$

The region of integration is now a hemisphere of radius 1, viz.

$$\xi^2+\eta^2+\zeta^2\leqslant 1 \quad \text{and} \quad \zeta\geqslant 0.$$

The Jacobian is given by the equation

$$d\kappa\, dE=(4mE'^2/\hbar^2)\zeta\, d\xi\, d\eta\, d\zeta. \qquad (4.18)$$

It is also convenient to introduce the following abbreviations

$$\alpha \,.\, \mathbf{i} \sec\theta(\hbar^2/2mE')^{1/2}=f, \qquad \gamma \sec\theta(\hbar^2/2mE')^{1/2}=d$$

$$\tau\cos\theta(2mE'/\hbar^2)^{1/2}=\lambda. \qquad (4.19)$$

Then from (4.5)

$$\begin{aligned}
&\mu_0{}^+-\mu_0{}^-=2(2mE'/\hbar^2)^{1/2}\cos\theta\zeta\\
&\mu_\alpha{}^+-\mu_\alpha{}^-=2i(2mE'/\hbar^2)^{1/2}\cos\theta\{(c-\xi)^2-(\xi^2+\zeta^2)\}^{1/2} \qquad (4.20)\\
&\mu_0-\mu_\alpha{}^-=(2mE'/\hbar^2)^{1/2}\cos\theta[f\pm\zeta+i\{(c-\xi)^2-(\xi^2+\zeta^2)\}^{1/2}].
\end{aligned}$$

We can expand the square root that occurs in the last two of these expressions, because $\xi^2+\eta^2+\zeta^2\leqslant 1$ and $c>2$ for a monovalent metal. The first term in the expansion is $(c-\xi)$. When $(c-\xi)$ occurs in the denominator of K (4.14) we replace it by c, but we shall not so change it in the exponent since this term oscillates. The integral (4.15) reduces, with these approximations, to

$$L=\frac{N_1N_2}{|\alpha_1\wedge\alpha_2|}\frac{4mE'^2}{\hbar^2}\frac{\sec^4\theta}{4i}\left(\frac{\hbar^2}{2mE'}\right)^2\frac{\exp[(if-c)M\lambda]}{c(f-nd+ic)(f-md+ic)}$$
$$\times\iiint\exp[M\lambda(\xi\pm i\zeta)]\,d\xi\,d\eta\,d\zeta. \qquad (4.21)$$

The triple integral over the hemisphere of radius 1 can be worked out by expanding the exponential and integrating first over a semicircle perpendicular to the ξ direction and then over ξ. The answer is

$$\iiint\exp[M\lambda(\xi\pm i\zeta)]\,d\xi\,d\eta\,d\zeta=\frac{2\pi}{3}\pm\pi i\sum_{p=0}^{\infty}\left(\frac{M\lambda}{2}\right)^{2p+1}\frac{1}{p\,!(p+2)\,!(2p+1)}. \qquad (4.22)$$

Because we require only L^++L^- (cf. (4.12) and (4.13)) the infinite sum is irrelevant. It is amusing to note that this is the same answer that would have been obtained if $(c-\xi)$ had been replaced by c in the exponential term of (4.14).

The next problem is the calculation of $V_{\alpha n}$ defined by (4.1)

$$V_{\alpha n}=\iint V(\rho,x)\,d\rho\,dx\Big/\iint d\rho\,dx. \qquad (4.23)$$

Again the coordinates are unnecessarily complicated, if we change to rectangular coordinates we introduce the Jacobian $\cos\theta$. Furthermore,

$$\alpha\,.\,\rho+n\gamma x=\left(\alpha-\frac{\alpha\,.\,\mathbf{i}}{\cos\theta}\mathbf{i}'+\frac{n\gamma}{\cos\theta}\mathbf{i}'\right).(\rho+x\mathbf{i})=\mathbf{k}\,.\,\mathbf{r} \qquad (4.24)$$

where $\mathbf{i}'$ is a unit vector perpendicular to the ρ plane. So our integral (4.23) is just

$$V_{\alpha n}=\int \exp(i\mathbf{k}\cdot\mathbf{r})V(\mathbf{r})\,d\mathbf{r}\Big/\int d\mathbf{r}. \quad . \quad . \quad . \quad (4.25)$$

No nucleus is at the origin of coordinates $\mathbf{r}$ but there is a nucleus at $\mathbf{r}=\tau\mathbf{i}/2$ (cf. (3.8)) so we have, for a potential spherically symmetrical about a nucleus,

$$V_{\alpha n}=\frac{(-1)^n}{\Omega}\int_{\text{cell}} V(\mathbf{r})\exp(i\mathbf{k}\cdot\mathbf{r})\,d\mathbf{r}=\frac{(-1)^n}{\Omega}\frac{4\pi}{k}\int_0^{r_s} rV(r)\sin kr\,dr, \quad (4.26)$$

where $\Omega=4\pi r_s^3/3$ is the volume of an atomic cell and we have used the Wigner–Seitz equivalent sphere. A simple potential to use is

$$V(r)=Ze^2\exp(-q'r)/r. \quad . \quad . \quad . \quad . \quad . \quad . \quad (4.27)$$

If we replace r_s by ∞ in the integral (4.26), this gives

$$V_{\alpha n}=\frac{(-1)^n}{\Omega}\frac{4\pi Ze^2}{q'^2+k^2} \qquad k^2=\alpha^2+(\alpha\cdot\mathbf{i}-n\gamma)^2\sec^2\theta \quad . \quad (4.28)$$

from (4.24).

Now it will be observed that $I_1(\mathbf{t})$ and $I_2(\mathbf{t},\mathbf{t}'|M)$ (4.12) and (4.13), involve a summation over n and m. If we leave out all the factors independent of n and m the required sum is

$$\begin{aligned}\sum_{nm}(-1)^{n+m}&\{(f-nd+ic)(f-md+ic)[\alpha^2+(\alpha\cdot\mathbf{i}-n\gamma)^2\sec^2\theta+q'^2]\\ &\times[\alpha^2+(\alpha\cdot\mathbf{i}-m\gamma)^2\sec^2\theta+q'^2]\}^{-1}=(\hbar^2/2mE')^2\\ &\times\{\sum_n(-1)^n(f-nd+ic)^{-1}][c^2+(f-nd)^2+q^2]^{-1}\}^2\\ &=(\hbar^2/2mE')^2\pi^2]S(\alpha,q)]^2, \quad . \quad . \quad . \quad . \quad . \quad . \quad . \quad . \quad . \quad (4.29)\end{aligned}$$

where q is defined as

$$q'(\hbar^2/2mE')^{1/2}=q. \quad . \quad . \quad . \quad . \quad . \quad . \quad . \quad . \quad (4.30)$$

The sum over n in $S(\alpha,q)$ can be easily evaluated by a contour integral (see Titchmarsh (1939), §3.3, p. 115). After a little manipulation we find

$$\begin{aligned}d^3S(\alpha,q)&=\sin F\pi\left\{\frac{\cosh C\pi}{Q^2S^2}-\frac{\cosh C'\pi}{Q^2S'^2}\right\}-i\cos F\pi\\ &\times\left\{\frac{\sinh C\pi}{Q^2S^2}-\frac{C}{C'}\frac{\sinh C'\pi}{Q^2S'^2}\right\}\\ S^2&=\sin^2F\pi+\sinh^2C\pi, \quad S'^2=\sin^2F\pi+\sinh^2C'\pi \quad . \quad (4.31)\\ Q&=q/d, \qquad F=f/d, \qquad C=c/d, \qquad C'=\sqrt{(C^2+Q^2)}.\end{aligned}$$

Notice that F and C are not only dimensionless but they are also independent of the lattice parameter $a=\tau\sqrt{2}$ and the Fermi energy E'. We have, therefore, worked out d^3S for seven different values of

$$Q=q'\tau/(\pi\sqrt{6}).$$

Collecting together all our formulae : (3.46), (4.11), (4.12), (4.13), (4.14), (4.15), (4.21), (4.22), (4.28), and (4.29) we find that the energy per unit area of two stacking faults M layers apart is

$$\frac{1}{N_1 N_2 |\tau_1 \wedge \tau_2|} \frac{1}{2\pi i} \Sigma_\kappa \int \log \frac{h_1}{h_2} dE \Big|_{t=0}^{t=(\tau_1+\tau_2)/3}$$

$$\frac{2me^4 Z^2}{\hbar^2} \frac{n}{a^2} \frac{2}{27\sqrt{3}\pi^3} \Sigma_\alpha \frac{d}{c} [d^3S(\alpha, q)]^2 \{(2 \exp [i\alpha \,.\, \mathbf{t}] - 2)$$

$$- \exp [2\pi(iF - C)M](2\exp [i\alpha \,.\, \mathbf{t}] - \exp [2i\alpha \,.\, \mathbf{t}] - 1)\} + \text{cc}, \quad . \quad (4.32)$$

where n is the number of electron per cell, i.e. for a monovalent metal 1. The first part in the curly brackets gives twice the self-energy ; the second part gives the interaction energy.

We have summed (4.32) over the six nearest neighbour α's, namely $\alpha_1, \alpha_2, \alpha_1+\alpha_2, -\alpha_1, -\alpha_2, -\alpha_1-\alpha_2$. The six next nearest neighbours make $\alpha \,.\, (\tau_1+\tau_2)/3 = \pm 2\pi$ and so do not contribute to the energy. We have neglected the next nearest neighbours because $d^3S(\alpha, q)$ decreases exponentially with C or c or $|\alpha|$.

In table 2, we show the numerical values of the surface energy per unit area as calculated from (4.32) with $Z=1$, $a=3{\cdot}61\times10^{-8}$ cm (the lattice parameter of copper) and for various values of $q'\tau$ as shown ($\tau=2{\cdot}55\times10^{-8}$ cm). Notice that our wave functions correspond to the 1s band because we have used the nearly free electron approximation so that it would be illogical to put $Z=29$.

Table 1. Energy of Two Faults M Layers Apart

M	1	2	3
Energy	$2W+4W'$	$4W+5W'$	$4W+6W'$
Interaction-energy	$-2W-2W'$	$-W'$	0

Table 2. Energy of Two Stacking Faults in Cu in ergs/cm^2

$q'\pi$	Self-energy	Interaction-energy		
		$M=1, \times10^2$	$M=2, \times10^5$	$M=3, \times10^7$
1	$+20{\cdot}3$	$+37$	-28	$-19{\cdot}2$
2	$+17{\cdot}0$	$+33$	-26	$-16{\cdot}7$
5	$+\ 5{\cdot}56$	$+16{\cdot}4$	$-15{\cdot}9$	$-\ 7{\cdot}45$
10	$+\ 0{\cdot}325$	$+\ 3{\cdot}34$	$-\ 4{\cdot}12$	$-\ 1{\cdot}29$
17	$+\ 0{\cdot}820\times10^{-3}$	$+\ 0{\cdot}498$	$-\ 0{\cdot}665$	$-\ 0{\cdot}178$
17·438	$+\ 0{\cdot}94\times10^{-6}$	$+\ 0{\cdot}451$	$-\ 0{\cdot}604$	$-\ 0{\cdot}162$
18	$-\ 0{\cdot}714\times10^{-3}$	$+\ 0{\cdot}399$	$-\ 0{\cdot}534$	$-\ 0{\cdot}142$

There are four points of interest in these results.

1. The self-energy changes sign at about $q'\tau=17{\cdot}438$ and for all $q'\tau$ bigger than this value the self-energy is negative. This is of course an unrealistically high q' for it makes the potential (4.27) almost a δ function at each nucleus.

2. The interaction energy is about a hundreth of the self-energy even for $M=1$. This means that the self-energy of a stacking fault of the second kind $ABC|B|ABC$ is just about twice the energy of a fault of the first kind $ABC|BCA$. For $q'\tau\doteq 17{\cdot}4377$, when the self-energy is zero, the interaction energy is still present.

3. The interaction energy oscillates in sign with a period of $M=3$ and decreases exponentially with distance M.

4. The self-energy for $Z=1$ and $q'\tau=1$ is very close to the experimental value of the self-energy of *twins* in copper (Fullman 1951).

These results should be compared with the calculations of the energy on the basis of van der Waal attraction between ions, which give :

1. A negative self-energy.

2. An interaction energy that is equal to minus the self-energy for $M=1$ and is negligible for $M=2, 3, \ldots$, so that the energy of a stacking fault of the second kind is equal to the energy of a fault of the first kind.

It seems wise at this point to warn the reader against an over naive extension of these results. It is not possible to calculate the energy of an arbitary number of faults by adding their self-energies and their interaction energies. For example a fault on every layer gives a cubic crystal again and should therefore have a zero energy, not the sum of the self-energies. The reason for this is that the interaction energy between two faults given by (4.13) is not correct when there is another fault between them. It may be that the energy of a twin is nearly the same as the energy of a fault and that the difference in energy between N layers of hexagonal and N layers of cubic is $N/2$ times the energy of a fault, but these results do *not* follow from this paper.

§ 5. Aluminium : The Energy of a Single Fault

In this section we shall outline a method for calculating the energy of a single stacking fault in a polyvalent metal. For reasons that will become apparent, this calculation cannot be so complete as that given in § 4 for a monovalent metal. From the very start it is necessary to put in numbers. We have therefore only considered aluminium.

The wave functions, (4.3) used in § 4 were based on first order perturbation theory, (4.6) (cf. Mott and Jones 1936, p. 60). For aluminium we must also consider electrons for which the wave vectors are close to the zone faces, so that, in eqn. (4.4) several $v_{\alpha\alpha' p}$'s are large (not just one), and degenerate perturbation theory must be used (Mott and Jones 1936, p. 61). This means that the determinant

$$h_1= \begin{vmatrix} v_{\alpha\alpha'}^{-} & v_{\alpha\alpha'}^{+}\exp(i\alpha\,.\,\mathbf{t}) \\ w_{\alpha\alpha'}^{-} & w_{\alpha\alpha'}^{+}\exp(i\alpha\,.\,\mathbf{t}) \end{vmatrix} \qquad (5.1)$$

derived from (3.21) has large off-diagonal terms in its sub-matrices. We decided only to retain zero order terms, thus reducing h_1 to finite order. $\mu_{\alpha'}$ and $v_{\alpha\alpha' p}$ were determined on the assumption that there were only two large $v_{\alpha\alpha' p}$ (this makes h_1 a 4×4). Both the real and the complex solutions of the quartic equation for $\mu_{\alpha'}$ (cf. Mott and Jones 1936, p. 60, eqn. (40)) were obtained. The solutions for $\mu_{\alpha'}$—only the real ones of course—are shown in fig. 1. We have plotted a cross section of the energy contours. The cross section is taken through the centre of the zone and containing the vectors $(\bar{1}11)$ and $(11\bar{1})$. Note that we are now taking the κ plane perpendicular to (011) so that the relation between κ, $\mu_{\alpha'}$ and **k** is given by (3.6). The numerical values for the energy gaps at the hexagonal and square faces were taken from Leigh (1951).

Fig. 1

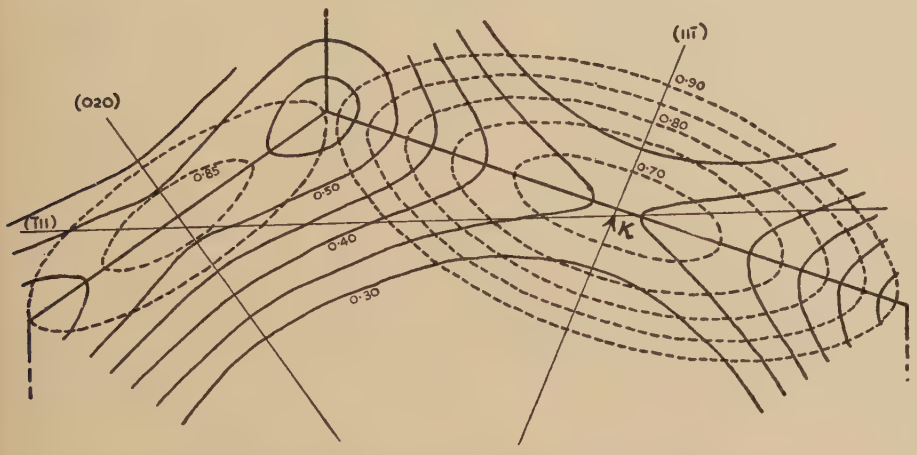

Cross section of the energy surfaces in aluminium. The full curves are for the upper band and the pecked curves are for the lower band. Contours are at intervals of 0·05 Rydbergs. A corner of the zone boundary between a square (020) and a hexagonal $(11\bar{1})$ face is shown. The line $(11\bar{1})$ is the intersection between the plane of the figure and the κ plane, which has an (011) normal. The intersection of the line $(\bar{1}11)$ starting at a given κ with the energy surfaces gives the value of μ (E). Note that for $E>0{\cdot}85$ Rydbergs there are, for most κ, four real μ's. While for $E<0{\cdot}85$ Rydbergs there are only two real μ's. The curves have been slightly adjusted near the edge between the square and the hexagonal faces.

A reasonably complete calculation would involve the computation of h_1 for many values of κ and E over the required range (up to about 0·9 Rydbergs). Actually we selected $3\times6\kappa$'s each one lying in the direction of one of the 6 zone faces. Five values of the energy, 0·70, 0·75, . . . 0·90 Rydbergs, all lying in the upper band were used for each of the three essentially different κ's.

In fig. 2 we show the results of a typcial calculation of the real and imaginary parts of h_1 for $|\kappa|=0{\cdot}70$ atomic units and κ in the α_1, i.e. $(11\bar{1})$ direction. The six graphs are for six values of $\alpha_1 \,.\, \mathbf{t} : 0, 1, 2, \ldots 5$. The curves for $\alpha_1 \,.\, \mathbf{t}=\alpha_1 \,.\, (\tau_1+\tau_2)/3=4\pi/3\doteq 4{\cdot}2$ (3.11), and $\alpha_1 \,.\, \mathbf{t}=0$ are the only ones of immediate interest, but the intermediate ones are

Fig. 2

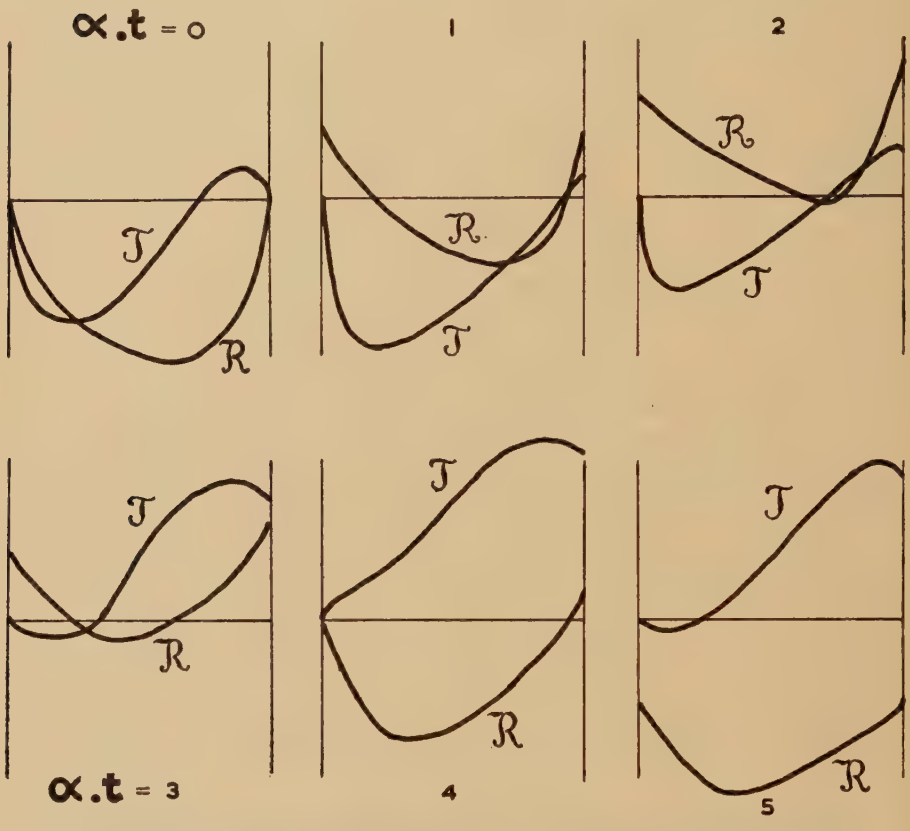

The real and imaginary parts of $h_1(E, \kappa, \mathbf{t})$ (ordinates) plotted against E (abscissae) for a given κ and for $\alpha_1 \,.\, \mathbf{t}=0,1, 2, \ldots 5$.

necessary to get the correct branch of $\arg h_1=\arctan(\Im h_1/\Re h_1)$. It will be noticed that for this particular κ $h_1=0$ at the bottom of the band when $\alpha_1 \,.\, \mathbf{t}=0$ and 3·8. This zero of h_1 actually moves out into the energy gap between the two bands (for this κ) and returns after

$$\mathbf{t}=(3{\cdot}8/4{\cdot}2)(\tau_1+\tau_2)/3.$$

This zero in the energy gap is, as we explained in § 3, the eigenvalue of a bound surface state that has for its wave vector parallel to the fault the value $\kappa-[(111) \,.\, \kappa/3](\bar{1}\bar{1}1)$. We found no surface states for the values of κ we chose when $\mathbf{t}=(\tau_1+\tau_2)/3$.

We estimated that the energy change due to the fault is about 2600 ergs/cm² for κ's near the hexagonal faces and about -1600 ergs/cm² for κ's near the square faces. So giving a total energy of the fault of 1000 ergs/cm² for electrons in the upper hand. We do not have much faith in this calculation, because it assumes that the energy change is the same for all κ's in the sectors terminating at the faces. It seems very likely that for κ's near the edge formed by two faces the energy would be entirely different, i.e. somewhat between $+2600$ and -1600.

Owing to the use in the total wave function, (2.8), (2.11), and (3.17), of complex wave vectors $\mathbf{k}$ in the direction perpendicular to the fault there will in general be a charge accumulation (positive or negative) in the region of the fault. Not only will this violate our condition (3.9); it will also give an electrostatic contribution to the surface energy. The electrostatic energy will be infinite unless the surface charge is screened, and the exact magnitude of the energy will depend on the rapidity of the screening. Suppose, for example, the charge density after screening was

$$\rho(z)=\rho_0[\exp(-\lambda_1|z|)-(\lambda_2/\lambda_1)\exp(-\lambda_2|z|)] \quad . \quad . \quad (5.2)$$

where z is the perpendicular distance from the fault. Then the self-energy of this charge distribution is

$$\pi\frac{(\lambda_1-\lambda_2)^2}{\lambda_1^3\lambda_2(\lambda_1+\lambda_2)}\rho_0^2 \quad . \quad . \quad . \quad . \quad . \quad . \quad (5.3)$$

per unit area. If we take $\rho_0=10^{-2}$, $\lambda_1=1$, and $\lambda_2=\frac{1}{2}$ in atomic units, the energy is approximately 200 ergs/cm². With $\rho_0=10^{-2}$, $\lambda_1=1$, and $\lambda_2=\frac{1}{4}$ the energy is greater by a factor of 6. These energies are of the same order of magnitude as those due to scattering of electrons by the fault.

Acknowledgments

We wish to thank Professor N. F. Mott for suggesting this problem. R. W. Attree, Ramsay Memorial Fellow in Chemistry (1950) wishes to thank the National Research Council (Canada) for a fellowship and the University of Bristol for a grant. J. S. Plaskett wishes to thank the Department of Scientific and Industrial Research for a Maintenance Grant and a Senior Award.

APPENDIX

The Zeros of Exponential Sums

In this Appendix we shall study the behaviour of the zeros of a finite exponential sum, say

$$\Delta(E,t,N)=\sum_{l=1}^{N} h_l(E,t)\exp(i\xi_l(E)N)$$

as a function of the parameter t for very large positive values of N. The steps to the proof of Theorem 2, which is used at the end of § 3, have been labelled Lemmas 1, 2, and 3. Lemmas 1 and 2 are independent of

one another, and give rather different bits of information on the zeros of Δ. Lemma 3 uses both these bits of information and the two theorems follow directly from it.

The following conditions are common to the whole Appendix (notice that no mention need be made of the parameter t until Theorem 2).

1. $g_l(E)$, $h_l(E)$ and $\xi_l(E)$ are regular functions of E in a region D of the E plane which has the closed interval (ϵ_1, ϵ_2) of the real axis in its interior.

2. The $\xi_l(E)$ are real for real values of E in D and can be labelled so that

$$\xi_1'(\epsilon)<\xi_l'(\epsilon)<\xi_2'(\epsilon), \qquad l\neq 1 \text{ or } 2$$

for all ϵ in the closed interval (ϵ_1, ϵ_2). We shall always write $E=\epsilon+i\eta$ so that ϵ and η are the real and imaginary parts of E.

Lemma 1. With the conditions 1 and 2

$$\Sigma h_l(E)\exp(i\xi_l(E)N)=\begin{cases}\exp[i\xi_1(E)N][h_1(E)+O(\exp -a\eta N)] & \eta\geqslant 0\\ \exp[i\xi_2(E)N][h_2(E)+O(\exp b\eta N)] & \eta\leqslant 0\end{cases}$$

for $|\eta|<\eta_0>0$ and $\epsilon_1-\eta_0<\epsilon<\epsilon_2+\eta_0$. a and b are positive (non-zero) and independent of E and N.

We only consider the case of $\eta\geqslant 0$

$$\Sigma h_l\exp(i\xi_l N)=\exp(i\xi_1 N)[h_1+\Sigma' h_l'\exp\{i(\xi_l-\xi_1)N\}]$$

but

$$i[\xi_l(E)-\xi_1(E)]=i[\xi_l(\epsilon)-\xi_1(\epsilon)]-\eta[\xi_l'(\epsilon)-\xi_1'(\epsilon)]+O(\eta^2)$$

and from condition 2 there exists an $a>0$ for which $\xi_l'-\xi_1'>2a$ for ϵ in $(\epsilon_1-\eta', \epsilon_2+\eta')$ for η' (>0) and small enough for all l. It follows that we can find an η'' (>0) so small that the term $O(\eta^2)<a\eta$ for $0\leqslant\eta<\eta''$ and so

$$|\exp\{i[\xi_l(E)-\xi_1(E)]N\}|\leqslant\exp(-a\eta N), \qquad 0\leqslant\eta<\eta_0<0$$

and $\epsilon_1-\eta_0\leqslant\epsilon\leqslant\epsilon_2+\eta_0$ where η_0 is the smaller of η' and η''. If η_0 is at the same time chosen so that this rectangle lies inside D then the $|h_l|$ are bounded and the lemma is proved.

Corollary. The zeros of $\Delta(E, N)$ for large N either tend to the zeros of h_1 $(\eta>0)$ or $h_2(\eta<0)$, if $|\eta|<\eta_0$ or are within a distance of $O(1/N)$ from the real axis provided h_1 and h_2 are not zero on the real axis. At a point on the real axis where h_1 or h_2 has a zero the zeros of Δ lie within a distance of $O(\log N/N)$ of the real axis.

Lemma 2. With the condition 1 and provided not all h_l are zero at the point $E=\epsilon$ the number of zeros of Δ within the square of side $2A/N$ (A arbitrary but independent of N) centred at ϵ is bounded (as $N\to\infty$). Furthermore, if circles of radius C/N ($C<0$ as small as one likes but independent of N) are cut out around each zero of Δ then in the remaining region of the square $|\Delta|$ has a positive lower bound (N big enough) that is independent of N.

Let us change the variable from E to z, $E=\epsilon+z/N$. Then

$$\Delta=\Sigma h_l(\epsilon)\exp[i\xi_l(\epsilon)N]\exp[i\xi_l'(\epsilon)z]+O(1/N),\qquad z<A\sqrt{2}.$$

Consider the first term and write it $\Sigma a_l\exp(ib_lz)=f(z)$ with

$$a_l=h_l\exp(i\xi_lN)\quad\text{and}\quad b_l=\xi_l'(\epsilon).$$

$f(z)$ has a finite number of zeros inside the square of side $2A$ centred at $z=0$ for any given a_l, i.e. given N. If we remove from the square circles of radius C centred at each zero then $|f(z)|$ has a positive lower bound in this region. The number of zeros of $f(z)$ and this lower bound depend on N through the a_l, but for all N the a_l only vary over *closed* regions since $|a_l|=|h_l|$, so the number of zeros has an upper bound independent of N and $|f(z)|$ has a positive lower bound independent of N. Now consider only those N's that are so large that the lower bound of $|f(z)|$ dominates the term $O(1/N)$ in Δ. Then from Rouché's theorem (Titchmarsh 1939, § 3.42) Δ has the same number of zeros as $f(z)$ and furthermore $|\Delta|$ has a positive lower bound independent N in the cut out region.

Lemma 3.

$$\int_\Gamma\frac{\Sigma g_l(E)\exp[i\xi_l(E)N]}{\Sigma h_l(E)\exp[i\xi_l(E)N]}dE=\int_{\Gamma_+}\frac{g_1}{h_1}dE+\int_{\Gamma_-}\frac{g_2}{h_2}dE+O(1/N)$$

where the closed contour Γ is composed of the two contours Γ_+ and Γ_-. Γ_+ starts at ϵ_2, ends at ϵ_1 and is always above the real axis except at the ends points. Γ_- starts at ϵ_1 ends at ϵ_2, and is always below the real axis except at its end points. h_1 is not zero on Γ_+ nor is h_2 zero on Γ_- including the end points. $\Sigma h_l\exp(i\xi_lN)$ is not zero on Γ. g_l, h_l, and ξ_l satisfy conditions 1 and 2.

Consider

$$\int_{\Gamma_+}\left[\frac{\Sigma g_l\exp(i\xi_lN)}{\Sigma h_l\exp(i\xi_lN)}-\frac{g_1}{h_1}\right]dE=\int_{\Gamma_+}\frac{\Sigma(g_lh_1-g_1h_l)\exp[i(\xi_l-\xi_1)N]}{\Sigma h_1h_l\exp[i(\xi_l-\xi_1)N]}dE.$$

By Lemma 1 the numerator is of order $\exp(-a\eta N)$ and, except in a neighbourhood of radius A/N of ϵ_1 and ϵ_2 (A sufficiently large), the denominator is dominated by h_1^2 and so has a lower bound. In this neighbourhood of ϵ_1 and ϵ_2 the denominator also has a lower bound independent of N by Lemma 2. An upper bound to the integral on the right is therefore

$$B\int_{\Gamma_+}\exp(-a\eta N)|dE|$$

where B is independent of N. This integral is of $O(1/N)$. The proof for Γ_- is similar.

Theorem 1. The number of zeros of Δ that lie inside the rectangle with corners $\epsilon_1\pm i\eta_0$ and $\epsilon_2\pm i\eta_0$ ($\eta_0>0$ but sufficiently small) is

$$\frac{N}{2\pi}\int_\epsilon^{\epsilon_2}[\xi_2'(\epsilon)-\xi_1'(\epsilon)]\,d\epsilon+O(1)$$

provided h_l and ξ_l satisfy conditions 1 and 2 and h_1 and h_2 are not zero at ϵ_1 and ϵ_2.

The number of zeros inside the rectangle is

$$\frac{1}{2\pi i}\int_\Gamma \Delta'/\Delta\, dE$$

where Γ is the boundary of the rectangle except where there is a zero on the boundary of the rectangle except where there is a zero on the boundary when Γ goes inside the rectangle to avoid it. Since

$$\Delta'=\Sigma(h_l'+h_l i\xi_l' N)\exp(i\xi_l N)$$

and the conditions of Lemma 3 are satisfied with either $g_l=h_l'$ or $h_l\xi_l'$ (we also modify Γ so as to avoid zeros of h_1 and h_2) we have for the number of zeros

$$\frac{iN}{2\pi i}\int_{\Gamma_+}\frac{h_1\xi_1'}{h_1}dE+\frac{iN}{2\pi i}\int_{\Gamma_-}\frac{h_2\xi_2'}{h_1}+O(1)$$

which proves the theorem once it is noted that the integrands of the Γ_+ and Γ_- integrals have no singularities and so can be deformed to lie on the real axis.

We now consider the variation of the parameter t contained in the h_l and impose the following condition in addition to 1 and 2.

3. $h_l(E, t)$ and $\partial h_l/\partial t$ are regular functions of E in D and continuous functions of t in some interval.

Theorem 2. If the zeros of Δ inside the rectangle with corners $\epsilon_1\pm i\eta_0$ and $\epsilon_2\pm i\eta_0$ ($\eta_0>0$ but sufficiently small, cf. Lemma 1) are at the points $E_p(t)$, $p=1, 2, \ldots$ for a given value of N, then

$$\frac{d}{dt}\sum_p E_p(t)=\frac{1}{2\pi i}\frac{d}{dt}\int_{\epsilon_1}^{\epsilon_2}\log\frac{h_1}{h_2}d\epsilon+O(1/N).$$

The zeros are to be counted with their correct multiplicity. Besides the conditions 1, 2, and 3 on h_l and ξ_l, $h_1(E, t)$ must have no zeros with $\eta\geqslant 0$ and h_2 must have no zeros for $\eta\leqslant 0$. (The result could easily be modified with the weaker condition that h_1 and h_2 should not be zero at ϵ_1 and ϵ_2.)

$$\sum_p E_p=\frac{1}{2\pi i}\int_\Gamma E\Delta'/\Delta\, dE,$$

where Γ is as in Theorem 1. So

$$\frac{d}{dt}\Sigma E_p=\frac{1}{2\pi i}\int_\Gamma E\frac{\partial^2}{\partial t\partial E}\log\Delta\, dE=\frac{1}{2\pi i}\int_\Gamma E\frac{\partial}{\partial E}\frac{\partial\Delta/\partial t}{\Delta}dE$$

integrating by parts we find

$$\frac{d}{dt}\Sigma E_p=-\frac{1}{2\pi i}\int\frac{\partial\Delta/\partial t}{\Delta}dE.$$

We now use Lemma 3 with $g_l=\partial h_l/\partial t$ and we find

$$\frac{d}{dt}\Sigma E_p=-\frac{1}{2\pi i}\frac{d}{dt}\int_{\Gamma_+}\log h_1\, dE-\frac{1}{2\pi i}\frac{d}{dt}\int_{\Gamma_-}\log h_2\, dE+O(1/N).$$

The theorem follows after the appropriate modification of the contours.

References

Bloch, F., 1928, *Z. Phys.*, **52,** 555.

Bouchaert, L. P., Smoluchowski, R., and Wigner, E., 1936, *Phys. Rev.*, **50,** 58.

Copson, E. T., 1935, *The Theory of Functions of a Complex Variable* (Oxford : University Press).

Floquet, G., 1883, *Ann. de l'Ecole norm. sup.* (2), **12,** 47.

Frank, F. C., 1951, *Phil. Mag.*, **42,** 809.

Fullman, R. L., 1951, *J. Appl. Phys.*, **22,** 448.

Heindenreich, R. D., and Shockley, W., 1948, *Report on the Strength of Solids* (London : The Physical Society), p. 57.

Ince, E. L., 1927, *Ordinary Differential Equations* (London : Longmans Green).

Kramers, H. A., 1935, *Physica*, **2,** 483.

Langer, R. E., 1931, *Bull. Amer. Math. Soc.*, **37,** 213.

Leigh, R. S., 1951, *Phil. Mag.*, **42,** 139.

Mott, N. F., and Jones, H., 1936, *Properties of Metals and Alloys* (Oxford : University Press).

Shockley, W., 1950, *Electrons and Holes in Semiconductors* (New York : Van Nostrand) ; 1952, *Imperfections in nearly perfect crystals* (New York : Wiley).

Tamarkin, J. D., 1927, *Math. Z.*, **27,** 24.

Titchmarsh, E. C., 1939, *The Theory of Functions* (Oxford : University Press).

Wilder, C. E., 1917, *Trans. Amer. Math. Soc.*, **18,** 415.

XCII. *Proton-Excited Energy Levels in* ^{14}N

By E. J. Burge
The Wheatstone Laboratory, King's College, University of London

and D. J. Prowse
H. H. Wills Physical Laboratory, University of Bristol †

[Received June 5, 1956]

Abstract

The nuclear energy levels of ^{14}N have been investigated up to an energy of 7·7 Mev by inelastic proton scattering. All the known levels appear to participate in the scattering. The energies of the levels have been determined as : $7{\cdot}60\pm0{\cdot}02$, $7{\cdot}40\pm0{\cdot}02$, $7{\cdot}03\pm0{\cdot}02$, $6{\cdot}46\pm0{\cdot}02$, $6{\cdot}23\pm0{\cdot}02$, $5{\cdot}83\pm0{\cdot}03$, and $5{\cdot}69\pm0{\cdot}03$ Mev. Some evidence was obtained for a level at 5·95 Mev, and a probable new level was observed at $6{\cdot}60\pm0{\cdot}04$ Mev.

The scattering of 9·5 Mev protons by nitrogen, accelerated by the 60 in. Birmingham cyclotron, has been studied by Freemantle *et al.* (1954) using the scattering camera described by Burrows *et al.* (1951). Nuclear energy levels were detected at 2·3, 3·9, 4·9 and 5·1 Mev, as well as at higher values. These higher levels have now been examined more carefully with plates from the same exposure and also from an exposure made in October 1955.

A study has been made of the factors limiting the application of nuclear emulsions to the detection and measurement of the energies of particles inelastically scattered from a target. A micrometer eyepiece ($\times 15$ Kellner) was used which allowed readings to be made to 0·01 mm (=1 division) in the focal plane. In conjunction with a $\times 95$ objective, it was found that repeated settings on the beginning and end of the same track gave the range with a mean deviation of 3 divisions, i.e. about 0·4 μ. An error was found to arise from the determination of the position of the first grain. This was aggravated by a concentration of background grains near the surface. The origin of this is obscure and it has not been found possible to eliminate it. To facilitate scanning in earlier work, where range was of importance only in order to assign a track to a well defined group, the surface had been rubbed with cotton wool dipped in alcohol to remove this ' deposit '. The rubbing was not so severe for the angles larger than 90° used in the present work, and it was allowed for by adding a constant amount to the projected range of every track such that the

---

† Communicated by Professor J. T. Randall, F.R.S.

Q-values of well-defined groups agreed with well-known levels found in other reactions. The maximum addition was 16 divisions which is equivalent to the removal of about 6 divs in depth ($=0{\cdot}7\,\mu$). In the more recent exposures no rubbing took place; this correction was therefore not necessary, but the surface conditions made scanning very difficult. A study of the average distances between successive grains for 81 tracks on a 'rubbed' plate, starting at the surface at an angle of dip of 21°, led to the following results: 1st to 2nd grain, 10 divs; 2nd to 3rd, 10 divs; 3rd to 4th, 8 divs; 4th to 5th, 6 divs. Thus an error in the determination of the first grain can lead to a significant broadening of the histogram for a given level.

Straight attacks found within an angle of $\pm ca.\ 4°$ of the mean direction were accepted, the micrometer eyepiece being aligned to each track. This criterion is an individual one and means that the number of tracks in the various groups are only a very approximate indication of the cross section for the corresponding energy levels. The mean direction is not the same as the line of traverse for a given angle, as can be easily verified from a consideration of the geometry. The area to be scanned for a given histogram needs to be small in both directions otherwise complicated corrections become necessary. Two effects limit the useful length of traverse, (1) the variation in the angle of dip, affecting the projected length, and (2) the variation of the correction for the stopping power of the gas in the camera. These effects act in opposite directions and for laboratory angles near 120° the latter proved to be about twice the former at a distance of about 5·6 cm from the point of scattering. The optimum width of the traverse is determined by the variation of the energy of protons with scattering angle. For a given Q-value, this variation is given by

$$E_2=E_1[a\ \cos\theta+(a^2\cos^2\theta+b+cQ/E_1)^{1/2}]^2$$

where E_1 is the energy of the incident particle of mass M_1,

$$a=M_1M_2/(M_2+M_3),$$

where M_2 is the mass of the scattered particle ($=M_1$ for simple scattering) and M_3 is the mass of the recoil nucleus,

$$b=(M_3-M_1)/(M_2+M_3),\ c=M_3/(M_2+M_3),$$

and θ is the scattering angle in the laboratory system. In the present work it was found that the expected variation in track length for a change in θ of $\pm 0{\cdot}5°$ (*ca.* 0·5 mm traverse width) was equal to that expected for a traverse length of 5 mm, the sum of the two effects amounting to about $\pm 0{\cdot}25\,\mu$, or ± 2 divs. For some histograms, where large areas were needed, the variation of θ was about $\pm 1°$.

The width of the scattering gap introduces another factor limiting the resolution. A given point in the traverse is able to accept protons scattered from a finite length of the beam, owing to the width of the gap. For a distance of about 5·6 cm, a mean scattering angle of 120° and a gap width of 4 mm, the range of scattering angles accepted is 121·7°–118·2°. This will therefore introduce a further spread in the measured lengths of

up to ± 3 divs. The width of the traverse is too small to make a significant increase in this correction. On the other hand, there is a variation in the correction due to the stopping power of the gas, arising from the different points in the beam at which scattering can occur. For the above conditions, this amounts to a path difference of *ca.* ± 1 mm, and a corresponding correction due to stopping power and angle of dip of $\pm 0{\cdot}6$ divs.

An important limiting condition is the straggling in the range of the particle. This is about $\pm 2{\cdot}5\%$ for a 400 divs track and $\pm 10\%$ for a 100 divs track (Rotblat 1950). So we may take it as ± 10 divs. The maximum total spread resulting from the area of the scan is ± 2 divs, and from the gap width $\pm 3{\cdot}6$ divs. These give a total standard deviation of about ± 11 divs. Although the maximum error due to the selection of the first grain can amount to ± 10 divs, the average value is considered unlikely to exceed ± 3 divs. Thus it can be seen that the major contribution to the standard deviation is due to the straggling, which is inherent in nuclear emulsion techniques, and not due to the design of the camera or the errors in scanning.

Results

Range histograms of tracks measured at four different angles, 140°, 130°, 120° and 60° are shown in the figure. Measurements have also been made at 80° and 110° and they confirm the level scheme given by the other angles. The mean proton beam energy determined from the range of the elastically scattered particles was $9{\cdot}45 \pm 0{\cdot}01$ Mev. The range energy relation of Gibson *et al.* (1954) was used. The correction made for the loss of energy in the gas was based on the values of Brolley and Ribe (1955).

It can be seen that levels are present at 7·60 (at 60°), 7·40 (at 60°), 7·03, 6·46, 6·23, 5·83 and 5·69 Mev. There is also a possible level present at about 6·60 Mev which had been suspected previously (Prowse 1954). The uncertainties amount to $\pm 0{\cdot}02$ Mev except those on the 6·60 Mev level and the 5·83–5·69 Mev doublet where they are 0·04 and 0·03 Mev respectively. These errors are derived from the statistical uncertainties plus the error in the beam energy.

The calculated position of the 6·60 Mev level does not coincide with the experimental position at all angles ; indeed, it appears at a higher range at low angles and at a lower range at high angles. This would apparently indicate that the level belongs to a lighter nucleus than nitrogen, e.g. carbon (the exact excitation energy would then be slightly different). If this were the case it would have been due to a gaseous impurity in the gas used in the scattering camera. Ordinary commercial nitrogen was used of 99% purity. Possible contaminations are carbon dioxide and oxygen. An oxygen impurity would result in a group of elastically scattered particles which, although not resolvable from the ^{14}N group, would have the effect of increasing the apparent beam energy at high angles. No such effect was observed. Similarly a ^{12}C impurity would lower the apparent beam energy at high angles. No tracks were observed which would be consistent with the 4·4 Mev level of ^{12}C. The loss of energy in the gas was such

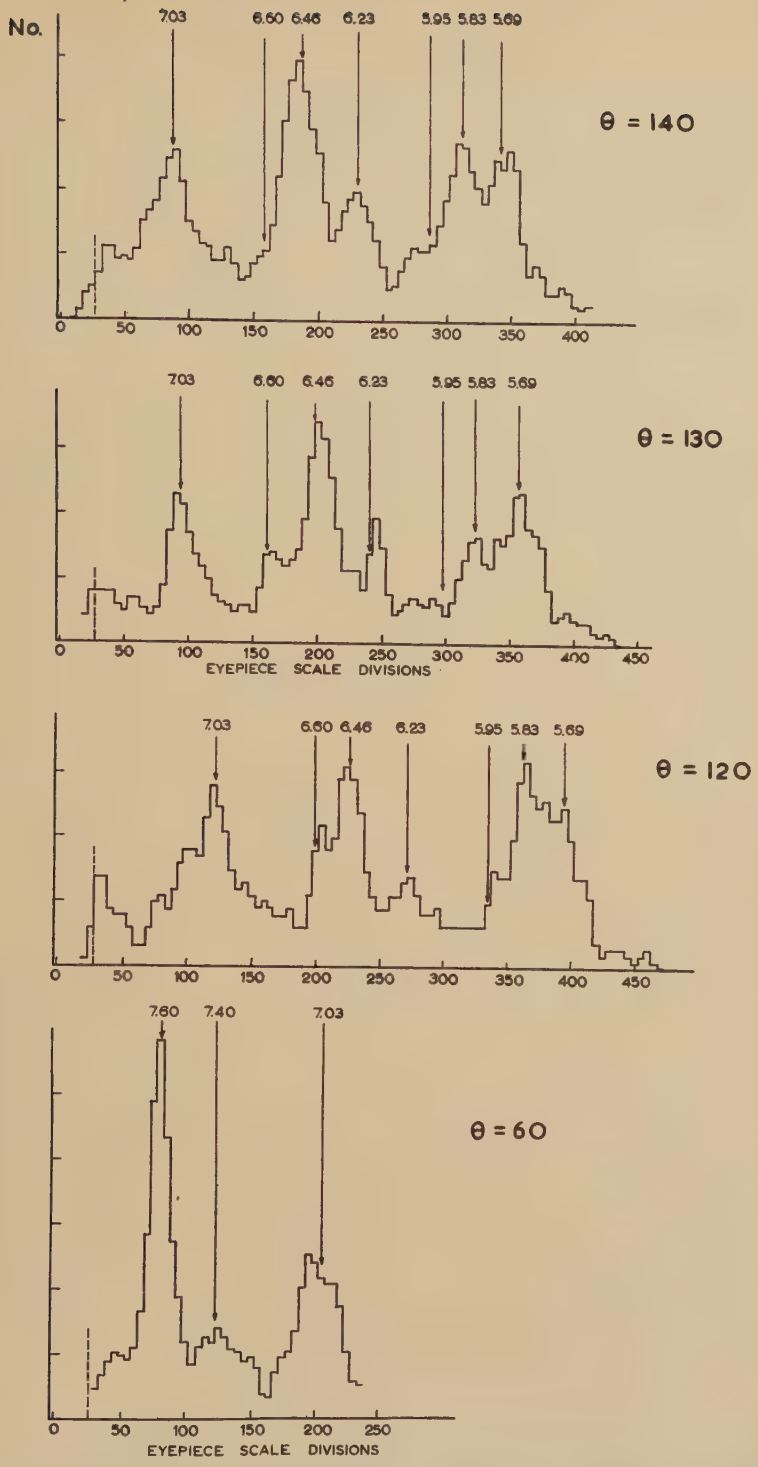

Range histograms of the tracks obtained at various angles. The excitation energies are the average values obtained from measurements at six different angles, except 7·60 (60° only) and 7·40 (60° and 80° only), and 5·95. The results have been smoothed by adding to the number of of tracks in a given 5 divs interval the average of the numbers in adjacent intervals. The scales on the ordinates are marked in multiples of 10 tracks.

that no tracks would have been expected from the 7·7 MeV level of ^{12}C which is known to participate in proton scattering (Hossain 1955). There remains, therefore, an anomaly which cannot be easily explained although it appears likely that an additional level at 6·60 MeV in ^{14}N would provide a solution. No such level has been previously reported from any other reaction.

A level at 5·98 MeV has been reported by Sperduto and Fader (1953) from the $^{16}O(d, \alpha)^{14}N$ reaction and also possibly by Benenson (1953) who obtained $6·1 \pm 0·1$ MeV from the $^{13}C(d,n)^{14}N$ reaction. It has not however given rise to a γ-ray in this or in the $^{13}C(p, \gamma)^{14}N$ reaction. In the figure the positions where it would be expected to appear have been marked and it can be seen that if it exists the cross section for proton scattering is low. The best values obtained for other levels compare well with those derived from γ-ray transition energies, quoted by Azjenberg and Lauritsen (1955), of $5·68 \pm 0·01$ and $5·83 \pm 0·02$ MeV. The 6·23 MeV level has been observed only in the $^{13}C(d,n)^{14}N$ reaction (Benenson 1953) and the error quoted was 0·05 MeV. The present results confirm this value and reduce the uncertainty. This level has also given rise to a $6·23 \pm 0·03$ MeV γ-ray. The same is true of the 6·44 MeV level which has been observed to lead to a 6·45 MeV γ-ray from $^{13}C(d,n)^{14}N$. The 7·03 MeV level has given a γ-ray of $7·05 \pm 0·04$ MeV although its excitation from neutron group measurements is $7·00 \pm 0·04$ MeV. Similarly the 7·40 MeV level has given a neutron group which results in an excitation energy of $7·50 \pm 0·04$ MeV but the γ-ray energy was $7·30 \pm 0·05$ MeV. The 7·60 MeV level has previously been reported at $7·72 \pm 0·04$ MeV, again from the (d,n) reaction, but γ-rays have not been observed. The levels of lower excitation, 5·10, 4·91, 3·95 and 2·31 MeV have all been observed in this experiment, the 4·91–5·10 MeV doublet being resolved at most angles despite the low cross section of the 4·91 MeV component. A figure of $3·0 \pm 1·0$ can be given for the ratio of the cross sections for scattering leading to these levels at this energy. No tracks were observed which could have resulted from a level at 3·15 MeV which has recently been reported by Quinton and Doyle (1956). In conclusion it may be stated that in resolving the levels at 5·69, 5·83, 6·23 and 6·46 MeV the limit of resolution has been reached for the scattering camera with the present aperture using photographic plates. (Similar resolution has been obtained by Burcham *et al.* (1953) using the same camera to investigate the doublets of ^{16}O.) Further investigations are proceeding to see whether, by slightly tilting the photographic plate in the microscope and thus rendering the proton tracks horizontal, better results might be obtained in judging which is the first grain of the track.

Acknowledgments

The authors wish to thank Professor C. F. Powell and Professor J. T. Randall, F.R.S. for their constant interest and encouragement; Professor J. Rotblat and Dr. W. M. Gibson for many informative discussions; and Professor W. E. Burcham, Dr. R. Freemantle, Dr. I. J. van Heerden and Mr. R. McKeague for their help with the exposures.

References

Azjenberg, F., and Lauritsen, T., 1955, *Rev. Mod. Phys.*, **27,** 77.
Benenson, R. E., 1953, *Phys. Rev.*, **90,** 420.
Brolley, J. E., and Ribe, F. L., 1955, *Phys. Rev.*, **98,** 1112.
Burcham, W. E., Gibson, W. M., Hossain, A., and Rotblat, J., 1953, *Phys. Rev.*, **92,** 1266.
Burrows, H. B., Powell, C. F., and Rotblat, J., 1951, *Proc. Roy. Soc.* A, **209,** 461.
Freemantle, R. G., Prowse, D. J., and Rotblat, J., 1954, *Phys. Rev.*, **96,** 1268.
Gibson, W. M., Prowse, D. J., and Rotblat, J., 1954, *Nature, Lond.*, **173,** 1180.
Hossain, A., 1955, *Thesis*, University of Bristol.
Prowse, D. J., 1954, *Thesis*, University of Bristol.
Quinton, A. R., and Doyle, W. T., 1956, *Phys. Rev.*, **101,** 669.
Rotblat, J., 1950, *Nature, Lond.*, **165,** 387.
Sperduto, A., and Fader, V. J., 1953, *M.I.T., Progress Report*, May.

XCIII. *The Heat Capacities of Chromium and Nickel*

By J. A. Rayne † and W. R. G. Kemp

Division of Physics, National Standards Laboratory, Commonwealth Scientific and Industrial Research Organization, Sydney ‡

[Received March 13, 1956]

Abstract

Heat capacity measurements have been made below 4·2°K on extremely pure specimens of chromium and nickel. In both cases the measurements give γ values lower than those obtained by former observers. The values of Debye temperature also differ significantly from those of previous work, it being found that $\theta=630$°K for chromium and $\theta=440$°K for nickel in contrast to the older figures of 418°K and 413°K respectively. These new results help to resolve the apparently anomalous nature of the θ versus T curves for the two metals. The influence of the magnetic heat capacity on the results for nickel is also discussed.

§ 1. Introduction

Measurements of the heat capacity of chromium have been made in the liquid helium region by Estermann *et al.* (1952) using a specimen of approximately 99·9% purity. Their data, when analysed in the usual way into a linear and cubic term, give a value for the Debye temperature of 418°K.§ As the results of Anderson (1937) on the heat capacity of chromium from 56 to 300°K show that the Debye temperature increases from approximately 450°K‖ at room temperature to 500°K‖ at 56°K the figure obtained by Estermann *et al.* implies that the curve of θ versus T has a maximum other than at $T=0$, contrary to theoretical expectations (Bhatia and Horton 1955). The present work on chromium was undertaken to investigate this anomalous behaviour and also, by using a specimen of high purity, to provide more accurate data concerning its electronic heat capacity, previous work (Rayne 1954) having shown that the γ value for transition metals is quite sensitive to small amounts of impurity.

† Now at Westinghouse Research Laboratories, East Pittsburgh, Pennsylvania, U.S.A.

‡ Communicated by the Authors.

§ After submitting this paper, the authors learnt of a more recent measurement of the low temperature heat capacity of chromium (Wolcott, N. M., 1955, Conference de Physique des Basses Temperatures, p. 286). His value of $\theta=585$°K is in good agreement with that found in the present work.

‖ These values of Debye temperature have been corrected for the electronic heat capacity of chromium and also for the difference between C_p and C_v.

Keesom and Clark (1935) have measured the heat capacity of nickel, of 99·8% purity, from 1 to 19°K. For temperatures below 9°K, they found that their data could be represented fairly well by $\theta=413$°K, this figure being derived from the room temperature elastic constants. Above 9°K their results, taken in conjunction with heat capacity data extending to higher temperatures (e.g. Busey and Giauque 1952), indicate that the Debye temperature rises to a maximum of 450°K at about 18°K and then falls to a constant value of 390°K at high temperatures (Clusius and Schachinger 1952). According to Bhatia a face-centred cubic metal can exhibit such a maximum at $T=0$ only if its elastic constants satisfy the condition

$$\sigma=\frac{C_{11}-C_{12}-C_{44}}{C_{44}}<-1\cdot39.$$

The low temperature elastic constants of nickel have not been measured, so that it is not known whether the above condition is satisfied or not. For copper, which is the element next to nickel in the periodic table and which also has a face-centred cubic structure, recent measurements (Gaffney and Overton 1954) give $\sigma=-1\cdot365$ in agreement with the fact that the θ versus T curve has a maximum at $T=0$. One might thus expect that nickel would behave in a similar fashion. The present work on nickel was undertaken to investigate this possibility and also to provide accurate data on the electronic heat capacity of pure nickel.

§ 2. Experimental Details

(*a*) *Apparatus*

The calorimeter employed in these experiments uses a mechanical heat switch, the possibility of extraneous effects arising from the use of exchange gas being thus avoided. Details of the apparatus are given in fig. 1.

Temperatures in the range 1·5–4·2°K are obtained by controlled pumping on liquid helium in the inner chamber A, which is filled from the main bath by means of the needle valve B. The working space below the inner chamber is normally evacuated but provision is made for admitting exchange gas to calibrate the resistance thermometer at the conclusion of a run.

Within the working space the specimen C is suspended by nylon threads from the disc D, which is thermally anchored to the bath by a copper strap E. Movement of the disc and specimen is effected by a stainless steel tube connected to a screw and bellows mechanism F at the top of the cryostat. By pressing the specimen against the flat bottom of the can, the sample may be brought to the inner bath temperature. Initial cooling from liquid nitrogen to liquid helium temperatures takes approximately 10 minutes.

The heater for the specimen is a 5000 ohm manganin resistance, which is wound on a copper former G screwed into the top of the specimen.

A 10 ohm Allen–Bradley carbon resistance, mounted in a copper sleeve H screwing into the side of the specimen, is used as a thermometer. Electrical connections to both the heater and thermometer are made with fine manganin wires, which are wound several times around the copper rod J to effect thermal contact with the inner bath and hence to reduce the heat leak to the specimen.

Fig. 1

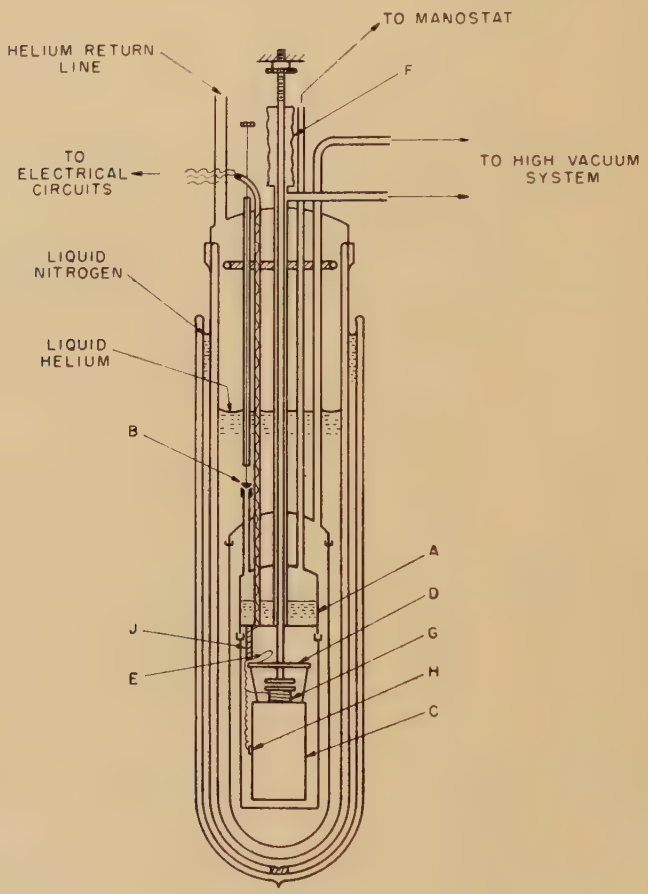

Details of Cryostat.

When the disc is raised so that the specimen is hanging freely, the only heat leak to the specimen arises from conduction down the thread and electrical connections, stray radiation and vibration. By keeping the temperature difference between the specimen and inner bath small, the stray input can be maintained below 100 ergs per minute. This enables the average random error in the individual heat capacity determinations to be reduced to about 1%.

The electrical and timing circuits are quite conventional and will not be described here.

(*b*) *Specimens*

A specimen of ductile chromium (Wain *et al.* 1954) of 99·998% purity was used in this work. The specimen was prepared by the Commonwealth Department of Supply in the form of a cylinder weighing 185·4 gramme. The nickel sample was a cylinder of mass 39·85 gramme, prepared by Johnson Matthey from spectrographically standardized sponge of 99·999% purity.

Fig. 2

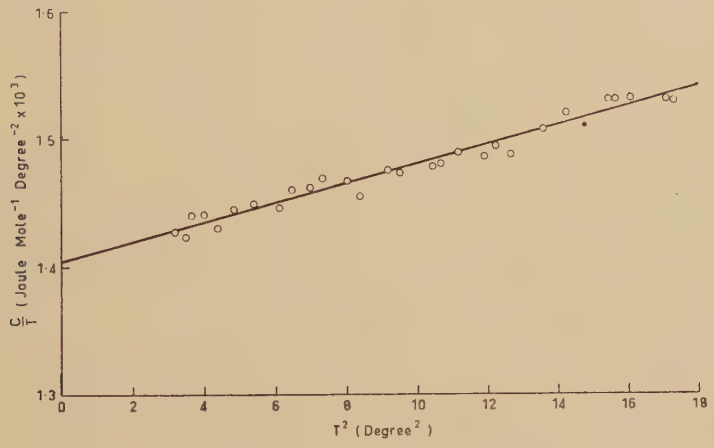

Atomic Heat of Chromium.

Fig. 3

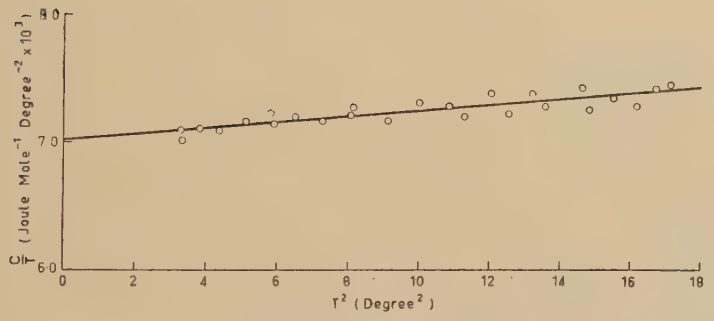

Atomic Heat of Nickel.

§ 3. Results

The experimental results, corrected for the heat capacity of the thermometer and heater and also for deviations from the 1948 temperature scale (Erickson and Roberts 1954), are presented in figs. 2 and 3 as plots of C/T versus T^2. For a normal metal this plot should give a straight line whose ordinate at $T=0$ is the value of γ for the metal and whose slope is

related to the Debye temperature by the relation

$$\beta = \frac{12}{5}\frac{\pi^4 R}{\theta^3} \quad . \quad . \quad . \quad . \quad . \quad . \quad . \quad . \quad . \quad . \quad (1)$$

R being the molar gas constant.

The straight lines shown are least squares fits to the points, the maximum deviation from the line being about 1·5%. The table gives the corresponding values of γ and θ together with the results of previous observers.

Observers	Chromium		Nickel	
	γ (Joule mole) (deg.$^{-2}\times 10^3$)	θ (°K)	γ (Joule Mole) (deg.$^{-2}\times 10^3$)	θ (°K)
Estermann *et al.*	1·59 ± 0·03†	418 ± 20 †		
Keesom and Clark			7·3 ± 0·2 †	413 ± 15 †
Present authors	1·40 ± 0·01 ‡	630 ± 30 ‡	7·02 ± 0·06 ‡	441 ± 15 ‡

† Errors (random only) estimated by present authors from plots of experimental data.

‡ Errors (random and systematic) estimated at a 90% confidence level.

§ 4. Discussion

The present work on chromium shows that its electronic heat capacity is very low for a transition metal. This result is in qualitative agreement with the data of Estermann *et al.*, who discuss the relation of the low γ value to possible theoretical forms for the band structure of chromium. Even if their work is corrected for errors in the 1948 temperature scale (Erickson and Roberts 1954), however, there is still a significant discrepancy between the two values of γ ; it is possible that this could be caused by impurity effects.

The new θ value for chromium is much higher than that previously obtained and gives a θ versus T curve of the form shown in fig. 4. As the data of Anderson only extends to 56°K the dotted portion of this graph is hypothetical, but it is clear that the new result is not inconsistent with a curve having a maximum at $T=0$. It is considered that the present θ value is the more reliable figure and that the previously implied anomaly in the θ versus T does not exist. No adequate explanation can be advanced for the discrepancy between the values of Debye temperature, as neither impurity effects nor errors in the 1948 temperature scale could materially alter the older value. Since the most recent measurements on copper (Corak *et al.* 1955) and on magnesium (Smith 1955) also give

similar disagreement with the results of Estermann *et al.*, it is possible that there were undetected errors in the latter's experiment.

Reference to the table shows that the agreement between the present γ value for nickel and that obtained by Keesom and Clark is within the combined limit of error. It is to be noted, however, that the present determination is considerably more accurate, particularly since the estimated uncertainty in the older work does not include systematic errors.

Fig. 4

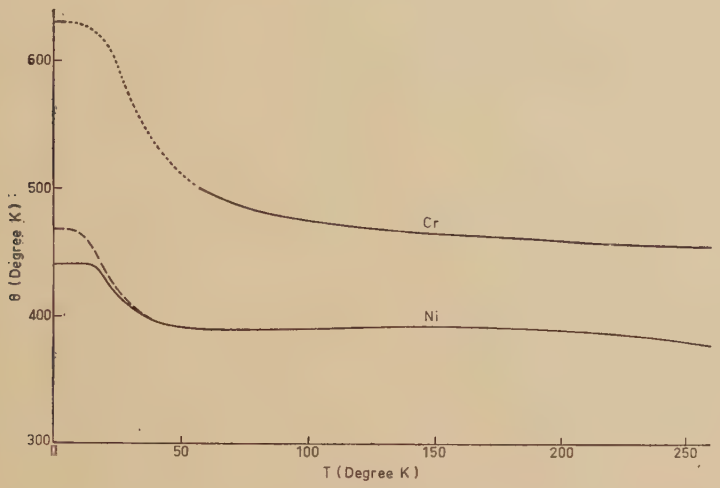

θ–T Curves for Chromium and Nickel.

Owing to its large electronic heat capacity, it is not possible to determine the value of Debye temperature for nickel with any great accuracy from measurements in the liquid helium region alone. To draw any conclusion from the present work regarding the θ versus T curve for nickel, it is necessary to make use of existing heat capacity data above 4·2°K. Unfortunately, most of these measurements have been made on specimens of high or unknown impurity content and hence cannot be related to the present results owing to the attendant uncertainty in the electronic heat capacity, which constitutes a large fraction of the total heat capacity at low temperatures. The only data on the heat capacity of high purity nickel above 4·2°K is that of Busey and Giauque but their work only extends to 13°K. The present values of γ and θ fit their low temperature results quite well, however, as may be seen from the fact that these parameters give a calculated value of heat capacity at 15°K of 0·183 joule mole^{-1} deg^{-2} as compared with Busey and Giauque's smoothed value of 0·180 joule mole^{-1} deg^{-2}. It is thus reasonable to conclude that the value of θ has a constant value of 440 ± 5°K up to 15°K. The resulting θ versus T curve then has the form shown in fig. 4, the anomalous maximum found by Keesom and Clark being no longer present. After correcting the latter's data for errors in the 1932 temperature scale (Keesom 1932) it

is still not possible to fit all their results with a single value of θ, so that the anomalous peak still remains. It is believed that this behaviour must be attributed to experimental error in their results.

Since nickel is ferromagnetic below 631°K, the heat capacity data include the contribution arising from the spontaneous magnetization. According to the Bloch spin wave theory, the heat capacity due to demagnetization for any cubic structure satisfies the equation (Mott and Jones 1936).

$$C=1{\cdot}18R\frac{\sigma_0-\sigma}{\sigma_0} \quad . \quad . \quad . \quad . \quad . \quad . \quad . \quad . \quad . \quad (2)$$

where σ is the magnetization at temperature T ($T \ll \theta$) and σ_0 is the saturation magnetization. The magnetization at low temperatures is given by the equation

$$\sigma=\sigma_0(1-AT^{3/2}) \quad . \quad . \quad . \quad . \quad . \quad . \quad . \quad . \quad . \quad (3)$$

the constant A for nickel being found experimentally to be $8{\cdot}9\times10^{-6}$ deg$^{-3/2}$ (Fallot 1936). Combining (2) and (3), the heat capacity of nickel due to demagnetization is found to be

$$C=8{\cdot}8\times10^{-5}\,T^{3/2} \text{ joule mole}^{-1} \text{ deg}^{-1}$$

so that the contribution to the total heat capacity is about 2% at 2°K, rising to 3% at 4°K. The accuracy of the present experiment is insufficient to distinguish this effect from slight alterations in the values of γ and θ. If these parameters are corrected for magnetization effects it is found that

$$\gamma=7{\cdot}05\times10^{-3} \text{ joule mole}^{-1} \text{ deg}^{-2}$$

$$\theta=468°\text{K}$$

giving a θ versus T relationship at low temperatures, which has the form shown by the dotted curve in fig. 4. While these corrected values are uncertain to a considerable extent because of doubt concerning the applicability of (2) to a real ferromagnet, it seems likely that the trend of the correction is as indicated, i.e. such as to make the θ versus T curve have a more pronounced maximum at $T=0$.

§ 5. Conclusions

Improved data for the heat capacity of chromium and nickel at liquid helium temperatures have been obtained by measurements on very high purity samples in a calorimeter employing a mechanical heat switch instead of exchange gas. The new results differ appreciably from those of previous observers and remove apparent anomalies in the θ versus T curves for the two metals.

Acknowledgments

The authors would like to express their appreciation to Mr. J. W. Smyth for the preparation of the liquid helium used in these experiments. Thanks are also due to Mr. J. Nish of the Defence Standards Laboratories, Commonwealth Department of Supply for providing the specimen of ductile chromium.

References

Anderson, C. T., 1937, *J. Amer. Chem. Soc.*, **59,** 488.
Bhatia, A. B., and Horton, G. K., 1955, *Phys. Rev.*, **98,** 1715.
Bloch, F., 1930, *Z. Phys.*, **61,** 1930.
Busey, R. H., and Giauque, W. F., 1952, *J. Amer. Chem. Soc.*, **74,** 3157.
Clusius, K., and Schachinger, L., 1952, *Z. Naturforsch.*, **7a,** 185.
Corak, William S., Garfunkel, M. P., Satterthwaite, C. B., and Wexler, Aaron, 1955, *Phys. Rev.*, **98,** 1699.
Erickson, R. A., and Roberts, L. D., 1954, *Phys. Rev.*, **93,** 957.
Estermann, I., Friedberg, S. A., and Goldman, J. E., 1952, *Phys. Rev.*, **87,** 582.
Fallot, M., 1936, *Ann. Phys.*, **6,** 305.
Gaffney, J., and Overton, W. C., 1954, *Phys. Rev.*, **95,** 602.
Keesom, W. H., and Clark, C. W., 1935, *Physica*, **2,** 513.
Mott, N. F., and Jones, H., 1936, *The Theory of the Properties of Metals and alloys* (London : Oxford University Press).
Rayne, J., 1954, *Phys. Rev.*, **95,** 1428.
Smith, P. L., 1955, *Phil. Mag.*, **46,** 744.
Wain, H. L., Henderson, F., and Johnstone, S. T. M., 1954–1955, *J. Inst. Metals*, **83,** 133.

XCIV. *The Drude Dispersion Formula shown to be Applicable to any Medium irrespective of the Polarization Field*

By Sir K. S. Krishnan, F.R.S., and S. K. Roy
National Physical Laboratory of India, New Delhi†

[Received April 10, 1956]

Abstract

It is shown that the well known dispersion formula of Drude is applicable to a dense medium even when the polarization fields associated with the different types of oscillators may all be different. The parameters involved in the formula are naturally the frequencies and the oscillator strengths of the oscillators in the medium, both of them as influenced by the mutual interactions between the oscillators, i.e. as influenced by the polarization fields. The observed data on dispersion will enable us to determine these parameters. In the Lorentz type of dispersion formula, on the other hand, the frequencies and the oscillator strengths involved are those of the *isolated* oscillators, which naturally are independent of the polarization field, and hence the effect of the polarization field on dispersion has to be taken into account explicitly. Because of this, the Lorentz type of formula needs for its formulation explicit information regarding the polarization field, which cannot be supplied by the observed dispersion data alone. The reduction of the Drude formula to one of the Lorentz type, and the appropriate information regarding the polarization field that is needed for this purpose, are also discussed in the paper.

§ 1. The Dispersion Formulae of Drude and of Lorentz

The well known dispersion formula of Lorentz for a dense medium is

$$\frac{K_\omega-1}{K_\omega+2}=\frac{4\pi}{3}\sum_{i=1}^{n}\frac{N_iF_ie_i^2}{\mu_i(\Omega_i^2-\omega^2)}=\frac{4\pi}{3}\sum_{i=1}^{n}\frac{A_i}{(\Omega_i^2-\omega^2)}, \text{ say} \quad . \quad . \quad (1)$$

where K_ω is the dielectric constant of the medium for frequency ω, N_i is the number per unit volume, F_i the oscillator strength, and μ_i the reduced mass, of oscillators of frequency Ω_i. This formula is derived on the basis that the actual field acting on an oscillator in the medium is not merely the field in the medium but includes in addition the polarization field, which is further taken to be $4\pi/3$ times the polarization per unit

† Communicated by the Authors.

volume. This introduces in the expression for $K_\omega - 1$ a multiplying factor $[1+(4\pi/3)\chi_\omega]=(K_\omega+2)/3$, where χ_ω is the polarization of the medium per unit volume per unit field in the medium.

On the other hand the Drude formula, namely

$$K_\omega - 1 = 4\pi \sum_{i=1}^{n} \frac{N_i f_i e_i^2}{\mu_i(\omega_i^2 - \omega^2)} = 4\pi \sum_{i=1}^{n} \frac{a_i}{\omega_i^2 - \omega^2}, \text{ say, } \ldots \quad (2)$$

which had been derived much earlier, did not naturally contemplate the presence of a polarization field. Hence the Drude formula is generally regarded as a special case of the Lorentz formula, applicable to media in which the polarization field is known to be zero.

For convenience in discussion we shall refer to the quantities A_i and a_i briefly as the oscillator strengths of the oscillators concerned in the two formulae, though actually they refer to N_i oscillators.

Many years ago Herzfeld and Wolf (1925) showed, however, that formula (1) *can always be reduced algebraically to* (2), the ω_i's and a_i's appearing in (2) being calculable functions of Ω_i's and A_i's. They derived (2) from (1) in the simple case when the number of frequencies involved in the formula is just two, but as they themselves pointed out, the reduction of (1) to (2) can be done also in the general case when the frequencies are more than two.

Further since the number of parameters involved in the two formulae is the same, it should be possible conversely to reduce (2) to (1), though the actual reduction, as we shall see later in the present paper, is not quite so simple as the reduction of (1) to (2).

From these considerations it follows that if the experimental data for the dispersion of any substance can be fitted with one of these formulae, they can be fitted equally well with the other formula too. The characteristic frequencies appearing in the two formulae will naturally be very different. From this circumstance it has been concluded by some of the later workers that by comparing the frequencies occurring in the two formulae with the observed frequencies of the medium it should be possible to decide between the two formulae : in other words to decide whether there is a polarization field of magnitude $4\pi/3$ times the polarization per unit volume, as contemplated in the derivation of the Lorentz formula, or it is zero as is taken to be implied by the Drude formula.

§ 2. The Dispersion Data can give no Information regarding the Polarization Field

In some earlier papers (Krishnan and Roy 1952, 1953) we have shown that such an appeal to observation, namely to find which set of frequencies deduced from the observed dispersion agrees with the observed resonance frequencies, whether it is the Ω_i's or the ω_i's, will not enable us to decide

on the existence or otherwise of a polarization field in the medium, and much less to determine its magnitude. Irrespective of whether a polarization field occurs or not, and irrespective of its magnitude when it occurs, the Drude formula (2) will always express correctly the observed dispersion, and the frequencies appearing in this formula will be the actual resonance frequencies of the medium. Since (2) can always be reduced algebraically to (1), again irrespective of the presence or not of an actual polarization field, the observed validity of (1) has by itself no physical significance, *unless the magnitude of the polarization field can be verified independently, or the frequencies Ω_i, whose significance will be stated presently, are known from other considerations.*

This arises from the following circumstance. The effect of the polarization field, whatever may be its magnitude, on the dielectric constant, can be taken into account in two alternative ways, which are mathematically equivalent, and which lead to the Lorentz and the Drude formulae respectively :

(1) The frequencies and the oscillator strengths may be taken to be those of the oscillators when isolated from one another, namely Ω_i and A_i respectively, and the effect of the polarization field on the dielectric constant is then taken into account explicitly.

(2) Alternatively, one may use the frequencies and the oscillator strengths, of the oscillators as influenced by the mutual interactions of the oscillators, i.e. as influenced by the polarization field, namely ω_i and a_i, in which case the whole effect of the polarization field on the dielectric constant is taken into account automatically.

The difference between the two approaches lies in this : whereas ω_i and a_i can be obtained directly from the dispersion data, Ω_i and A_i cannot be.

§ 3. Scope of the Present Paper

It was also emphasized in these papers that the polarization fields associated with the different types of oscillators present in the medium, as for example the electronic and the reststrahlen oscillators in the alkali halide crystals, may be widely different. It was further mentioned, without a statement of the proof, that the Drude formula (2) will hold even in the most general case when the polarization field acting on an oscillator of type i due to all the oscillators of type j in the medium is p_{ij} times χ_j, where χ_j is the contribution from oscillators of type j to the polarization per unit volume per unit field in the medium, and the p_{ij}'s *may all be different.* Since this result is of some importance, and the proof is not obvious, the proof is given in the present paper.

The conditions under which the Drude formula, which is generally applicable to any medium, can be reduced to one of the Lorentz type are also discussed in this paper.

§ 4. The Basic Expression for Refractivity and its Reduction to the Drude Formula

When the different p_{ij}'s, which we may refer to as the polarization field factors, may be different, the basic expression for the dielectric constant of the medium takes the form

$$K_\omega - 1 = 4\pi\chi = 4\pi \sum_{i=1}^{n} \chi_i, \qquad \ldots\ldots (3)$$

where

$$\chi_i = \frac{N_i F_i e_i^2}{\mu_i(\Omega_i^2 - \omega^2)} \left(1 + \sum_{j=1}^{n} p_{ij}\chi_j\right) \qquad \ldots\ldots (4)$$

Obviously the χ's, like K, would be functions of the incident frequency ω, but for convenience in writing, we have dropped the subscripts ω except in the case of K.

We now proceed to demonstrate that the basic eqns. (3) and (4) can be reduced to formula (2) of Drude.

Using the n equations similar to (4), and using also (3), one can eliminate all the χ_i's and obtain therefrom

$$\begin{vmatrix} -\chi & 1 & 1 & \ldots & \ldots & 1 \\ 1 & p_{11} - \frac{1}{b_1} & p_{12} & \ldots & \ldots & p_{1n} \\ 1 & p_{21} & p_{22} - \frac{1}{b_2} & \ldots & \ldots & p_{2n} \\ \ldots & \ldots & \ldots & \ldots & \ldots & \ldots \\ \ldots & \ldots & \ldots & \ldots & \ldots & \ldots \\ 1 & p_{n1} & p_{n2} & \ldots & \ldots & p_{nn} - \frac{1}{b_n} \end{vmatrix} = 0, \qquad \ldots (5)$$

where

$$b_i = \frac{N_i F_i e_i^2}{\mu_i(\Omega_i^2 - \omega^2)} = \frac{A_i}{\Omega_i^2 - \omega^2} \qquad \ldots\ldots (6)$$

Let

$$\Delta = \begin{vmatrix} p_{11} - \frac{1}{b_1} & p_{12} & \ldots & \ldots & p_{1n} \\ p_{21} & p_{22} - \frac{1}{b_2} & \ldots & \ldots & p_{2n} \\ \ldots & \ldots & \ldots & \ldots & \ldots \\ \ldots & \ldots & \ldots & \ldots & \ldots \\ p_{n1} & p_{n2} & \ldots & \ldots & p_{nn} - \frac{1}{b_n} \end{vmatrix} \qquad \ldots (7)$$

which is a polynomial of degree n in ω^2, which cannot be zero for all values of ω^2.

Now let P_{ij} be the co-factor of the ijth element in the determinant Δ. One then obtains from (5)

$$\chi = -\sum_{i,j=1}^{n} P_{ij}/\Delta. \quad \ldots\ldots\ldots \quad (8)$$

In (8) the P_{ij}'s are polynomials of degree $n-1$ in ω^2, whereas Δ is of degree n in ω^2. Hence the right-hand side of (8) can be expanded into partial fractions, thus leading to the expression

$$K_\infty - 1 = 4\pi\chi = 4\pi \sum_{i=1}^{n} \frac{a_i}{\omega_i^2 - \omega^2}, \quad \ldots\ldots \quad (9)$$

where $\omega_1^2, \omega_2^2, \ldots \omega_n^2$ are the n roots of the equation $\Delta(\omega^2)=0$. ω_i and a_i will be functions of the Ω's, the A's and the p's, and will be independent of ω.

Equation (9) can be immediately recognized as the Drude formula.

§ 5. The Dispersion Data in Relation to the Polarization Field

This derivation emphasizes the basic nature of the Drude formula for dispersion. Far from being a special case of the Lorentz formula for zero polarization field, it is physically a more significant formula than Lorentz's, even when there is a polarization field, which may be large and complicated. Just as for the isolated oscilators, their optical behaviour is determined uniquely by their characteristic frequencies Ω_i and their oscillator strengths A_i, so also the optical behaviour of a dense assemblage of such oscillators is determined by the corresponding quantities ω_i and a_i characteristic of the medium. The parameters involving explicitly the polarization fields get eliminated.

For the same reason the dispersion data by themselves cannot give any information regarding the polarization field. If the medium has n characteristic frequencies, the observed dispersion data, which obviously should fit into (9), can supply $2n$ parameters, namely the ω_i's and the a_i's which would be just sufficient to determine the frequencies Ω_i and the oscillator strengths A_i of the n oscillators, *when all the* p_{ij}*'s are known*.

Now if the p_{ij}'s were all different their number would be n^2, in which case, the p's would be too numerous to be calculated from the $2n$ parameters available from the dispersion data, even if all the Ω_i's and the A_i's were known; except in the trivial case when $n=1$. But actually the p_{ij}'s are not quite so many, since in general p_{ij} should be equal to p_{ji}, in which case the number of different p_{ij}'s reduces to $\frac{1}{2}n(n+1)$. If the Ω_i's and the A_i's are known, then all the p_{ij}'s should be determinable from the dispersion data when $n \leqslant 3$. With $n=3$ or even with $n=2$, it would be possible in practice to describe satisfactorily the dispersion over a fairly wide region of the spectrum.

The result obtained just now may be of even deeper practical interest. Till now we have been concerning ourselves with the dispersion formula alone, i.e. the expression for K as *a function of the frequency* ω, which

enables us directly to determine only the parameters ω_i and a_i, and in which the polarization fields do not appear explicitly. On the other hand the expression for K as *a function of the density of the medium* would involve the polarization field explicitly. In particular, for molecular substances like benzene, naphthalene and other organic compounds, in which the molecules retain their individuality in the condensed state, one can obtain the Ω_i's and the A_i's from the dispersion in the vapour state, in which the polarization fields are negligible, and the corresponding ω_i's and a_i's in the condensed phase from the dispersion data for this phase. A comparison of the two sets, referring respectively to the two phases, should enable us to determine all the p_{ij}'s, provided we choose a spectral region in which 3 frequencies would be adequate to represent correctly the dispersion data.

On the other hand the variation of dispersion with density, in the condensed phase, which may be secured by varying the temperature, would not be so helpful, since the p's also are functions of the density.

§ 6. Reduction of the Basic Formula to One of the Lorentz Type

Having shown that the basic formulae of dispersion, namely (3) and (4), do reduce to Drude's even when the p_{ij}'s are all different, we may proceed to enquire whether in this general case, (3) and (4) can also be reduced to one of the Lorentz type, by which we mean a formula of the type

$$\phi(K)=4\pi\sum_{i=1}^{n}\frac{A_i}{\Omega_i^2-\omega^2}, \qquad \ldots\ldots \quad (10)$$

in which the Ω_i's and the A_i's refer to the *isolated* oscillators, and have the same significance as in (1). The answer is that this can not be done in the general case when the p_{ij}'s are all different.

The problem is really one of finding an expression for K, i.e. for χ, which will not involve the component polarizabilities χ_i separately. One obvious method of doing this is to eliminate the χ_i's between (3) and (4), and this procedure, as we have seen, yields the Drude formula, which involves the characteristic frequencies ω_i of the medium, and not the frequencies Ω_i of the isolated oscillators, which we now wish to retain. On a closer examination of (4) and (3) one can see that the separate χ_i's can be eliminated, without at the same time eliminating the Ω_i's also, only when the p_{ij}'s have all the same value, say p.

When this is the case, the explicit expression for $\phi(K)$ appearing in (10) becomes

$$\frac{\chi}{1+p\chi}=\sum_{i=1}^{n}\frac{A_i}{\Omega_i^2-\omega^2} \qquad \ldots\ldots \quad (11)$$

or

$$\frac{K-1}{K+\alpha}=p\sum_{i=1}^{n}\frac{A_i}{\Omega_i^2-\omega^2} \qquad \ldots\ldots \quad (12)$$

where $\alpha=4\pi/p-1$,

§ 7. Reduction of the Drude Formula to one of the Lorentz Type

We have shown that the basic formulae of dispersion, namely (3) and (4), can be reduced to the Drude formula (9) even when the p_{ij}'s are all different, and that in the special case when they have all the same value p, (3) and (4) reduce to (12) also. Hence it follows when all the p_{ij}'s have the same value, it should be possible directly to reduce (9) to (12), i.e. to obtain the constants Ω_i and A_i in terms of ω_i and a_i when $\alpha=4\pi/p-1$ is known. The reduction is done in the following manner.

Starting with (10), and remembering that $\alpha=4\pi/p-1$, one obtains immediately

$$\frac{K-1}{K+\alpha}=\left(p\sum_{i=1}^{n}\frac{a_i}{\omega_i^2-\omega^2}\right)\Big/\left(1+p\sum_{i=1}^{n}\frac{a_i}{\omega_i^2-\omega^2}\right)$$

$$=\frac{p\sum_{i=1}^{n}a_i\prod_{\substack{j=1\\j\neq i}}^{n}(\omega_j^2-\omega^2)}{\prod_{i=1}^{n}(\omega_i^2-\omega^2)+p\sum_{i=1}^{n}a_i\prod_{\substack{j=1\\j\neq i}}^{n}(\omega_j^2-\omega^2)} \quad . \quad . \quad . \quad . \quad (13)$$

Now knowing ω_i and a_i and knowing further that every p_{ij} has the same value $p=4\pi/(\alpha+1)$, we may put the denominator on the right-hand side of (13)$=0$, and treating it as an equation in ω^2, obtain the n roots of the equation, namely M_1^2, M_2^2, ... M_n^2, and thence obtain

$$\frac{K-1}{K+\alpha}=\frac{p\sum_{i=1}^{n}a_i\prod_{\substack{j=1\\j\neq i}}^{n}(\omega_j^2-\omega^2)}{\prod_{i=1}^{n}(M_i^2-\omega^2)} \quad . \quad . \quad . \quad . \quad . \quad . \quad (14)$$

Since the M_i's are now known, the numerator on the right hand side can be put equal to $p\sum_i C_i\prod_{\substack{j=1\\j\neq i}}^{n}(M_j^2-\omega^2)$ where the C_i's can be readily obtained. We thus obtain

$$\frac{K-1}{K+\alpha}=p\sum_{i=1}^{n}\frac{C_i}{M_i^2-\omega^2}, \quad . \quad . \quad . \quad . \quad . \quad . \quad (15)$$

in which the C_i's are obviously independent of ω.

Comparing (15) with (12) one can immediately see that if the basic assumption that every p_{ij} has the same value, namely p, is correct, then every M_i and C_i appearing in (15) should be identical with every Ω_i and A_i respectively.

But the important point to emphasize is that the values of M_i and C_i thus obtained will represent correctly the frequencies and the oscillator strengths of the isolated oscillators only to the extent to which our knowledge of the polarization field is dependable. Since the dispersion data themselves do not supply any information regarding the polarization

field, one may choose any arbitrary α, and find the corresponding M_i and C_i which will make (15) algebraically identical with (9). Since the Drude formula (9) represents correctly the observed dispersion, (15) too, with the appropriate choice of the M_i's and C_i's corresponding to our choice of α, will represent equally well the observed dispersion, and this will be so irrespective of the actual values of the different p_{ij}'s ; but then the M_i's and C_i's that appear in the formula will not be the actual Ω_i's and the A_i's of the isolated oscillators.

References

Herzfeld, F. F., and Wolf, K. L., 1925, *Ann. d. Physik*, **78**, 35.
Krishnan, K. S., and Roy, S. K., 1952, *Phil. Mag.*, **43**, 1000 ; 1953, *Ibid.*, **44**, 19.

XCV. *Some Observations on the Solid State of Argon*

By D. Stansfield†
H. H. Wills Physical Laboratory, University of Bristol‡

[Received April 25, 1956]

Summary

A polycrystalline specimen of solid argon has been grown using a modification of Bridgman's method ; grains of up to 4 mm diameter have been produced. A technique was used to etch the specimen thermally, and the results are described in this paper.

In order to conduct experiments on the plastic properties of solid argon, some preparatory observations on the solidification of argon have been made. Polycrystalline specimens with a grain size of about 4 mm have been obtained by solidification from the melt, and thermally etched superficial markings observed.

The purity of the gas used in these experiments was quoted by the suppliers as 99·93%, the main impurity being nitrogen. Initial experiments were made by reducing the temperature of a bulb containing about 1 ml of liquid argon to just below its triple point (83·8°K). It was seen that argon formed ' vapour snakes ' of the kind observed in several compounds by Verschingel and Schiff (1954). The conditions given by them as necessary for vapour snake formation (viz. high triple point pressure, and a high value for the ratio between the latent heats of evaporation and fusion) are satisfied by argon, for which the triple point pressure is 516 mm of mercury, and the latent heats of evaporation and fusion are 1557 and 280 cals/g mole respectively (Guggenheim 1945). No special care was necessary for the snakes to form, the temperature of the walls above the argon surface not being higher than that of the lower walls. When only the lower part of a glass tube having two bulbs joined by a narrow vertical neck was cooled, the argon froze inwards from the walls until the neck was completely blocked by the solid. The contraction resulting from further cooling then caused vapour snakes to grow in the lower bulb ; a free solid-vapour interface is therefore not necessary for their formation.

Transparent polycrystalline specimens were obtained by progressive freezing from the melt, as in Bridgman's method. The argon tube was slowly lowered into liquid oxygen at about 70°K, and a stream of argon gas into the tube was maintained so that the solid grew at the rate of about

---

† Communicated by the Author.

‡ Now at H.M. Underwater Detection Establishment, Portland, Dorset.

1 mm/minute. The solid was covered by a thin layer of liquid, the top of which was heated by condensation of the gas, so that the temperature gradient in the liquid was about 5 deg/mm. This method of growth resulted in the production of polycrystalline specimens having mean grain diameters of about 4 mm, the diameter also of the central part of the argon tube. Faster rates of growth caused smaller grain sizes, but subsequent spontaneous grain growth produced specimens similar to those resulting from slower rates.

It was found that the solid argon could readily be freed from the glass walls of the surrounding tube by immersing the tube in unstirred liquid oxygen at constant temperature, with the oxygen level above that of the argon. Sublimation of the solid next to the walls then took place, vapour condensing on the cooler parts of the walls near the oxygen surface, and the solid argon specimen becoming detached progressively, from the top downwards, from the containing walls. The freshly exposed solid-vapour surfaces rapidly showed thermally etched markings, which were visible when viewed by transmitted light, using a narrow aperture at the objective of the viewing microscope.

The later specimens were grown in tubes having a narrow neck of rectangular (6 mm $\times$ 2 mm) cross section between bulbous ends, and the lower tail of the enclosing dewar vessel was of square section. By this arrangement the astigmatic effects of cylindrical walls were eliminated, and the argon surface could be studied more easily. The plate shows two photographs of typical solid argon surfaces. It should be noted that etched markings on both front and back surfaces are visible, particularly in fig. 1 (Plate).

The observations of Chalmers *et al.* (1948) on the thermal etching of silver suggest that the strong markings to be seen in the photographs are due to grain boundary grooves. That this is true in this case is supported by the observation of lines traversing the surface between the stronger markings, as in fig. 2 (Plate). These indicate that the strong lines enclose regions having a unique crystallographic axis, and we may there-therefore assume that these markings are in fact due to grain boundary grooves. Moreover, the fact that the grain boundaries do not show many kinks indicates that most of them are visible, as junctions with other grain boundaries usually cause sharp angles. This deduction is confirmed by the observation that the lighter surface markings in general terminate only at the visible grain boundaries.

Grain boundary grooves are due to the excess free energy resulting from local atomic disorder, which gives rise to forces analogous to surface tensions (see Chalmers *et al.* 1948). The shape of any groove thus depends on the relative free energies of the grain surfaces in contact with each other and with the adjoining atmosphere. A few boundaries may be seen to terminate at no other visible boundary, and fig. 2 shows surface striations bounded on one side by a line (AA) which is not itself visible. These observations indicate that the grains may in some cases

be twinned, the grooves formed at twin boundaries being shallower (and therefore not so clearly visible) because of the low free energy of the twin boundary.

Chalmers *et al.* observed the formation on silver of striations on the surfaces of the grains themselves, and showed that they were oriented along simple crystallographic planes. Such markings are due to the decrease in surface free energy sometimes made possible by the formation of steps, the faces of which are simple crystallographic planes. Similar striations are visible on argon surfaces, as shown particularly in fig. 2, but it may be noted that the lines are not quite straight. Figure 2 shows part of the surface of a specimen which had not been strained by application of an external load, but may have been subjected to considerable strains due to temperature changes in the specimen. These markings are not however slip lines, since they do not appear until the argon surface has been free for about twenty minutes.

The conditions necessary for the visual observation of the surface markings should be noted, as they give some indication of the scale of the etching. Light from the illuminating source is deflected by the curved sides of the surface grooves, so that some rays which would have entered the microscope aperture are prevented from doing so. The grooves therefore show as dark lines on a bright background, the contrast being improved by using a narrow slit source and a narrow aperture. The geometrical conditions necessary for surface steps to be visible are much less likely to be satisfied, the sides of the steps being plane. It is not surprising, therefore, that surface striations are visible on only a small number of grains. Further, for appreciable deflections to be caused, the grooves or steps must be at least one wavelength of light deep.

It is not probable that the abrupt termination of some grain boundary marks is caused by non-satisfaction of the necessary geometrical conditions, as such an explanation involves pairs of conjoining grain boundaries being invisible, or else sharp kinks in some boundaries. If a grain is twinned, however, the grain boundary groove at the edge of one twin may be visible whilst its continuation at the edge of the other twin is too shallow to be seen. In a few cases, surface striations have indicated twinning in a region with edges marked by faint parallel straight lines extending across a grain.

Preliminary observations of the properties of solid argon under applied stresses have also been made. The ultimate tensile strength at 75°K was found to be about 50 g/mm^2, and, rather surprisingly, the final fracture diameter after necking was seen to increase with rise of temperature. The motion of grain boundaries during straining and subsequent annealing and recrystallization has also been observed (Domb 1955).

This note is presented to indicate that specimens of solid argon having a grain size of several millimetres may readily be grown from the melt, and their surface etched to give information about their structure and about the behaviour of grain boundaries under internal or external stresses.

The thickness of the specimens grown in these experiments was only two millimetres, and Beck (1954) has reviewed evidence that the largest grain size obtained by spontaneous grain growth is limited by the smallest dimension of the specimen. However, later work has suggested that impurities are probably the most important factor determining the maximum grain sizes obtained in these experiments. There would appear to be no fundamental difficulties in the growth of single crystals of argon.

Acknowledgment

This work was supported by the Department of Scientific and Industrial Research by the award of a Maintenance Grant.

References

Beck, P. A., 1954, *Advanc. in Phys.*, **3**, 245.
Chalmers, B., King, R., and Shuttleworth, R., 1948, *Proc. Roy. Soc.* A, **193**, 465.
Domb, C., 1955, *Nature, Lond.*, **175**, 661.
Guggenheim, E. A., 1945, *J. Chem. Phys.*, **13**, 253.
Verschingel, R., and Schiff, H. I., 1954, *J. Chem. Phys.*, **22**, 723.

XCVI. *Density Changes in Neutron Irradiated Quartz*

By P. G. Klemens
Division of Physics, Commonwealth Scientific and Industrial Research Organization, Sydney †

[Received April 17, 1956]

Wittels (1953) and Wittels and Sherrill (1954) measured the density changes produced in quartz by fast neutron irradiation in a pile. The density was found to decrease with increasing dose, and the density change attained a saturation value of about 15% for doses in excess of 2×10^{20} neutrons/cm^2. However, the rate of density change did not decrease steadily, but increased at first (beyond cumulative doses of 7×10^{19}), reached a value of about two to three times the initial value at a cumulative dose of 10×10^{19}, and decreased only at higher doses—see also Kinchin and Pease (1955). To explain this increase in the rate of density change Primak (1955) suggested that the disorder is due to thermal spikes—regions whose temperature had been temporarily increased by the energy from the slowing down of a fast particle—and that these regions would retain their thermal energy longer in the partly disordered crystal because of the reduction in the thermal conductivity known to be associated with such disordering (Berman *et al.* 1950, Berman 1951). Primak considered that this would enhance the density change produced by each new thermal spike.

Primak's explanation does not seem tenable when it is considered that the thermal conductivity of unirradiated quartz at the temperatures within the pile would be only two or three times the thermal conductivity after an irradiation of 7×10^{19}, and that in any case a less rapid quenching of the temperature of a spike due to a decrease in the thermal conductivity would be expected to give rise to less, rather than more, disorder frozen into the spike.

A different explanation of this increase in the rate of density change will be given here, based on the formation of disordered regions within the crystal, which are under compression until the number of such regions is sufficiently large that the stresses in the crystal are relieved by plastic flow.

From the changes in the low temperature thermal conductivity on irradiation it can be concluded (Klemens 1951) that the imperfections responsible for the additional thermal resistance above liquid hydrogen temperatures are isolated imperfections of atomic dimensions, whereas

---

† Communicated by the Author.

the additional resistance at lower temperatures is due to imperfect regions of larger size, though fewer in number. This picture is consistent with the theory of radiation damage (Seitz 1949). An atom, knocked out by a fast neutron, causes further displacements while being slowed down and stopped. In the initial part of the slowing-down process, the displacements are well separated spatially, but a substantial part of the energy is lost at the end of the range, where many displacements are concentrated in a small region.

With increasing neutron dose the thermal conductivity curve approaches in character the curve for fused silica (Berman 1951), which suggests that within one of these larger disordered regions the material is of vitreous structure, as is reasonable from the glass-forming tendency of quartz.

A similar picture of the vitrification of a region within the crystal by the slowing down of a particle was proposed by Primak (1954), who suggested that the substances which can be vitrified by fusion can also be vitrified by irradiation. Quartz is indeed turned into an amorphous state† by heavy irradiation (Wittels and Sherrill 1954, Primak 1955).

The vitreous material formed by heavy irradiation is about 15% less dense than crystalline quartz. If a small vitreous inclusion is formed inside the crystal, it will be unable to expand completely (i.e. 15%), because of the constriction of the surrounding crystalline material. Thus the vitreous material will be in a state of compression, while the surrounding material will be displaced outwards, being sheared without dilatation. The resulting volume increase of the crystal can be calculated in terms of the elastic constants of both materials : for reasonable values of their Poisson ratios, and if their Young's moduli do not differ greatly, the expansion is between one-half and one-third of what the expansion would have been if the vitreous material could have expanded fully.

Thus for low doses the volume of the crystal will increase by 5–8% of the volume of the vitrified regions : at the same time shear stresses will be set up in the crystalline regions. When an appreciable fraction of the volume has been vitrified, the shear stresses at some points will be large enough to start plastic flow, and the stress system will be partly relieved. The mechanism of this stress relief is necessarily complicated and obscure, but the only way of relieving the stresses is by an increase in the volume of the crystal. In this way expansion will occur which was earlier prevented by the constraints of the surroundings, and the rate of density change due to irradiation will increase.

---

† But this state differs from the state of fused silica, whose density is about 2% lower. Presumably the vitreous state is not unique, but different degrees of order are possible. Berman (1951) found small differences in the thermal conductivity of different specimens of fused silica. It would be interesting to compare the thermal conductivity of fused silica in the unirradiated and the heavily irradiated state. The latter, being denser, should be more ordered, and should have a longer phonon mean free path.

Primak *et al.* (1953) have studied the density changes of an irradiated crystal on annealing. Annealing at high temperatures increased the density to its original (crystalline) value : this is presumably due to recrystallization. However, annealing below 600°C caused a further *decrease* of the density. This is in agreement with the present picture : some plastic flow takes place when the temperature is raised, so that some of the stresses in the crystal are relieved and the latent volume increase realized, but the temperature is not high enough to produce recrystallization.

It appears from an examination of the curve of density change versus dosage of Wittels and Sherrill (1954) that about one quarter of the material has been vitrified at a cumulative dose of 5×10^{19} neutrons/cm^2, the density change being 2%. It is reasonable that the rate of density change should increase beyond this point, since the joining up of vitreous inclusions and the consequent formation of systems of high stress extending over large distances should be quite frequent. At twice the dose all single crystal x-ray reflections disappear.

The fraction of material vitrified can also be estimated from Berman's measurements of the thermal conductivity at low temperatures, and using the dosage values for these measurements deduced by Kinchin and Pease (1955), it is found that the two methods of estimating the fraction vitrified agree to within a factor 2, the thermal conduction values giving a lower fraction of vitrified material. The discrepancy could be due to a difference in the neutron flux calibration.

According to the present model there is no direct relation between changes in hydrostatic density and changes in the lattice parameters determined by x-ray diffraction. Vitreous inclusions should produce very diffuse diffraction rings, as were indeed observed by Wittels. Diffraction spots and lines in the Laue and Debye–Sherrer patterns should become diffuse because of the inhomogeneous strain of the crystalline material, and long range order should progressively diminish. This is also in accordance with observations. However, apart from minor effects due to isolated point imperfections, there should be no net dilatation of the crystalline regions. The line broadening due to the inhomogeneous shear strain should be extremely skew, for in any volume element the compression along one principal axis should be twice the expansion in the other two directions. Thus the mean of a line should not be shifted, but the intensity maximum should be displaced in the sense of lattice expansion, to be compensated by a long tail of low intensity on the compression side. This could create the impression of overall lattice expansion and may explain at least a part of the lattice expansion reported by Wittels (1953) and by Johnson and Pease (1954).

Acknowledgment

The author is indebted to Mr. A. F. A. Harper for helpful criticism.

References

Berman, R., 1951, *Proc. Roy. Soc.* A, **208,** 90.
Berman, R., Klemens, P. G., Simon, F. E., and Fry, T. M., 1950, *Nature, Lond.*, **166,** 864.
Johnson, F. B., and Pease, R. G., 1954, *Phil. Mag.*, **45,** 651.
Kinchin, G. H., and Pease, R. S., 1955, *Rep. Progress Phys.*, **18,** 1.
Klemens, P. G., 1951, *Proc. Roy. Soc.* A, **208,** 108.
Primak, W., 1954, *Phys. Rev.*, **95,** 837 ; 1955, *Ibid.*, **98,** 1708.
Primak, W., Fuchs, L. H., and Day, P., 1953, *Phys. Rev.*, **92,** 1064.
Seitz, F., 1949, *Disc. Faraday Soc.*, No. 5, 271.
Wittels, M., 1953, *Phys. Rev.*, **89,** 656.
Wittels, M., and Sherrill, F. A., 1954, *Phys. Rev.*, **93,** 1117.

XCVII. *The Ratio of K-Capture to Positron Emission in Fluorine* 18

By R. W. P. Drever, A. Moljk, and J. Scobie
Department of Natural Philosophy, University of Glasgow†

[Received August 15, 1956]

Abstract

The existence of electron capture in the decay of ^{18}F has been revealed by the detection of K-radiations of oxygen in a proportional tube spectrometer containing a gaseous BF_3 source. The K/β^+ ratio determined from the number of counts in the observed K-peak and the total number in the positron spectrum is 0·030, with an estimated accuracy of 6%. A scintillation spectrometer investigation showed the absence of any gamma rays with intensity greater than 0·5% of the positrons, suggesting that both K-capture and beta decay are ground state to ground state transitions. A comparison between theoretical and measured values of the K/β^+ ratio gives, for the ratio of the axial vector and tensor coupling constants, $C_A/C_T=(0\cdot4\pm2)\%$.

§ 1. Introduction

The ratio of the probabilities of K-capture and positron emission in an allowed transition is of interest for beta decay theory. Analyses of the measured shapes of allowed beta spectra have shown that Fierz interference terms arising from the linear combination of different interactions are not large. If such terms are neglected, the probabilities λ_K for K-capture and λ_+ for positron emission can be written

$$\lambda_K=\frac{G^2}{4\pi^2}(W_0+W_k)^2\,g_k^2|M|^2,\quad \lambda_+=\frac{G^2}{2\pi^3}f_+(Z,\ W_0)\,|M|^2$$

where G is the Fermi constant, W_0 the maximum positron energy, W_k the energy of the K electron, g_k the large component of the wave function of the K electron at the nucleus,

$$f_+(Z,W_0)=\int_1^{W_0}W(W^2-1)^{1/2}(W_0-W)^2F(Z,W)dW^2$$

with $F(Z,W)$ the Fermi function, and M is the nuclear matrix element. The K/β^+ ratio λ_K/λ_+ does not involve the Fermi function constant and the matrix element, and is therefore particularly suitable for experimental verification. Moreover, agreement between experimental and theoretical values of the K/β^+ ratio can set a closer limit to the Fierz interference terms than that given by spectrum shape measurements.

The ratios of K-capture to positron emission have been determined for a number of nuclei, and the results have been reviewed recently by Radvanyi (1955). However, the comparison with theory is not entirely satisfactory since the data concern nuclei with complex decay schemes,

† Communicated by the Authors.

not always well established. Further, indirect methods for measuring K-capture involving considerable corrections have usually been employed, and in most cases experimental errors are large. A K/β^+ determination for a simple ground state to ground state transition would provide a more reliable comparison with theory. In the case of a low Z nucleus such a measurement can be made directly using proportional counter gaseous source technique. With these considerations in mind, the present study of fluorine 18 was undertaken.

Fluorine 18 is a positron emitter, of half-life 112 minutes (Blaser *et al.* 1949), with a simple spectrum of allowed shape and maximum energy 649 kev (Ruby and Richardson 1951). No gamma emission has been detected (Knox 1948). The transition is superallowed with $\log fT = 3{\cdot}6$. Fluorine 18 is an odd-odd $N=Z$ nucleus with a spin of 1 (Moszkowski and Peaslee 1954), assigned on the basis of isotopic spin selection rules which indicate that the transition to ^{18}O, with spin $J=0$ and isotopic spin $T=1$, involves a Gamow–Teller interaction.

Electron capture is expected, but it had not been observed before the present work, mainly because the absence of gamma emission prevents the application of the usual indirect methods for measuring K-capture. In ^{18}F K-capture can only be detected by the K-radiation of oxygen subsequently emitted. This has an energy of 530 ev and, on account of the low fluorescence yield, 99·5% of the K-capture events lead to the emission of Auger electrons instead of K x-rays. A proportional tube spectrometer can be used for the measurement of electrons in this low energy region, and this instrument is particularly suitable for the present experiment since the ratio of K-capture to positron emission can be found directly from the pulse height distribution.

§ 2. Source Preparation

A radioactive gas to be measured in a proportional counter should not have a high attachment coefficient which might affect the performance of the counter, and of course should not react chemically with the wall material. For these reasons fluorine itself cannot be used, but preliminary experiments showed that boron trifluoride and methyl fluoride are more suitable. The former was employed in most of the measurements.

The ^{18}F was made by (γ, n) reaction on fluorine using the gamma beam from the Glasgow 340 Mev electron synchrotron. With a total output of 2×10^9 equivalent quanta per minute, the intensity of the effective part of the bremsstrahlung spectrum in the neighbourhood of 20 Mev is just sufficient to give a source of the required specific activity.

Calcium fluoride, the target material, was irradiated for 4 hours and boron trifluoride was then prepared by heating the calcium fluoride with boric oxide and sulphuric acid. The gas was freed from condensable impurities by cooling with solid carbon dioxide. Since the target material was exposed close to the vacuum chamber of the synchrotron, the neutrons present produced an appreciable amount of ^{37}A by (n, α) reaction

on calcium. This radioactive impurity was removed by freezing the boron trifluoride with liquid air and pumping out.

The boron trifluoride prepared contained some silicon tetrafluoride which is undesirable in a counter because of its high electron attachment coefficient. However, the short half-life of ^{18}F prevented the extensive purification required to remove the silicon tetrafluoride. The presence of this gas set a limit of about 4 mm of mercury to the partial pressure of the source that could be used in the counter.

§ 3. Measurements

The proportional counter employed had a diameter of 10 cm and a sensitive length of 58 cm, defined by field correcting tubes. A trace of gaseous source was introduced into the counter and methane to 10 cm of mercury, and argon to 3 atmos, was added. The total pressure was chosen so that the rise of the pulse spectrum at low energies, caused by escaping positrons that spend only part of their energy in the counter, would not be excessive. The pulse distribution was analysed with a multichannel kicksorter.

Fig. 1

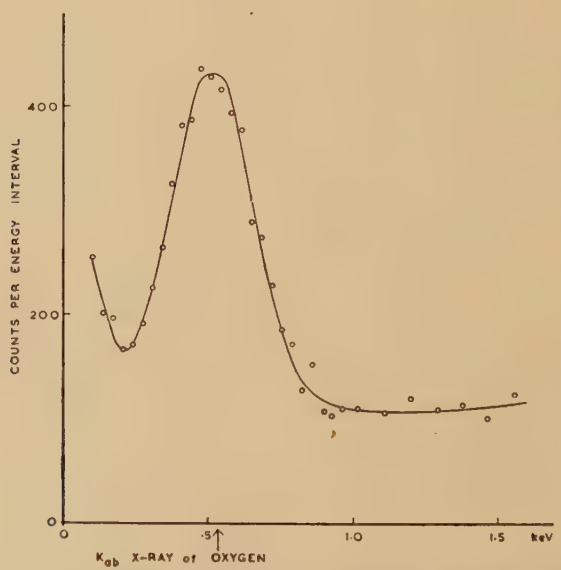

K-capture peak of ^{18}F measured in a proportional counter with a gaseous source.

The gain of the counter was adjusted using the 9·2 kev x-rays from a ^{71}Ge source for calibration, and the low energy part of the pulse spectrum was examined. A peak was detected in the region of 500 ev and is shown in fig. 1. To avoid the possibility of errors due to space charge the energy of the observed peak was determined more accurately by using the 2·8 kev K-radiation from an ^{37}A source introduced into the counter. This

confirmed that the energy of the peak corresponds to the K absorption energy of oxygen. Such a peak can only be caused by K-capture since, in a counter with 4π geometry, any multiple event such as the emission of x-rays following ionization in positron decay would give an integrated pulse due to both components. The ratio of the counting rate in the peak to the counting rate in the continuous spectrum was found to remain constant as the source decayed, and the half-life agreed closely with that of ^{18}F. Some long-lived activity due to impurities was apparent after several half-lives, but its intensity was low and it merely led to a slight increase in the continuous background.

The relative intensity of K-capture was determined from the number of counts in the peak and the total number of counts in the spectrum. The peak is superimposed on a continuous positron pulse distribution, which rises at low energies and introduces some uncertainty in the position and shape of the line defining the base of the peak. Errors due to such uncertainties depend on the width of the peak, which, in low energy measurements, is relatively large because of fluctuations in the number of ion pairs produced. In the present case the width is increased even further by electron attachment in the source and by the effects of the high counting rate of large positron pulses. To reduce these errors a comparison method was used when determining the area of the peak. After the K-capture measurement, when the source had decayed, ^{37}A was introduced into the counter and the shapes and relative areas of the 230 ev L-peak and the 2·8 kev K-peak were measured. The base of the fluorine K-capture peak was established by comparison with these, and the number of K-capture pulses was thus determined.

The high absorption of oxygen K x-rays in argon, and the small fluorescence yield, make any errors due to escape of photons from the counter completely negligible. The number of counts in the observed peak therefore gives the number of K-capture events that have occurred in the sensitive volume.

The number of positrons was obtained from the total number of pulses recorded, taking into account background and the weak long-lived activity revealed by the decay curve. A correction, calculated to be 4·6%, was applied for positrons that enter the sensitive volume from the ends of the counter.

Boron trifluoride is a reactive gas, so a separate experiment was carried out to measure any adsorption on the wall. The counter was filled with the source and, 1 hour later, was pumped out. The residual counting rate was then determined, and it was found that 23% of the ^{18}F activity had been deposited on the brass wall of the counter. The decay curves taken with gaseous sources indicated that no loss of source occurred during the measurements, so it may be assumed that the adsorption takes place immediately after filling. Previous work has shown that such an adsorbed source would not contribute to the K-capture peak. The positron counting rate was corrected accordingly when calculating the K/β^+ ratio.

The results of a number of separate measurements give a mean value for the ratio of K-capture to positron emission of

$$\lambda_K/\lambda_+ = 0{\cdot}030.$$

The main uncertainty in the experiment arises in determining the number of pulses in the K-peak and, taking this into account, the estimated accuracy of the above result is 6%.

§ 4. Decay Scheme

Although previous work (Knox 1948) has shown the absence of gamma rays above 100 kev with intensity greater than 10% of the beta disintegrations, this does not rule out the possibility that the K-capture transition now observed might go to an excited state of ^{18}O. A more detailed search for gamma rays has therefore been made using a scintillation spectrometer. In view of the difficulty of detecting a weak photoelectric peak above the Compton distribution due to the annihilation radiation, the measurement was made by comparing the spectra obtained from ^{18}F with that given by another pure positron source, in this case ^{11}C.

Fig. 2

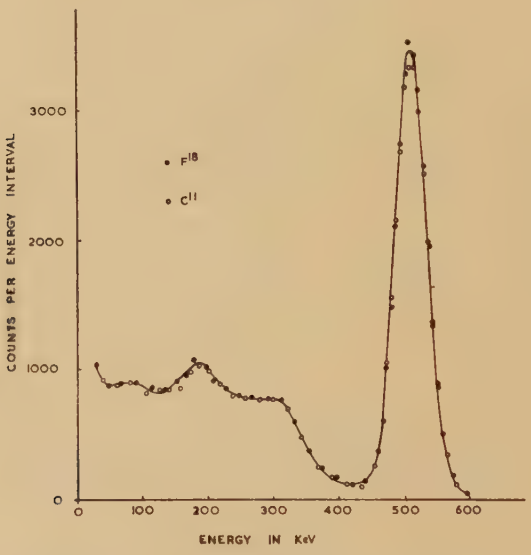

Scintillation counter spectra of ^{18}F and ^{11}C.

A thin layer of irradiated calcium fluoride was placed in front of the NaI (Tl) crystal, which had a diameter of 4·2 cm and a height of 2·5 cm, and was covered with a Perspex absorber. The pulse spectrum in the region between 30 kev and 700 kev was measured. The experiment was then repeated with a ^{11}C source, prepared by (γ, n) reaction from spectroscopically pure graphite. Carbon 11 is a pure positron emitter with an end point energy of 990 kev and a half-life of 20 minutes. No gamma emission has been detected (Siegbahn and Peterson 1946). The spectra obtained from both the ^{18}F and ^{11}C sources are given in fig. 2, normalized

to the same total number of counts. The close correspondence of the two spectra indicates that no gamma ray above 30 kev with intensity greater than 0·5 % of the positrons is emitted by either isotope.

The energy region below 50 kev was examined with the proportional counter and gaseous source. No peaks other than that due to the K-capture radiation were detected. It may therefore be assumed that the decay of ^{18}F is simple, and the observed K-capture is a ground state to ground state transition.

§ 5. Discussion

The theoretical value of the K/β^+ ratio for ^{18}F has been calculated using the table of Fermi functions by Rose (1955) with the screening correction factors of Reitz (1950). When the Fierz interference terms are neglected, the value R_0 of the K/β^+ ratio was found to be $R_0=0{\cdot}0295$, which is close to the measured value.

By comparing the theoretical and experimental values of the K/β^+ ratio it is possible to set a limit to the ratio C_A/C_T of the axial vector and tensor coupling constants in the Gamow–Teller interaction. Studies of the shapes of allowed beta spectra, together with measurements of the angular correlation between electron and neutrino emission, indicate that C_A/C_T is not more than a few per cent. There are several estimates of the upper limit for this ratio : 0·02 (Konopinski and Langer 1953), 0·04 (Davidson and Peaslee 1953), and 0·20 (Winther and Kofoed-Hansen 1953). A determination of the K/β^+ ratio of ^{22}Na by Sherr and Miller (1954) gives $C_A/C_T=(-1\pm2)\%$, though there may be some doubt whether this decay is allowed.

If the K/β^+ ratio calculated for a small finite value of C_A/C_T has the value R, then it may be shown (see De Groot and Tolhoek 1950) that

$$\frac{C_A}{C_T}=\frac{R-R_0}{2R_0(1+\langle W^{-1}\rangle)}$$

where $\langle W^{-1}\rangle$ is the average of W^{-1} over the beta spectrum, W being the positron energy. For ^{18}F the value of $\langle W^{-1}\rangle$ is 0·69. Substituting the present values of the experimental and theoretical values of the K/β^+ ratio for R and R_0 gives $C_A/C_T=(0{\cdot}4\pm2)\%$.

This result is very similar to that obtained from the ^{22}Na measurements referred to above, and satisfactorily confirms conclusions drawn from the shapes of allowed beta spectra.

Acknowledgments

We would like to thank Professor P. I. Dee for his interest and encouragement, Dr. W. McFarlane and the Synchrotron crew for their cooperation, and Dr. G. M. Lewis for some helpful discussions. The authors are indebted to the D.S.I.R. for financial support (R.W.P.D.), and to the University of Glasgow for a scholarship (J.S.). One of the authors (A.M.) is grateful to the University of Ljubljana, Yugoslavia, for leave of absence.

References

Blaser, J. P., Boehm, F., and Marmier, P., 1949, *Phys. Rev.*, **75,** 1953.
Davidson, J. P., and Peaslee, D. C., 1953, *Phys. Rev.*, **91,** 1232.
de Groot, S. R., and Tolhoek, H. A., 1950, *Physica*, **16,** 456.
Knox, W. J., 1948, *Phys. Rev.*, **74,** 1192.
Konopinski, E. J., and Langer, L. M., 1953, *Ann. Rev. Nucl. Sc.*, **2,** 261.
Moszkowski, S. A., and Peaslee, D. C., 1954, *Phys. Rev.*, **93,** 455.
Radvanyi, P., 1955, *Ann. de Phys.*, **10,** 584.
Reitz, J. R., 1950, *Phys. Rev.*, **77,** 10.
Rose, M. E., 1955, in *Beta and Gamma Ray Spectroscopy*, edited by K. Siegbahn (Amsterdam : North-Holland Publishing Company).
Ruby, L., and Richardson, J. R., 1951, *Phys. Rev.*, **83,** 698.
Sherr, R., and Miller, R. H., 1954, *Phys. Rev.*, **93,** 1076.
Siegbahn, K., and Peterson, S. E., 1946, *Ark. Mat. Astr. Fys.*, **32B**, No. 5.
Winther, A., and Kofoed-Hansen, O., 1953, *Kgl. Danske Videnskab Selskab Mat.-Fys. Medd.*, **27,** No. 14.

XCVIII. *The Reaction* ^{9}Be (α, n) ^{12}C

By D. B. James,† G. A. Jones‡ and D. H. Wilkinson
Cavendish Laboratory, Cambridge §

[Received February 23, 1956]

Summary

The angular properties of the reaction ^{9}Be (α, n) ^{12}C have been investigated in some detail in the range $E_\alpha = 0{\cdot}4$ to $1{\cdot}3$ MeV. Analysis of the results in terms of overlapping resonances has led to tentative assignments of spin and parity to certain levels in ^{13}C. The possibility that the reaction may proceed partly by a stripping mechanism has been considered; it has been concluded that the results do not specifically demand such a mechanism.

§ 1. Introduction

The suggestion by Madansky and Owen (1955) that the reaction ^{9}Be (α, n) ^{12}C may proceed by a stripping mechanism attaches renewed interest to some work done in this laboratory in 1951 and submitted in Ph.D. Theses by two of the authors (D.B.J. and G.A.J.) but not previously published.

Work ante-dating our own included that of Halpern (1949) who measured the total neutron yield up to $E_\alpha = 5{\cdot}3$ MeV using α-particles from polonium, and Bradford and Bennett (1950) who, at $E_\alpha = 1{\cdot}4$ MeV, measured the 0° : 90° ratios of abundances of the two groups of neutrons to the ground state and first excited state of ^{12}C at 4·43 MeV with $E_n \sim 6\frac{1}{2}$ and 2 MeV respectively. On the basis of these latter measurements, Haefner (1951) has assigned a spin of 5/2 to the relevant level in ^{13}C, but, as our own work shows, data at 0° and 90° are quite insufficient to make a reliable assignment.

Post-dating our work, Talbott and Heydenburg (1953) have measured the γ-ray yield up to $E_\alpha = \sim 3$ MeV; they locate a well-pronounced resonance at $E_\alpha = 1{\cdot}9$ MeV followed by a weaker, broader resonance at $E_\alpha = 2{\cdot}6$ MeV and a rising background. Bennett *et al.* (1953, only in abstract) report the existence of a narrow resonance at $E_\alpha = 0{\cdot}61$ MeV and a broad one at $E_\alpha = 0{\cdot}53$ MeV. Tanner (1955) has measured angular distributions of the γ-radiation at energies between $E_\alpha = 1{\cdot}3$ and $1{\cdot}9$ MeV and has estimated the total cross section at the $1{\cdot}9$ MeV resonance peak.

† Now at Bell Telephone Laboratory, Murray Hill, New Jersey, U.S.A.
‡ Now at A.E.R.E., Harwell.
§ Communicated by the Authors.

In this paper we present the excitation function of both groups of neutrons and of the γ-radiation in the range E_α=0·4 to 1·3 MeV, the angular distributions of the ground state neutrons at a number of energies in this range, also, at fewer energies, the angular distributions of the low energy group, of the γ-radiation and the n–γ correlation.

Attempts were made in the Theses to describe quantitatively in terms of three overlapping levels the angular distributions of the ground state neutrons. The qualitative success achieved did not encourage further application to the other distributions and correlations. Only the qualitative conclusions from these analyses are given here since in any case what was considered to be a single resonance at $E_\alpha \sim 0{\cdot}6$ MeV has been resolved into two (Bennett *et al.* 1953) so that at least four overlapping states would be required to give a complete picture. When the analysis of angular distribution patterns demands such complexity as this there can be little profit in pursuing it further.

§ 2. Measurements and Results

The neutron detector used in these measurements was a spherical ionization chamber of volume 500 cm^3, filled with deuterium to a pressure of 40 atmospheres. The chamber was constructed by G. H. Stafford and a similar one filled with hydrogen has been described by him (Stafford 1948). A typical 'spectrum' from the reaction ^{9}Be (α, n) ^{12}C (thin target) is shown in fig. 1; two groups of neutrons are discernible with approximate energies of cut off of $6\frac{1}{2}$ and 2 MeV respectively, and of relative intensities, after allowing for corrections listed later, of roughly 1 : 3.

For measuring the angular distributions of the neutron groups, the chamber was mounted on a rotatable framework centred upon the target where it subtended of solid angle of approximately 0·1 steradian. The yield was monitored by measuring the γ-flux through a brass-walled Geiger counter at a fixed position—roughly forward. The target, an evaporated layer of beryllium on 0·010 in. copper sheet, was soldered to 1/32 in. brass plate which formed the end of the target tube. The target thickness had previously been estimated from a comparison of the yield, from this target and from a thick target, of γ-radiation from the reaction ^{9}Be (p, γ) ^{10}B. Knowledge of the width of the broad resonance at E_p=1 MeV (Γ=94 kev Fowler and Lauritsen 1949) gave a target thickness of 6 kev for protons of 1 MeV or approximately 40 kev for α-particles of 1 MeV (Allison and Warshaw 1953).

In measuring the angular distributions of the ground-state neutrons, pulses due to deuterons recoiling from neutrons of the low energy group were biased out. To detect this low energy group, a lower bias point was chosen in addition (just above noise due to build up of γ-ray pulses etc.) and from the shape of the 'spectrum'—see fig. 1—a suitable correction was made for the presence of the high energy group. Since this correction was only about 25% of the total count errors in it are of little significance,

The angular distributions of the two groups presented in figs. 2 and 3 have been corrected both for motion of the centre of gravity of the reacting system and for variation of detecting efficiency with neutron energy, which depends on the angle of observation. No correction for finite solid angle of detection has been made, because in general the statistical accuracy does not justify making this rather complicated correction.

Fig. 1

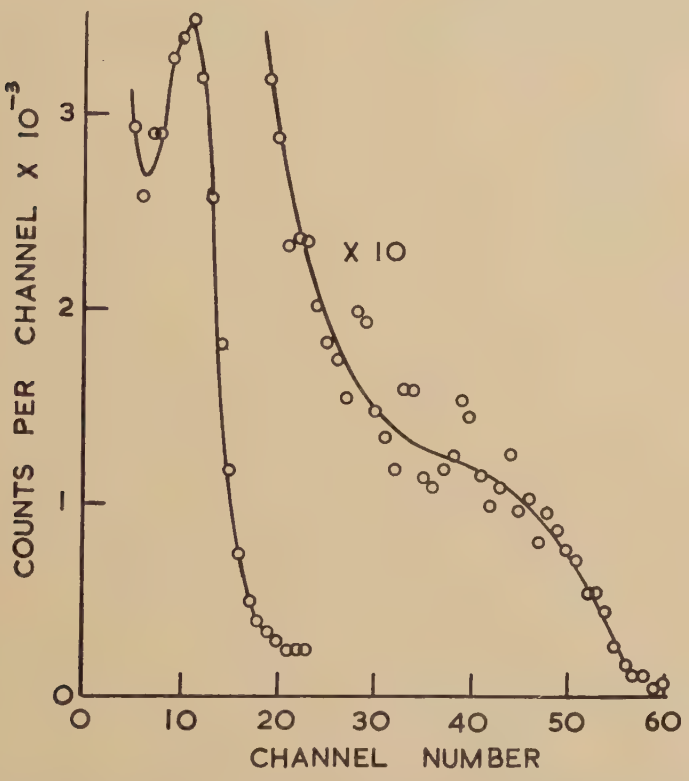

The deuterium recoil spectrum of the neutrons from Be (α, n) ^{12}C at $E_\alpha = 1{\cdot}12$ MeV.

The detecting efficiency varies with neutron energy on four counts: (1) the n–d scattering cross section varies with the neutron energy; (2) the deuteron angular distribution, and therefore the shape of the pulse spectrum, is a function of neutron energy; (3) the discriminator bias cuts out a smaller fraction of the pulses at higher neutrons energies; and (4) the wall effect is larger for higher neutron energies, since the mean probability that a recoil deuteron be stopped within the chamber decreases as the length of the recoil track increases.

The n–d scattering cross section is given by Adair (1950). The effect of (2) is sufficiently small to be ignored. Corrections for (3) and (4) are

Fig. 2

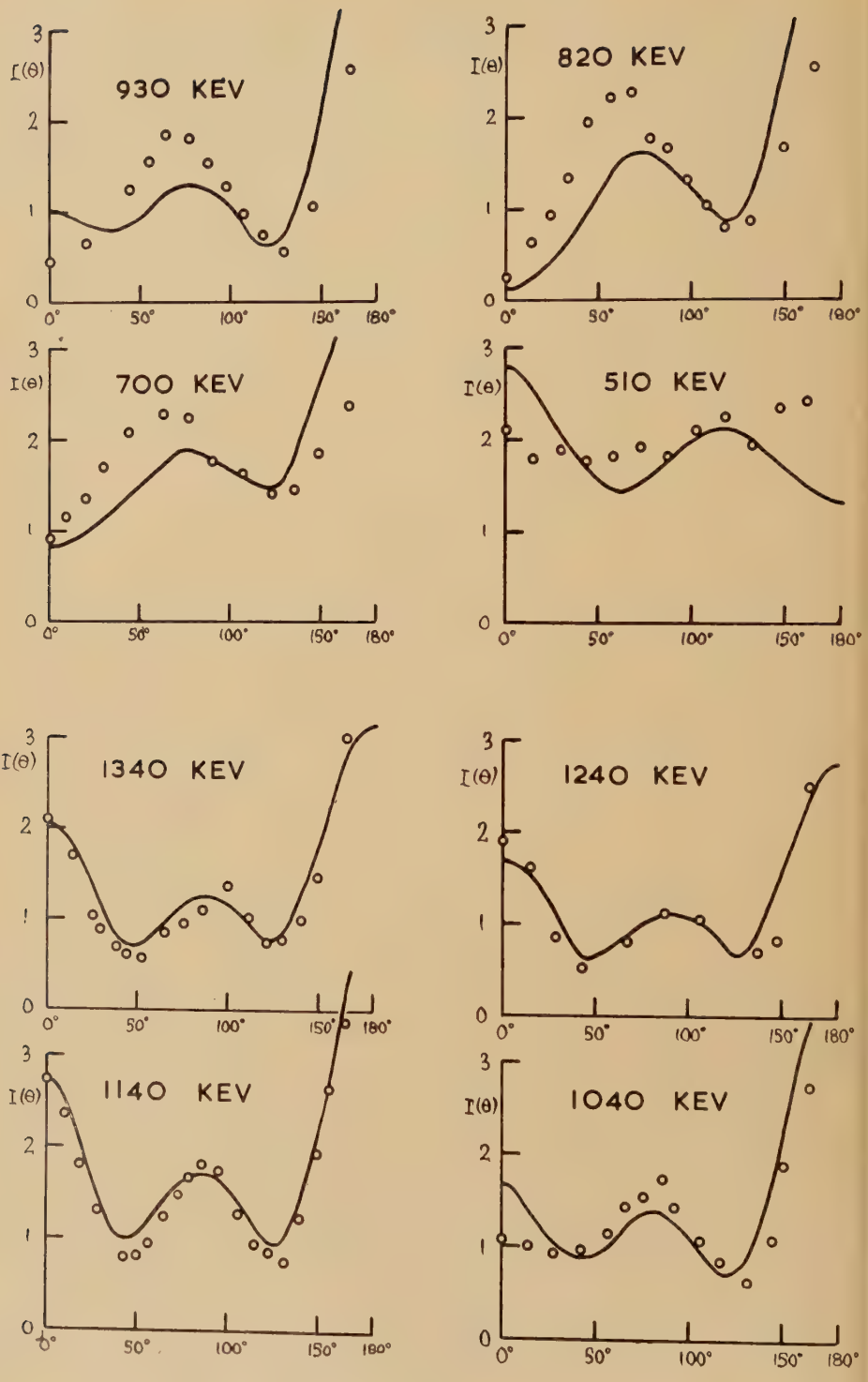

Angular Distributions of ground state neutrons.

complicated and tedious to make and will not be discussed in detail; they are not independent.

The over-all correction for the ground-state neutrons resulted in an increase of about 20% in the backward direction falling to zero in the forward, while for the low energy group the corresponding range of increase was 100% to zero. Though the corrections are large in this latter case, they are derived from well understood processes and should be reliable.

The integrated cross section for emission of the ground-state neutrons, fig. 4, has been derived from measurements made at 0° and 60° and the

Fig. 3

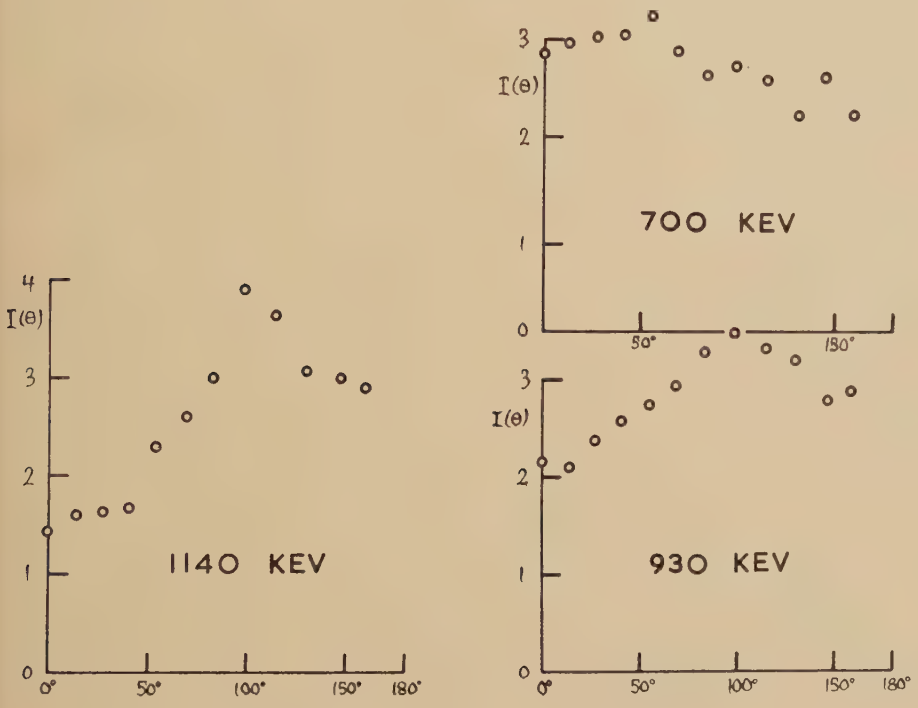

Angular Distributions of low energy neutrons.

observed angular distributions. Those for the low energy neutrons and γ-radiation, fig. 5, have not been corrected for the angular distributions, but, since the measurements were made at 90° and the respective angular distributions are not very strong, the correction is in any case quite small. It will be noticed that the three excitation functions are somewhat similar in shape indicating that the branching ratio between transitions to the excited state and ground state of ^{12}C does not change very much with bombarding energy in our range. The yield in fig. 4 is given in terms of the absolute partial cross section for production of high energy neutrons; it is based upon estimates of yields of $1{\cdot}3\times10^{-10}$ and 9×10^{-10} n per α at

E_α=0·65 and 1·3 MeV respectively and upon the estimated target thickness of 6 kev to protons of 1 MeV, or $1{\cdot}8\times10^{18}$ Be nuclei per cm^2, using a value of the stopping power of beryllium for protons given by Madsen and Venkateswarlu (1948) and Allison and Warshaw (1953). The yields in fig. 5 are given in arbitrary units, but, as has previously been stated, the low energy neutron group is about three times as intense as the high.

A thick walled brass Geiger counter, similar to that used for monitoring, was used as a detector in measuring the angular distribution of the γ-radiation. The corrections applied here were for purely experimental

Fig. 4

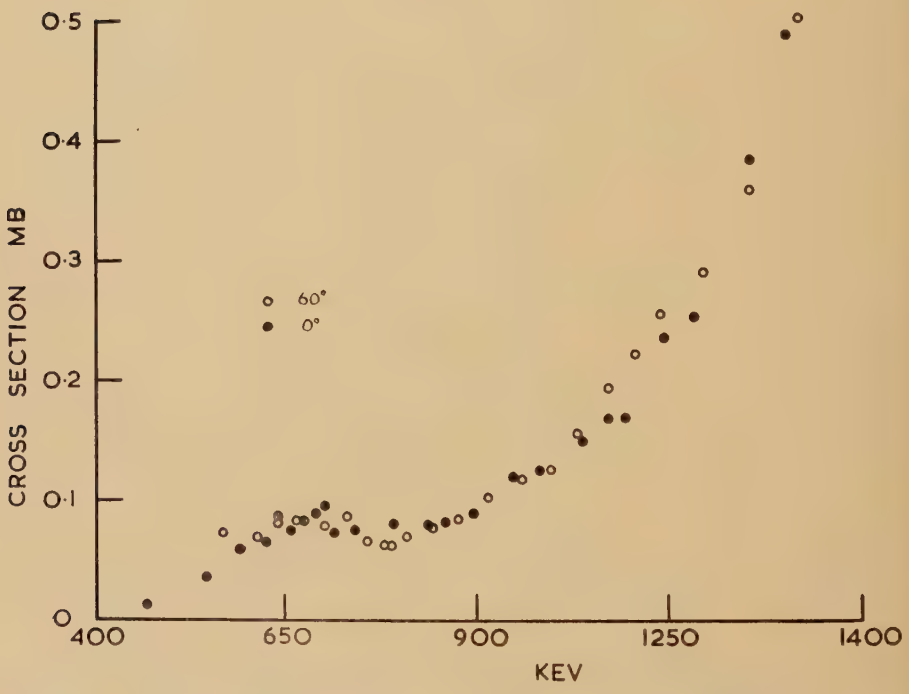

Excitation Function for ground state neutrons.

reasons such as for eccentricity of the geometrical arrangement and for absorption of radiation in the target backing. Since this part of the experiment was carried out in much better geometry this latter correction was found to be considerable when observing in a direction nearly parallel to the surface of the target, though very small in other directions. No correction was made for motion of the emitting nucleus. The results are shown in fig. 6.

The angular correlation between the low energy neutrons and the γ-radiation was measured only in the plane perpendicular to the α-particle beam. Liquid scintillation counters were used to detect both types of

Fig. 5

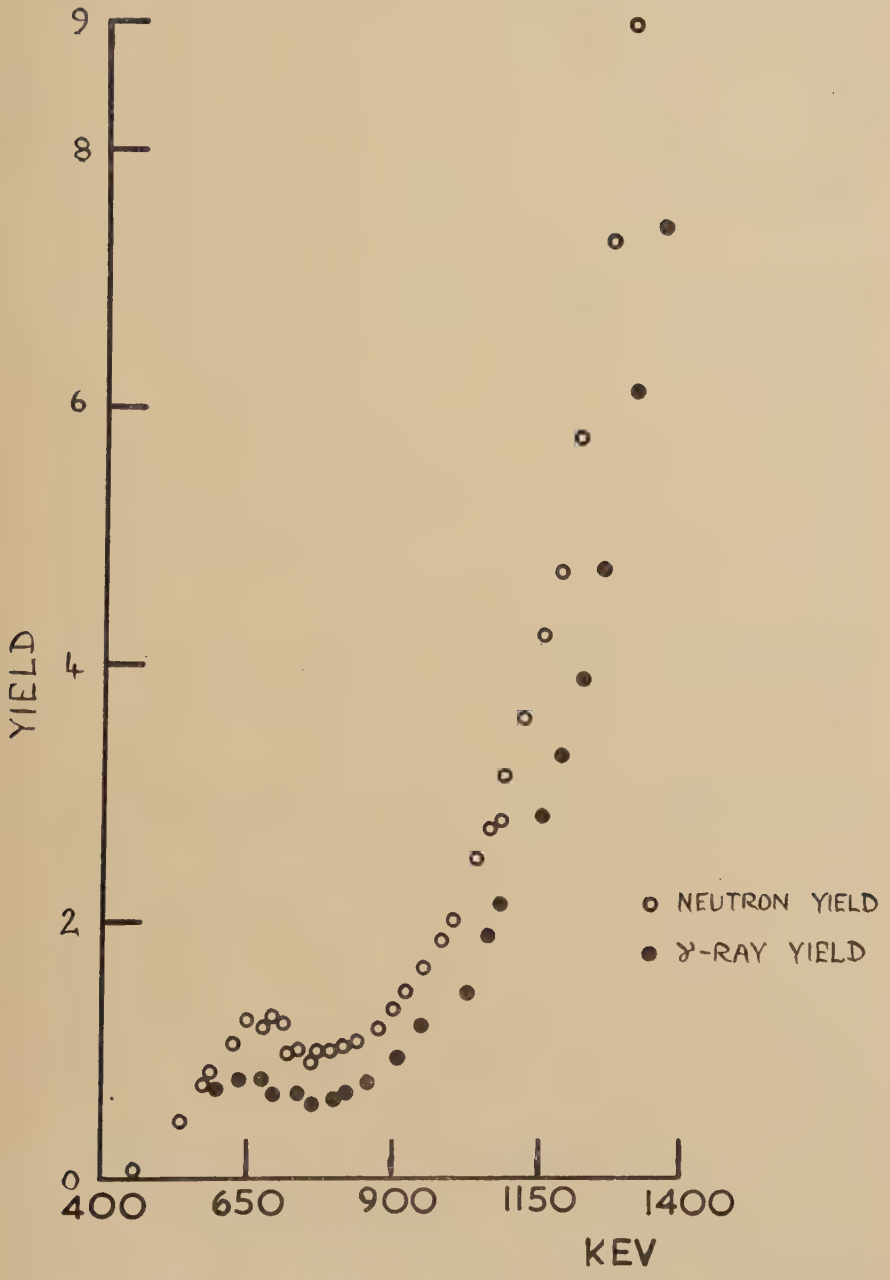

Excitation Functions for low energy neutrons and γ-radiation.

Fig. 6

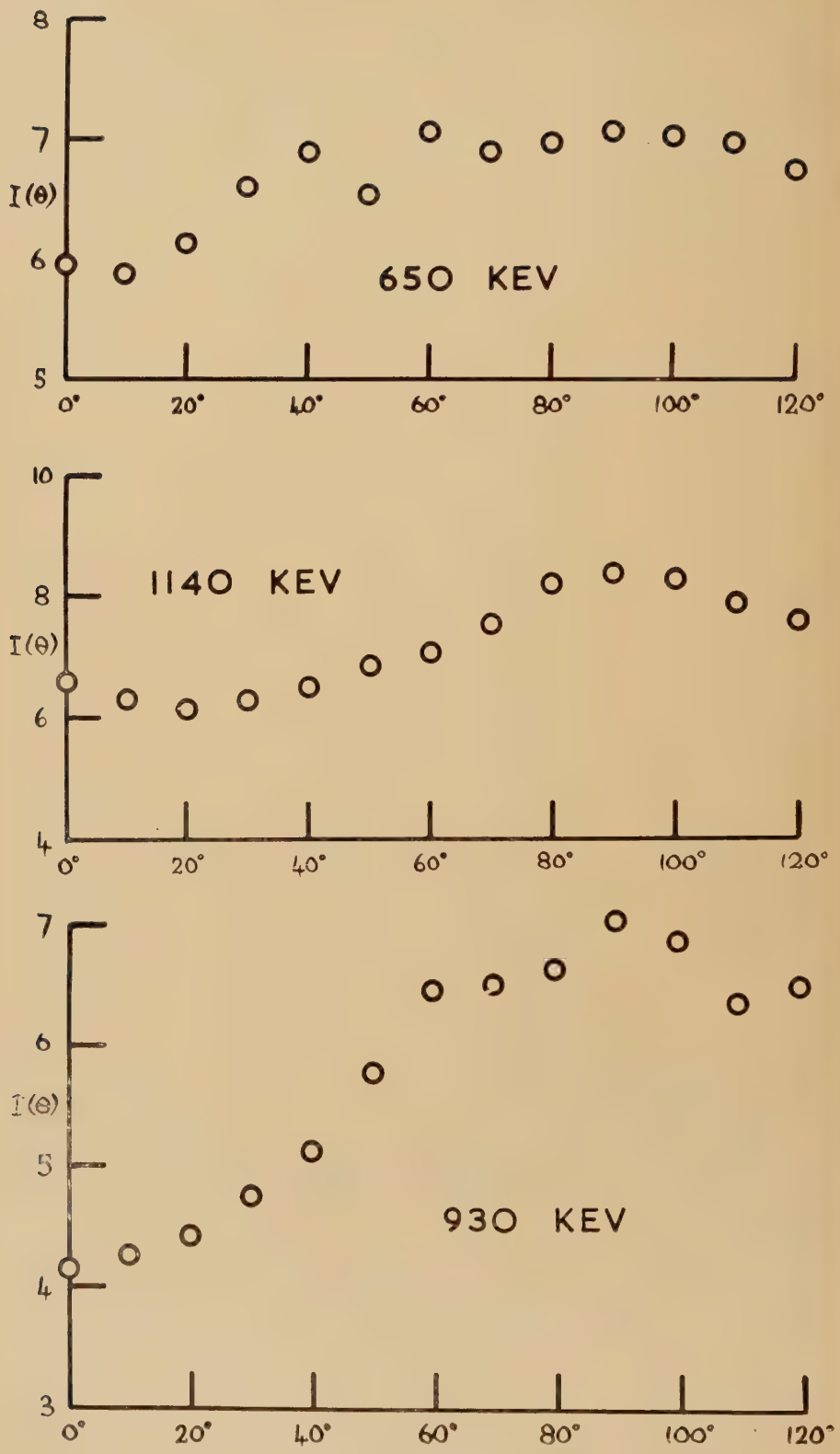

Angular Distributions of γ-radiation.

radiation †, the γ-radiation chiefly by production of Compton electrons, and the neutrons by production of knock-on protons, within the scintillation material (a solution of terphenyl in toluene). A coincidence circuit giving a resolving time of $1\text{–}2\times10^{-8}$ sec was employed; the complete

Fig. 7

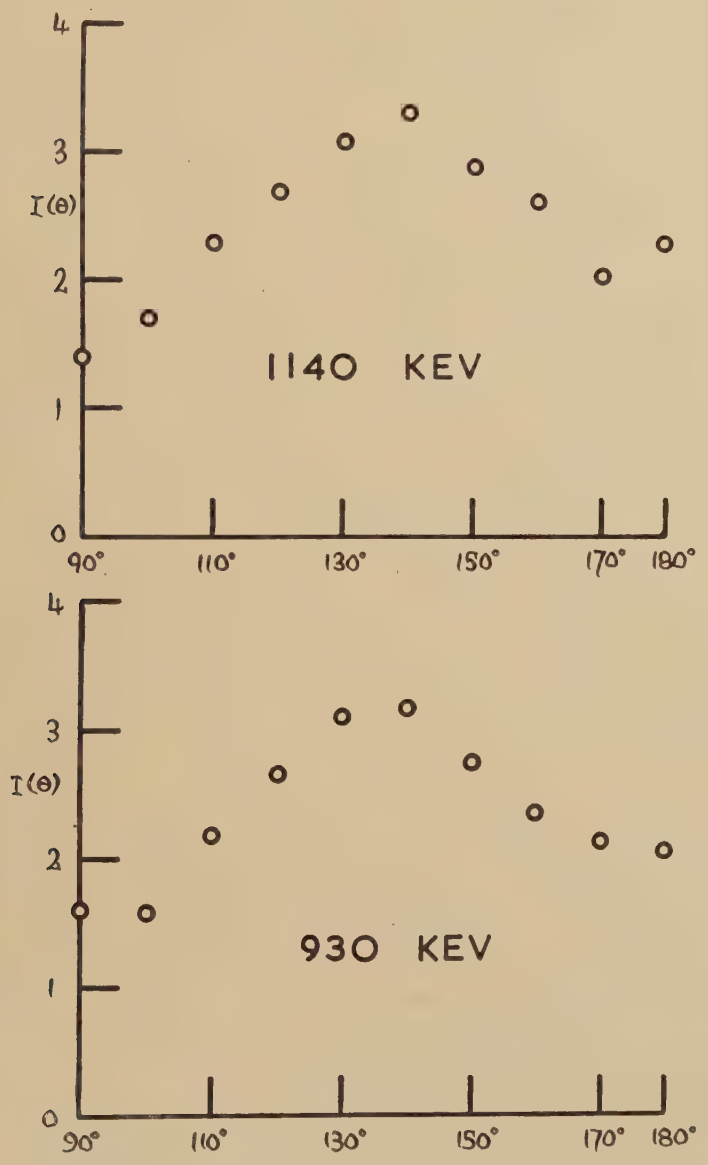

Angular Correlations between neutrons and γ-rays.

† NaI (Tl) crystals for γ-detection were not available in the laboratory at the time.

apparatus has been described by James and Treacy (1951). The need for fast coincidence techniques here was rather different than that usually encountered namely to discriminate against a high background rate from competing or spurious reactions ; the reaction now under consideration is virtually free from background but has a poor yield necessitating the use of large volumes of scintillating material for efficient detection. The rather poor light collection from these detectors made it necessary to run well into photomultiplier noise to realize this high sensitivity.

To eliminate coincidences due to scattering of a neutron or γ-ray from one detector into the other, measurements were taken only in the 90°–180° sector. This eliminated completely the effect of neutron scattering by hydrogen nuclei since neutrons scattered through angles greater than 90° (which requires multiple scattering) would have low energies and take longer than the resolving time to travel between detectors. The photons scattered through angles greater than 90°, and the neutrons scattered from carbon nuclei in the scintillators were absorbed by putting an inch of lead and a few inches of paraffin wax between the detectors. This was, of course, not possible at and near the 180° position ; nothing was done about the neutron scattering from carbon, the probability of its occurrence in this position being quite small, but the γ-ray scattering was effectively eliminated by surrounding completely one of the detectors by 1 cm of lead, even in the direction of the target. This reduced the coincidence rate slightly (without affecting the correlation), but absorbed strongly the back-scattered photons, of energy about 250 kev.

The angular correlations at two energies are presented in fig. 7. No correction has been made for finite size of detectors, which subtended $\pm 15°$ at the target.

It might be remarked here that this correlation could be measured more accurately and reliably using NaI(Tl) crystals, now available, and slow coincidence techniques since the γ-radiation could be efficiently detected with energy discrimination eliminating scattering events.

§ 3. Discussion

Analysis of the angular distributions of the ground state neutrons into powers of $\cos\theta$ is given in the table. The fact that odd powers of $\cos\theta$ occur requires interference between states of unlike parity. In addition it has been found that the combination of even powers cannot be obtained without introducing interference between states of like parity. Thus at least three states of the intermediate system are required to interpret the results in terms of resonance reaction †. An attempt was therefore made to fit the angular distributions and the excitation function by the overlap of three resonances.

† This conclusion is also apparent from the excitation function which indicates a resonance at or near 600 kev, while other work at higher energies (Talbott and Heydenburg 1953) indicate resonances in the neighbourhood of 2 Mev of which the ' tails ' of at least two may be important at low energies.

After exhaustive search of all reasonable sets of spin and parity assignments it was found that the combination $(\frac{1}{2}+)$ $(\frac{1}{2}-)$ and $(7/2-)$ for the relevant states in ^{13}C was most promising and that the presence of a state of characteristics $(5/2+$ or $-)$ was very unlikely since the 'pure' angular distributions from such states differed so much from the observed

Analysis of angular distributions of ground state neutrons into powers of $\cos\theta$

E_α (kev)	C^0	C^1	C^2	C^3	C^4
510	1	$-0{\cdot}10\pm0{\cdot}04$	—	—	—
700	1	$+0{\cdot}85\pm0{\cdot}11$	$-0{\cdot}03\pm0{\cdot}06$	$-1{\cdot}28\pm0{\cdot}14$	—
820	1	$+1{\cdot}64\pm0{\cdot}10$	$-0{\cdot}02\pm0{\cdot}07$	$-2{\cdot}44\pm0{\cdot}13$	—
930	1	$+1{\cdot}22\pm0{\cdot}08$	$-1{\cdot}39\pm0{\cdot}20$	$-1{\cdot}97\pm0{\cdot}11$	$+1{\cdot}45\pm0{\cdot}18$
1040	1	$+0{\cdot}81\pm0{\cdot}07$	$-2{\cdot}16\pm0{\cdot}18$	$-1{\cdot}53\pm0{\cdot}11$	$+2{\cdot}58\pm0{\cdot}18$
1090	1	$+0{\cdot}63\pm0{\cdot}12$	$-2{\cdot}47\pm0{\cdot}29$	$-1{\cdot}33\pm0{\cdot}18$	$+3{\cdot}11\pm0{\cdot}31$
1140	1	$+0{\cdot}30\pm0{\cdot}05$	$-2{\cdot}98\pm0{\cdot}14$	$-0{\cdot}79\pm0{\cdot}08$	$+3{\cdot}73\pm0{\cdot}15$
1240	1	$+0{\cdot}07\pm0{\cdot}14$	$-2{\cdot}92\pm0{\cdot}34$	$-0{\cdot}69\pm0{\cdot}20$	$+3{\cdot}84\pm0{\cdot}35$
1340	1	$+0{\cdot}00\pm0{\cdot}12$	$-2{\cdot}66\pm0{\cdot}33$	$-0{\cdot}43\pm0{\cdot}20$	$+3{\cdot}63+0{\cdot}37$
1140 (repeat)	1	$+0{\cdot}21\pm0{\cdot}12$	$-2{\cdot}81\pm0{\cdot}33$	$-0{\cdot}73\pm0{\cdot}20$	$+3{\cdot}61\pm0{\cdot}36$

patterns. However, as has been mentioned previously, Haefner's tentative assignment of spin 5/2 to the state at $E_\alpha = 1{\cdot}9$ Mev cannot be considered well founded. The complete expression for the differential cross section for this combination of states is, with $\cos\theta$ abbreviated to c :

$$W(\theta) = \frac{3}{28}A^2(13-10c^2+45c^4) + \frac{5}{28}D^2(9-36c^2+141c^4-98c^6)$$
$$+ \frac{3}{28}\sqrt{5}AD\cos(\alpha-\delta)(3-75c^2+285c^4-245c^6) + \tfrac{1}{2}B^2 + \tfrac{1}{2}C^2$$
$$- \frac{3}{2}\sqrt{\frac{1}{14}}AB\cos(\alpha-\beta)(3-30c^2+35c^4) + \tfrac{1}{2}\sqrt{\frac{5}{14}}BD$$
$$\cos(\beta-\delta)(3-30c^2+35c^4)$$
$$-BC\cos(\beta-\gamma)(c) + 6\sqrt{\frac{1}{41}}AC\cos(\alpha-\gamma)(3c-5c^3) - 2\sqrt{\frac{5}{14}}DC$$
$$\cos(\delta-\gamma)(3c-5c^3),$$

where A and α denote the amplitude and phase associated with neutron emission from the $(\frac{7}{2}-)$ state formed by d-wave α-particles, D and δ refer to the same state but formed by g-wave α-particles, B and β refer to the $(\frac{1}{2}-)$ state, which can be formed only by d-wave α-particles, and C and γ refer to the $(\frac{1}{2}+)$ state, which can be formed only by p-wave α-particles.

The above combination of states can be made to yield the required experimental angular distributions at all energies if the relative amplitudes and phases are considered arbitrary. This is not the case, however, and on imposing the conditions that the yield curves for the individual states

and also the phases should have the usual restricted energy variation, dependent upon the location of the resonance, its width, and the barrier penetration function, great difficulty is experienced in fitting the data. The best fit is obtained when the $(\frac{1}{2}+)$ state is assigned to the resonance near 600 kev, with its yield curve distorted by the barrier function to produce a considerable high energy tail. The contribution to the yield of the $(\frac{7}{2}-)$ and $(\frac{1}{2}-)$ states near and below this resonance is very small, but both rise steadily in intensity until at the high energy limit of our observations, they account for most of the yield. The analysis seemed to favour a sharper rise in intensity of the $(\frac{1}{2}-)$ state giving a slight preference for assigning these characteristics to the resonance at 1·9 Mev.

The full lines in fig. 2 are the theoretical angular distributions for this scheme and indicate that, though qualitatively they have the correct behaviour, much is still to be desired. The calculations were based upon a somewhat larger than normal nuclear radius for α-absorption (this point is discussed later) but for neutron emission the radius recommended by Feshbach and Weisskopf (1949) was used †.

On adopting widths for the levels, the relative amplitudes and phases for all energies are defined by the resonance and Coulomb factors except for the relative importance of d- and g-wave for forming the $(\frac{7}{2}-)$ state. Since relative barrier penetrability strongly favours d-waves, the g-wave contribution was neglected.

The shape of the excitation function also leads to some difficulty since, using the conventional nuclear radius to calculate α-particle penetrabilities, it is not possible to produce the desired shape of the resonance near 600 kev ; for such a slow rate of rise below resonance, the total width required is such that a minimum in the total yield would not occur. Neither does the yield rise sufficiently quickly at high energies. For these reasons a radius for ^{9}Be of approximately twice the conventional value was taken ; subsequent estimation based upon the considerations of Scott (1954) on proton absorption indicate that such a choice may not be unreasonable. It is interesting to note in this connection that Thomas *et al.* (1949) give excitation functions for ^{9}Be (p, d) and (p, α) which seem to indicate no great increase in penetrability above a proton energy of about 350 kev.

It is very likely that the resolution by Bennett *et al.* (1953) of what we have taken to be a single resonance near 600 kev into two, one broad, one sharp, may allow of a reduction in nuclear radius. The broad resonance will account for the slow rise at low energies, while the sharp resonance—blurred out by lack of resolution in our work—can be made to account for the slight dip in yield above the resonances. The rather slow rise at high energies may then arise from the higher contribution to the yield at

† There is no necessity that the two radii should be the same. The analysis seemed to depend uncritically on the radius for neutron emission so the conventional value was taken.

high energies of the broad resonance for which the resonance denominator works against the increase in penetrability.

The intrusion of another state into the picture increases the possibility of fitting the angular distributions.† No further attempt has been made by the authors to do this since the picture has now reached such a stage of complexity as to make it not worthwhile especially when the final conclusions, namely the assignment of spins and parities to certain levels in ^{13}C at excitation energies of about 11 MeV, are not likely to be of much value. It is clear however that our results are capable of being explained adequately in terms of the conventional resonance theory ; in particular no stripping mechanism of the type described by Madansky and Owen (1955) is demanded, but we cannot rule out the possibility that a small part of the intensity arises in this way. Although there is some tendency for the neutrons to be emitted backwards, this can easily be described as we have seen in terms of compound nucleus formation. Indeed the backward emission appears to depend too sharply on angle to be consistent with the stripping process but it is possible that stripping-compound nucleus interference may sharpen the backward rate of rise near 180°. The excitation function of Talbott and Heydenburg (1953) confirms and strengthens our conclusion since a non-resonant process such as stripping can hardly produce what appears to be such a well formed resonance at 1·9 MeV.

Concerning the absolute yield at 1·9 MeV, from γ-ray measurements by Tanner (1955), the assignment $(\frac{7}{2}-)$, but not $(\frac{1}{2}-)$, to the relevant state in ^{13}C leads to an interpretation consistent with this measurement and also Dearnaley's upper limit for $\sigma(\alpha, \alpha)$ quoted by Tanner. Taking 200 kev for the width of this state, this latter measurement gives 30 kev as an upper limit for Γ_α, from which results a total neutron cross section at resonance of 0·18 b. Allowing perhaps for 10–20% background intensity from other resonances gives a total neutron cross section at 1·9 MeV of 0·20–0·22 b against Tanner's measurement of 0·33 b to a factor of two.

The assignment of $(\frac{7}{2})$ to this state and a partial width for α-particle emission of 30 kev at 1·9 MeV is not inconsistent with our measurement of the absolute cross section for emission of high energy neutrons at 1·3 MeV, but the attempt to correlate these data is very much dependent upon the penetrability function. Taking an effective nuclear radius of 6×10^{-13} cm the total neutron cross section from this resonance should decrease from 0·18 b at 1·9 MeV to $\sim$1·6 mb at $E_\alpha = 1{\cdot}3$ MeV. We find that the cross section for high energy neutrons at 1·3 MeV is 0·5 mb and for all neutrons approximately 2·0 mb. Since our analysis has indicated that this

† The $(\frac{1}{2}+)$ state in our analysis was taken to be at resonance at $E_\alpha = 650$ kev, from the shape of the excitation function. In fact the variation with energy of the angular distributions (see fig. 2) would suggest that this resonance should be at a lower energy ; the location suggested by Bennett *et al.* namely $E_\alpha = 530$ kev would immediately lead to a better fit for the angular distributions

resonance should account for roughly half the total yield at this energy, the agreement is, perhaps fortuitously, excellent. At $E_\alpha = 1{\cdot}3$ MeV, we deduce $\Gamma_\alpha \sim 3$ kev and the reduced width $\gamma_\alpha{}^2 \sim 0{\cdot}84$ MeV cm or $\sim 12\%$ of the Wigner Limit.

Assuming that the yield at $E_\alpha \sim 0{\cdot}65$ MeV arises chiefly from the $(\frac{1}{2}+)$ level, to which we have assigned a total width $\Gamma = 70$ kev, we deduce that $\Gamma_\alpha \sim 20$ ev and $\gamma_\alpha{}^2 \sim 0{\cdot}5$ MeV cm or $\sim 7\%$ of the Wigner Limit. In view of our complete lack of knowledge concerning the sharp resonance (except that, since we did not observe it, perhaps its intensity may be small), these latter figures are to be taken with reserve. Since both our estimates of $\gamma_\alpha{}^2$ are rather larger than is normally encountered, it seems probable that we have not underestimated the effect of the Coulomb barrier despite the fact that a large effective radius has been taken.

With no completely adequate account of the ground state transition, analysis of the other angular distributions seems profitless, but one point of interest arises from the n–γ correlations. Rotation in the plane perpendicular to the beam from 90° to 180° relative to the neutron axis corresponds to a rotation from 90° to ~60° relative to the impact axis under the experimental conditions. For a stripping reaction it is the impact axis which is of importance rather than the neutron axis. That the correlation should change so much in this range is additional evidence against the importance of the stripping mechanism.

§ 4. Conclusions

We consider that the experimental investigation of the reaction ^{9}Be (α, n) ^{12}C up to $E_\alpha = 1{\cdot}3$ MeV reveals no clear indication of a stripping mechanism and that the main contribution to the yield in this region arises from four resonances: a broad resonance at $E_\alpha = 0{\cdot}53$ MeV corresponding to a level in the compound nucleus ^{13}C of characteristics $(\frac{1}{2}+)$; a sharp resonance at $E_\alpha = 0{\cdot}61$ MeV of unknown character; and two resonances at higher energies one of which is certainly that of $E_\alpha = 1{\cdot}9$ MeV, the other most probably that of $E_\alpha = 2{\cdot}6$ MeV (see Talbott and Heydenburg 1953) of characteristics $(\frac{7}{2}-)$ and $(\frac{1}{2}-)$. In order to account for the cross section at $E_\alpha = 1{\cdot}9$ MeV we assign the characteristics $(\frac{7}{2}-)$ to the corresponding state in ^{13}C.

References

Adair, R. K., 1950, *Rev. Mod. Phys.*, **22**, 249.
Allison, S. K., and Warshaw, S. D., 1953, *Rev. Mod. Phys.*, **25**, 779.
Bennett, W. E., Roys, P. A., and Toppel, B. J., 1953, *Phys. Rev.*, **93**, 924.
Bradford, C. E., and Bennett, W. E., 1950, *Phys. Rev.*, **78**, 302.
Feshbach, H., and Weisskopf, V. F., 1949, *Phys., Rev.*, **76**, 1550.
Fowler, W. A., and Lauritsen, C. C., 1949, *Phys. Rev.*, **76**, 314.
Haefner, R. R., 1951, *Rev. Mod. Phys.*, **23**, 228.
Halpern, I., 1949, *Phys. Rev.*, **76**, 248.
James, D. B., and Treacy, P. B., 1951, *Proc. Phys. Soc.* A, **64**, 847.
Madansky, L., and Owen, G. E., 1955, *Phys. Rev.*, **99**, 1608.

Madsen, C. B., and Venkateswarlu, P., 1948, *Phys. Rev.*, **74,** 648.
Scott, J. M. C., 1954, *Phil. Mag.*, **45,** 411.
Stafford, G. H., 1948, *Nature, Lond.*, **162,** 771.
Talbott, F. L., and Heydenburg, N. P., 1953, *Phys. Rev.*, **90,** 186.
Tanner, N. W., 1955, *Proc. Phys. Soc.* A, **68,** 1195.
Thomas, R. G., Rubin, S., Fowler, W. A., and Lauritsen, C. C., 1949, *Phys. Rev.*, **75,** 1612.

XCIX. *The Cold Work Introduced during the Fatigue of Copper*

By R. D. McCammon and H. M. Rosenberg
The Clarendon Laboratory, Oxford †

[Received May 19, 1956]

§ 1. Introduction

Recent work (e.g. Wood 1955, Clarebrough *et al.* 1955) has suggested that the damage to the crystalline structure of a metal subjected to deformation depends upon the mode of cold working. In particular, the damage produced by fatiguing a metal is of a different nature from that produced by unidirectional strain. In the paper by Wood (1955) it is shown that the x-ray back reflection photograph of a polycrystalline copper specimen, fatigued in a compression–tension machine, differs from that obtained for a similar specimen strained in tension to the same degree of hardness. Furthermore, the temperature at which the damage anneals out, as determined by the x-ray photographs, is different in the two cases. The work of Clarebrough *et al.* (1955) showed that the energy which is stored in a metal when it is fatigued is released at a different temperature and at a different rate from that which is stored in a metal which has been strained in tension. The present note presents further evidence, from a different type of experiment in support of this view.

§ 2. The Experiments

The specimens were of polycrystalline high conductivity copper from I.C.I., annealed at 600°c for three hours in argon and furnace cooled. They were deformed in fatigue or tension by means of a Goodman's vibration generator. By feeding a.c. or d.c. into this machine one obtains either an alternating (fatigue) or unidirectional stress. It has the advantage that the stress–strain curve of a specimen can be taken after it has been fatigued or strained without the necessity of handling the specimen between the two experiments. The degree of work hardening produced in a specimen after deformation is measured by taking a stress–strain curve at room temperature.

Specimens were fatigued at various low temperatures at a given stress for $6{\cdot}75\times10^4$ cycles (previous work showed that the work hardening reached a saturation value after less than 10^4 cycles). It was found that the work hardening so produced decreased with decreasing temperature of fatiguing, even down to 4·2°K—these particular experiments will be reported in detail in a future publication. The observations which are of interest in the present connection arose when a fatigue experiment was

† Communicated by the Authors.

done at 100°C (the specimen being actually immersed in boiling water) in order to see whether the work hardening introduced would follow the same trend as the earlier experiments and hence be greater than that introduced after fatiguing at room temperature. It was found that this was not the case, but that the work hardening was considerably less than the room temperature value.

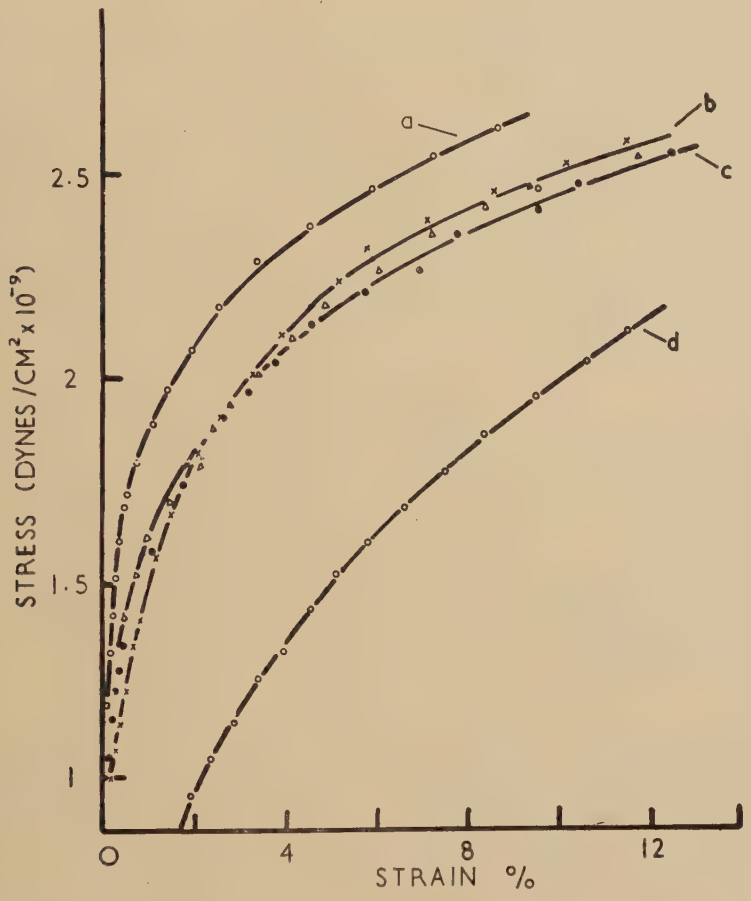

Stress–strain curves for copper specimens (*a*) fatigued at room temperature; (*b*) fatigued at room temperature and then heated to 100°C for 60 min. △, for 90 min ×; (*c*) fatigued at 100°C; (*d*) virgin annealed specimen.

It seemed improbable that this result could be ascribed to a reversal of the fatigue characteristics of copper between room temperature and 100°C. The most likely explanation appeared to be that some of the work hardening had annealed out at 100°C, although this was thought to be rather a low tempreature for any annealing to take place. To check this another two specimens were fatigued at the same loading at room temperature, heated to 100°C for 60 and 90 minutes respectively

and stress–strain curves then taken at room temperature. It was found that these curves almost coincided with the one obtained from the specimen which had been fatigued at 100°C. These curves are shown in the figure, together with the stress–strain curve for a specimen which has been fatigued at room temperature at the same alternating stress but not annealed at 100°C. A stress–strain curve for the virgin annealed copper is shown for comparison.

These experiments show that an appreciable amount of work hardening, although by no means all of it, anneals out at a comparatively low temperature which is far lower than the annealing temperature of the work hardening introduced by unidirectional strain. In order to confirm this, and also to check that the effect was not due to the apparatus, stress–strain tests were done on specimens which had previously been stretched so as to give approximately the same hardness as had been produced in the fatiguing experiments. It was found in this case that the stress–strain curves were the same whether the specimens were or were not heated to 100°C after the initial extension.

§ 3. Conclusion

It is thus apparent that the nature of the work hardening introduced by fatiguing is different from that produced by tensile straining. It is not as yet possible to say why the fatigue cold work partially anneals out at such a low temperature. At 100°C it is highly improbable that dislocations can themselves migrate. On the other hand it does seem that the dislocation configuration, which is produced by fatigue, is such that some of the ' pile-ups ' involved can become unlocked at this temperature and hence produce the observed softening.

Acknowledgments

We should like to thank Professor Sir Francis Simon, F.R.S. for the interest he has taken in this research. This work was done under a contract from the Ministry of Supply and during the tenure by R. D. McC. of a British Oxygen Company Research Fellowship.

References

Wood, W. A., 1955, *Phil. Mag.*, **46**, 1028.

Clarebrough, L. M., Hargreaves, M. E., Head, A. K., and West, G. W., 1955, *Trans. A.I.M.E.*; 1955, *J. Metals*, **7**, 99.

C. CORRESPONDENCE

Energy Levels of ^{40}A

By I. J. VAN HEERDEN † and D. J. PROWSE
H. H. Wills Physics Laboratory, University of Bristol ‡

[Received May 29, 1956]

VERY few experiments have been performed to determine the energy levels of the ^{40}A nucleus. They could be obtained from an analysis of the neutrons from the ^{39}K (d, n) ^{40}A reactions ; but the (d, p) reaction demands a supply of the rare isotope ^{39}A. The ^{37}Cl (α, p) ^{40}A reaction has been investigated by Kranz and Watson (1953), but no levels in ^{40}A were observed by them. It is also difficult to attack the problem through any form of resonance reaction. The easiest approach is to make experiments on inelastic scattering. Heitler *et al.* (1947) observed the scattering of 4·2 MEV protons by argon, and found that the elastic scattering obeyed the Rutherford law to a high degree of approximation. They also found evidence for excited levels at 1·46 and 2·4 MEV. The first level has also been obtained from an examination of the γ-radiation following K-capture of ^{40}K (e.g. Bell and Cassidy 1950).

The elastic and inelastic scattering of 9·5 MEV protons by ^{40}A has been studied by bombarding a gaseous argon target with protons from the beam of molecular hydrogen accelerated in the 60–in. Birmingham cyclotron. The angular distribution of the protons elastically scattered from ^{40}A has already been given by Freemantle *et al.* (1954 b) ; in addition to the elastic group, an energy level was reported at 1·48$\pm$0·02 MEV.

The experimental arrangement and procedure has already been described (e.g. Burrows *et al.* 1951). Owing to the low cross section for inelastic scattering, it was necessary to work close to the scattering gap to obtain a sufficient density of tracks in the photographic plate. In this region of the plate, however, the locus of protons scattered through a given anlge is not parallel to the direction of the tracks themselves.

The plate was scanned along the locus corresponding to the desired angle, and the projected track lengths were then corrected for ' skewness '. The true range of any particle in the emulsion was then deduced from its corrected track length and the angle of dip. To eliminate broadening of the groups due to single scattering, only those tracks which were nearly rectilinear and parallel to the correct direction were accepted. This procedure results in estimates of cross sections which are too low for the scattering process unless suitable corrections are applied, but it increases

† On leave from the National Physical Laboratory, Pretoria.
‡ Communicated by Professor C. F. Powell.

the resolution in energy. The tracks were measured on a Cooke, Troughton and Simms M 4000 microscope ; those $>100\,\mu$, with a ratchet device; those $<100\,\mu$, by means of an eyepiece scale. The loss of energy suffered by the scattered protons whilst traversing the gas was calculated from values of the stopping power of argon given by Brolley and Ribe (1955). The energy of the primary protons has been determined from the ranges of the elastically scattered protons, and the value thus obtained is $9{\cdot}51\pm0{\cdot}01$ MEV. The range–energy relation used was that of Gibson *et al.* (1954).

The number of background tracks (presumably due to particles scattered by the walls of the brass collimating tube), are at a minimum of angles of scattering of 115° (lab.). This is therefore a good angle to use in an experiment in which groups with a low cross section have to be resolved against a relatively high background.

Fig. 1

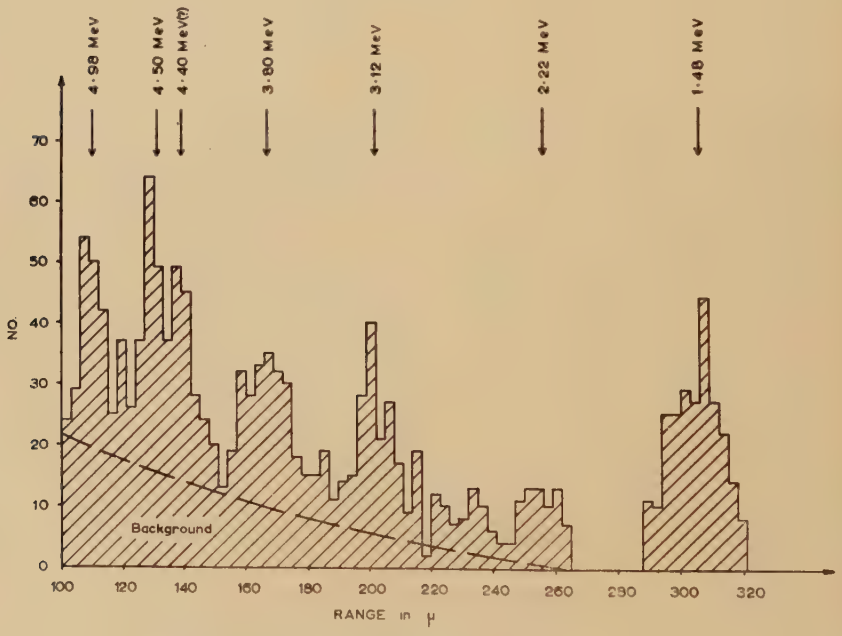

Histogram of the tracks measured at 115° (lab.).

A histogram of the tracks obtained at an angle of scattering 115° (L-system) is shown in fig. 1. It shows the presence of levels at $1{\cdot}48\pm0{\cdot}02$, $2{\cdot}22\pm0{\cdot}04$, $3{\cdot}12\pm0{\cdot}03$, $3{\cdot}80\pm0{\cdot}03$, $4{\cdot}50\pm0{\cdot}05$ and $4{\cdot}98\pm0{\cdot}05$ MEV. The errors quoted combine the calculated standard deviations in the measured ranges and beam energy, and allow for straggling effects. There is also a possible group at 2·66 MEV. Further measurements at 80° and 130° (L-system) confirm the presence of the levels deduced from observations at 115°. The 2·4 MEV level observed by Heitler *et al.* may have arisen from incomplete resolution of the 2·22 and possible 2·66 MEV levels shown

in fig. 1. The group at 1·48 MeV is in very good agreement with the previous work ; the other levels appear to be new. It is possible that some of these may be doublets ; thus, there are indications that the 4·50 MeV level is accompanied by another at 4·40 MeV. The observed width of the group at 3·80 MeV suggests that this level also is a doublet.

In view of the appearance of a large number of levels, the question of the purity of the argon used is of great importance. The argon gas was of normal commercial purity. Fortunately, the presence of impurities can be detected experimentally by observations on the groups scattered

Fig. 2

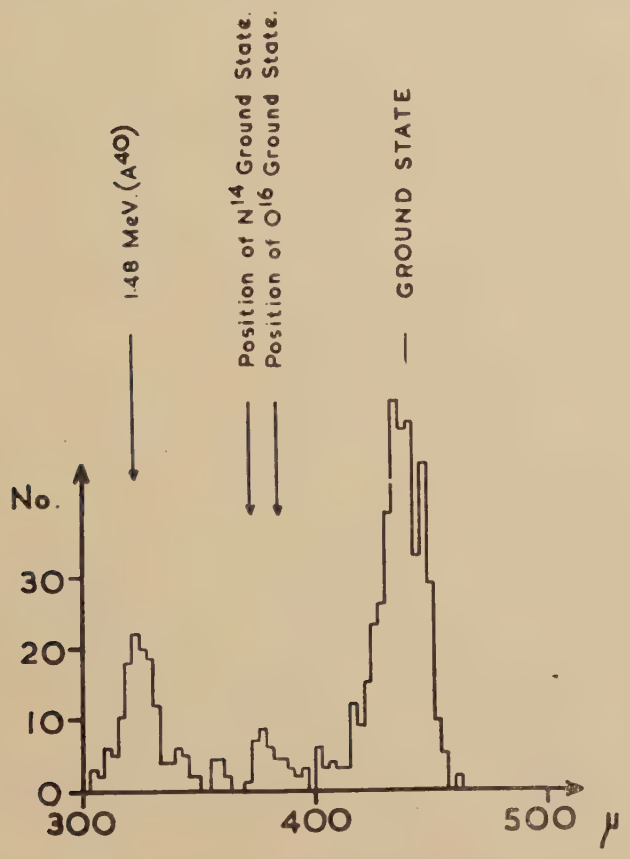

Histogram of the tracks $>300\mu$ in length, measured at 80° (lab.) showing the presence of impurity groups at $\sim 380\mu$.

elastically by other nuclei. At all angles above about 40°, such groups from any oxygen or nitrogen atoms will be resolved from those from argon, but above 135°, these groups will begin to overlap with those due to inelastic scattering by argon with the formation of the excited state at 1·48 MeV.

A histogram of the tracks obtained at $\theta = 80°$ is shown in fig. 2. It is clear that there are impurity groups between those due to argon, but

it is not certain whether they are due to oxygen or nitrogen ; from the shape of the angular distributions it seems more probable that the principal impurity is nitrogen, as would be expected from on other grounds. The absolute differential cross sections for the scattering of 10 MEV protons by oxygen, nitrogen and argon are known (Freemantle *et al.* 1953, 1954 a and 1954 b) and they enable us to deduce the percentage impurity in the argon employed. From measurements at various angles, it has been calculated that the maximum nitrogen impurity is $1{\cdot}0\pm0{\cdot}2\%$. From the known cross sections for the 2·3 and 3·9 MEV levels of ^{14}N, it then follows that less than 1 track due to the 2·3 level, and only 4 tracks due to the 3·9 level, would be expected to be present in the histogram shown in fig. 1.

In addition, we have obtained indications of levels in ^{40}A at energies >5 MEV (corresponding to ranges $<100\,\mu$). Further work is proceeding to confirm or deny the existence of these highly excited states.

ACKNOWLEDGMENTS

The authors wish to thank Professor C. F. Powell for his guidance and encouragement, Professors W. E. Burcham and J. Rotblat for many discussions, and Drs. W. M. Gibson and R. G. Freemantle for their help with the exposures.

REFERENCES

BELL, P. R., and CASSIDY, J. M., 1950, *Phys. Rev.*, **79**, 173.
BROLLEY, J. E., and RIBE, F. L., 1955, *Phys. Rev.*, **98**, 1112.
BURROWS, H. B., POWELL, C. F., and ROTBLAT, J., 1951, *Proc. Roy. Soc.* A, **209**, 461.
FREEMANTLE, R. G., GIBSON, W. M., PROWSE, D. J., and ROTBLAT, J., 1953, *Phys. Rev.*, **92**, 1268.
FREEMANTLE, R. G., PROWSE, D. J., and ROTBLAT, J., 1954 a, *Phys. Rev.*, **96**, 1268.
FREEMANTLE, R. G., PROWSE, D. J., HOSSAIN, A., and ROTBLAT, J., 1954 b, *Phys. Rev.*, **96**, 1270.
GIBSON, W. M., PROWSE, D. J., and ROTBLAT, J., 1954, *Nature, Lond.*, **173**, 1180.
HEITLER, H., MAY, A. N., and POWELL, C. F., 1947, *Proc. Roy. Soc.*, **190**, 180.
KRANZ, A. Z., and WATSON, W. W., 1953, *Phys. Rev.*, **91**, 1472.

Long Range Nuclear Interaction in Paramagnetic Resonance

By J. E. BENNETT and D. J. E. INGRAM
University of Southampton †

[Received April 12, 1956]

IT is well known that considerable information can be obtained from the hyperfine structure of paramagnetic resonance spectra, concerning both the nuclear parameters and the electronic state of the atom. In most cases so far investigated the hyperfine pattern has taken the form of $(2I+1)$ lines, where I is the nuclear spin of the paramagnetic atom. Recent work (Owen and Stevens 1953) has shown, however, that 'covalent'

† Communicated by the Authors.

bonding between the central paramagnetic atom and its nearest neighbours may result in partial sharing of the magnetic electrons, and there is thus a contribution to the hyperfine pattern from these neighbouring nuclei. Such spectra have been analysed in detail for various chloroiridate compounds (Griffiths and Owen 1954), and a similar interaction with surrounding halogen nuclei has also been found in some of the iron-group fluorides (Tinkham 1955).

We have recently investigated a copper compound in which the halogen atoms are very far removed from the central paramagnetic atom, and yet have still obtained a marked contribution to the hyperfine pattern from them. The compound was copper tetra-phenyl porphin (Barnes and Dorough 1950), and the spectra of both the chlorinated and unchlorinated derivatives were studied. The phenyl groups are connected to the four carbon atoms round the edge of the central porphin ring system, and in the chlorinated derivative the outermost hydrogens of these four phenyl groups are replaced by chlorine atoms. The structural formula for the chlorinated derivative is shown in fig. 1, and it can be seen that there are seven atoms between each chlorine and the central copper atom.

The hyperfine pattern observed from the unchlorinated derivative had the four equally spaced components of the normal copper spectrum, and the separations and g values were very close to those obtained for copper phthalocyanine, which has a similar central structure (Bennett and Ingram 1955). The pattern corresponding to the parallel direction is shown in fig. 2 (*a*), which is reproduced on the plate.

When the chlorinated derivative was investigated, however, a very marked change in the pattern was observed and it had the standard 'christmas tree' appearance previously found in the chloroiridate spectra (Griffiths and Owen 1954). The pattern corresponding to the parallel case is shown in fig. 2 (*b*) and nine lines can be clearly resolved with faint signs of others in the wings. Since there was no appreciable change in the g value of 2·18, this type of structure can only be explained by assuming an interaction with other nuclei, and as the addition of the chlorines was the only change in the derivative, such an interaction would appear to be with the chlorine nuclei. Nitrogen nuclei are the only others present in the molecule possessing magnetic moments, other than protons, and any interaction with these would have been seen in both the unchlorinated derivative and the phthalocyanines.

It is hoped that larger single crystals of the chlorinated derivative will enable a more detailed analysis of the spectra to be obtained, but a synthesis of the pattern of fig. 2 (*b*) can be made if it is assumed that the magnetic electron of the copper is interacting with two chlorines at any given time, and that the chlorine hyperfine splitting is half that of the copper compounds, i.e. $A_{Cu}=0{\cdot}025$ cm ^{1} $A_{Cl}=0{\cdot}012$ cm^{-1}. Four overlapping sets of seven lines are then obtained, each with an intensity ratio of 1 : 2 : 3 : 4 : 3 : 2 : 1, and these four sets are shown added together in fig. 2 (*c*) with the envelope of the integrated absorption from them all. This has a fairly close resemblance to the photograph of fig. 2 (*b*) and would

Fig. 1

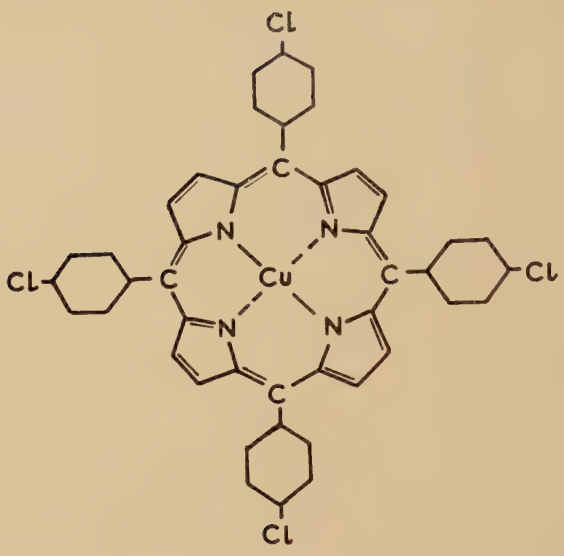

Structural formula of chlorinated copper tetra-phenyl porphin.

Fig. 2 (*c*)

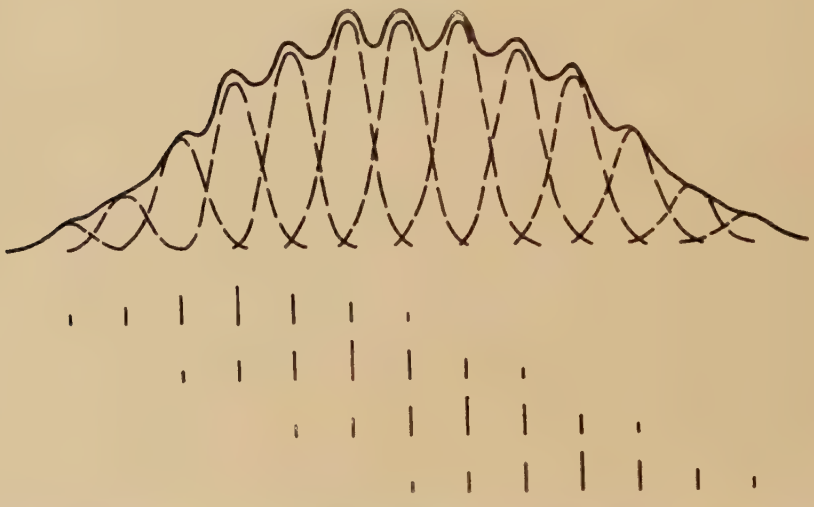

Synthesis of pattern for chlorinated derivative, assuming chlorine hyperfine interaction half that of copper. Groups of 7 lines centred on the four copper components are shown below.

seem to confirm that the interaction is with the chlorine nuclei. Although there are four equivalent chlorine atoms in the molecule the simultaneous interaction with only two might be expected as the resonating structure of the porphin ring has two sets of conjugated bond systems which are

equally probable. It is possible that the interaction in the parallel direction is with clorine nuclei of adjacent molecules. The large splitting observed shows that even in this case an unpaired electron must be associated with the chlorine for an appreciable time.

It would therefore seem that the magnetic electron associated with the central copper atom can move out to the edge of very large molecules via the π-orbitals of the ring system and may interact with nuclei present there. Although such long range interaction has been found in organic free radicals where the electrons move in non-localized orbitals, it does not appear to have been observed before with normal paramagnetic atoms. The apparent ease with which such interaction is possible may account for the strong exchange effects observed in many copper salts (Bagguley and Griffiths 1950, Bleaney and Bowers 1952).

References

Bagguley, D. M. S., and Griffiths, J. H. E., 1950, *Proc. Roy. Soc.* A, **201**, 366.
Barnes, J. W., and Dorough, G. D., 1950, *J. Amer. Chem. Soc.*, **72**, 4045.
Bennett, J. E., and Ingram, D. J. E., 1955, *Nature Lond.*, **175**, 130.
Bleaney, B., and Bowers, K. D., 1952., *Proc. Roy. Soc.* A, **214**, 451.
Griffiths, J. H. E., and Owen, J., 1954, *Proc. Roy. Soc.* A, **226**, 96.
Owen, J., and Stevens, K. W. H., 1953, *Nature, Lond.*, **171**, 836.
Tinkham, M., 1955, *Disc. Faraday Soc.*, **19**, 174.

The Bombardment of Osmium by Nitrogen Ions

By G. W. Greenlees and L. G. Kuo
Physics Department, University of Birmingham

[Received March 28, 1956]

§ 1. Introduciton

Reactions caused by bombardment with heavy ions from a 60 in. cyclotron (maximum energy ~130 mev) are likely to involve large spin changes because of the high values of incident angular momentum involved. Heavy ion bombardments could therefore be a means of exciting high spin isomeric states (Greenlees and Souch 1955). This could occur via a direct excitation mechanism and it was therefore decided to bombard a target with heavy ions and examine the activities of the target atoms themselves after chemical separation. Osmium was chosen for these experiments since shell model considerations indicate the likelihood of the presence of low lying levels of high spin.

§ 2. Procedure

The bombardments were made using the internal nitrogen 14 beam of the 60 in. Nuffield cyclotron. The beam had a continuous energy distribution of maximum energy about 130 mev with an intensity fall-off by a

factor of two for each 10 MeV rise of energy above 50 MeV. The target consisted of spongy osmium covered by a 5μ foil of aluminium. This target was placed in a screened probe similar to that described by Chackett *et al.* (1954). A 5μ aluminium screening foil was used. Beam currents of approximately 5×10^{-7} A were available and bombardments of about 1μ A hour used.

The osmium activities were separated chemically from the active target. The target was fused with sodium peroxide and the osmium distilled off as the tetroxide into alkaline solution. The osmium was then obtained as the sulphide by precipitation with H_2S. This separation took about $1\frac{1}{2}$ hours so that any short lived osmium activities would not be observed in the separated fraction. The chemical extraction efficiency was about 70%.

§ 3. Experimental Results and Discussion

The γ-ray spectrum of the separated osmium was observed using a shielded NaI (Tl) scintillation counter. A peak was found at 63 kev corresponding to the Kα x-ray energy for osmium. The decay curve for this peak is given in the figure. This curve analyses into three half lives of $7{\cdot}2\pm1$ hours, 39 ± 2 hours and 26 ± 2 days.

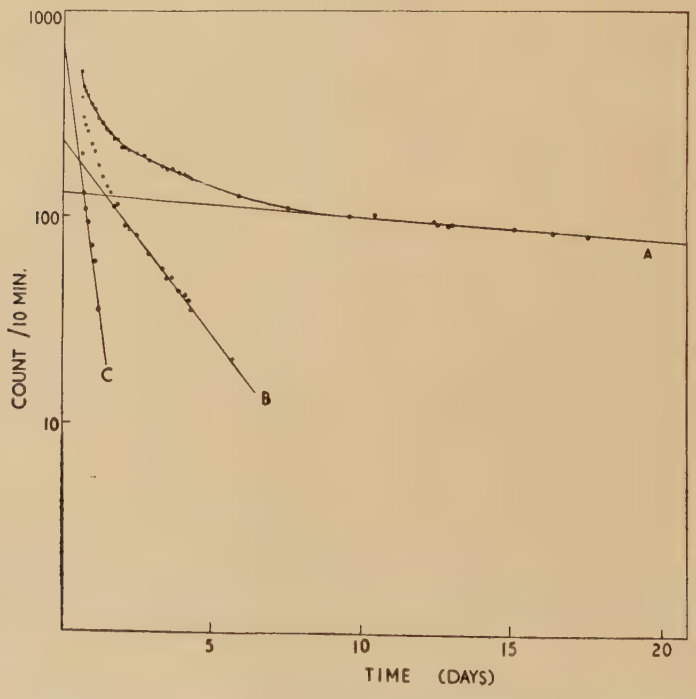

Analysis of decay curve of 63 kev γ-ray peak from osmium.
A, Half life 26 ± 2 days; B, Half life 39 ± 2 hours; C, Half life $7{\cdot}2\pm1$ hour.
Counts/10 min. Time-days.

These three half lives can be associated with some weak activities detected by Chu (1950). Chu bombarded rhenium with α particles and examined the iridium activities using a G.M. counter technique. On separating osmium from the iridium samples he found weak activities of half life 9·5 min, 6 hours, ~35 hours and ~50 days. The last three can be identified with the present results. The 9·5 min activity would not be observed in the present work because of the time required for chemical separation. In Chu's work the only mass numbers to be expected are 186, 187, 188, 189 and 190. All isotopes of osmium with these mass numbers are stable and hence the x-rays observed in the present experiments cannot be due to K-capture or the internal conversion of γ-rays following β decay. This x-ray peak is therefore associated with the internal conversion of γ-rays from isomeric transitions in osmium. Such transitions might be expected to be highly converted which would explain the absence of the corresponding γ-ray peaks with the scintillation counter.

One concludes, therefore, that there are present at least three isomeric transitions in osmium isotopes with mass numbers 186–190. From Chu's work it is reasonable to associate the $7{\cdot}2\pm1$ hours half life with Os^{190}, the 39 ± 2 hours half life with Os^{187} and the 26 ± 2 day half life with Os^{188}. The absence of any γ-ray half lives due to known radioactive osmium isotopes is evidence that the observed isomeric states are formed, in the present experiments, by a direct excitation mechanism.

Acknowledgments

The authors wish to thank Dr. K. F. Chackett for his help in devising the chemical separation procedure. One of us (L.G.K.) wishes to thank the Nuffield Foundation for financial support covering the period of this work.

References

Chackett, K. F., Fremlin, J. H., and Walker, D., 1954, *Phil. Mag.*, **45**, 173
Chu, T. C., 1950, *Phys. Rev.*, **79**, 582.
Greenlees, G. W., and Souch, A. E., 1955, *Phil. Mag.*, **46**, 682.

Periodicity in Ice-Flowers

By F. C. Frank and A. Keller

[Received May 16, 1956]

The accompanying photographs show ice-flowers formed on the inner surface of the panes of a cold green-house during the recent severe frost, and were taken on the morning of February 4th.

Presumably the pattern developed on the evening of January 31st, on which day (following a period of mild weather) the temperature fell from 0°C at midday to −10°C in the night. The air temperature remained

below freezing during the following three days, but there were some periods of sunshine followed by similarly low night temperatures.

The feature of interest is the regular periodic marking along the ' stem ' of each ' fern-leaf '. The period was about the same in all " fern-leaves" on any one pane, but varied with position in the green-house from about 5 mm to about 30 mm. The periodic dark spots are regions of weaker light-scattering in the direction of view. This peculiarity in the frost-flowers was first noticed at night, on the evening of February 3rd, when the ice surfaces were more sharply etched, and at first sight gave the impression of an ice layer of considerable, sinusoidally varying, thickness. Holding the light in a suitable position, the banding while most prominent along the stem was seen to spread almost in semi-circles across the full width of each ' fern-leaf '. In the morning, when the sun was shining and some evaporation had occurred, it could only be seen on the stems. The periodic bands were not visible between crossed polaroids, which enabled one to see, however, that the crystal orientation fanned out in the same manner as the surface striations, which were probably parallel to the hexagonal axes of the ice crystals.

It is possible that this periodicity arose from a rhythmic crystallization analogous to Liesegang rings. Perhaps more probably it corresponded to a slow twist about the hexagonal axis (at the rate of 60° per apparent period) in the crystal growth. Such twisting, though unexplained, is a common accompaniment, usually with a much smaller period, of fanning crystallization, as in spherulites (see references).

References

Bernauer, F., 1927–7, *Neues Jb. Minér., Beilage Band*, A, **55**, 92 ; 1929, *Gedrillte Kristalle* (Berlin : Verlag Borntraeger).

Gaubert, P., 1908, *C.R. Acad. Sci., Paris*, **146**, 829 ; 1909, *Bull. Soc. franç. Minér.*, **32**, 421 ; 1913, *Ibid.*, 36, 45 ; 1927, *C.R. Acad. Sci., Paris*, **184**, 1565 ; and several others in the same journals.

Levy, M., and Munier-Chalmas, 1892, *Bull. Soc. franç. Minér.*, **15**, 159.

Wallerant, F., 1907, *Bull. Soc. franç. Minér.*, **30**, 43.

CI. REVIEWS OF BOOKS

Recent Advances in Optics. By. E. H. Linfoot. (Oxford: Clarendon Press.) [Pp. ix+286.] Price 50*s*.

This monograph gives an account of researches carried out in some selected branches of Optical Theory within the last twenty years. The first chapter deals with the Optical Image, more especially with the Geometrical Theory of error balancing, with diffraction images in the presence of aberrations and with the theory of partial coherence. Then follow chapters on the theory of the Foucault test, the theory of the Schmidt Camera and finally plate-diagram analysis with some of its applications, especially to plate mirror systems used in Astronomical Photography.

The standard of presentation is unusually high. In particular, the handling or approximations so important in the theory of aberrations could hardly be improved upon. It is to be regretted, however, that from the wealth of material that undoubtedly comes under the title of this book, only very few topics are in fact covered; much more could have been included in the space available if the topics were treated in less detail. Several small mistakes were noted by the reviewer: In equations (2.21), (2.22), (2.36) and (2.37) a multiplicative factor 4 is erronously included. It is not correct, as mentioned on p. 73, that the theory of partial coherence was first investigated by Van Cittert in 1934. Earlier investigations are due to Von Laue (1907) and Berek (1926). The author follows (regretfully, in the reviewer's opinion) some recent practice of defining the degree of coherence without any reference to a time average; this will make it difficult for the non-initiated reader to appreciate the physical significance of this quantity.

Much can be learned from this book not only about the subject matter it covers, but also about the elegance and precision with which theoretical optics can be presented. E. W.

Annual Review of Nuclear Science, Volume 5, 1955. Edited by J. G. Beckerley, M. D. Kamen and L. I. Schiff. (Published by Annual Reviews Inc., Stanford, California; London agents, Messrs. H. K. Lewis, Gower Street, W.C.1.) [488 pp.] Price £3, or $7.50 postpaid.

This valuable series always covers a broad field of activities, and this time there is less than usual for the pure physicist. Four of the fourteen articles are on biological subjects connected with radioactivity, and four are chemical. These consist of one on methods of chemical separation, two on the chemical effects of irradiation, and one on the mass spectrometer in industrial chemistry.

The physical articles include an especially clear and critical review of our understanding of nuclear gamma-ray transitions, by Goldhaber and Weneser. Peaslee writes on nuclear reactions, Ford and Hill discuss the distribution of charge in heavy nuclei, and Fretter reviews recent work on cloud- and bubble-chambers.

In another interesting article, Borst offers critical advice to those who are wondering on what kind of reactor they should put their money (or their uranium). In discussing safety precautions, he remarks that there is, especially in universities, "a tendency to avoid the routine and take short cuts; and it is this virtue of the research scientist, making him outstanding in his field, which can constitute a significant and real danger."

This volume contains an index to the first five volumes. J. M. C. S.

The Fundamentals of Electroacoustics. By F. A. Fischer. (Translated by S. Ehrlich and F. Pordes. (Interscience Publishers London.)

This book, as the author informs us, resulted from the need to instruct young physicists and electronic engineers in the fundamentals of acoustics in order that they can work independently in this field as soon as possible. No special knowledge of acoustics beyond what is taught in this country at pass degree standard is required. The treatment is in the main theoretical though the text is written with an eye to practical applications and a bibliography of experimental treatises is appended.

The author has certainly succeeded in his aim, though perhaps one should add that the reader whose training has been in electrical engineering will find himself more at home than one who has had courses in physics. The electrical aspects of the subject are in fact emphasized to some neglect of the hydrodyhamical aspects, so that the student might remain unaware, for example, of the effects of viscosity in causing damping.

The translation is clear and the mathematics well presented. E.G.R.

Basic Statistical Concepts. By Joe Kennedy Adams. (McGraw-Hill, 1955.) [Pp. xvi+304.] Price 41*s.* 6*d.*

This book is written by a professor of psychology with the aim of explaining the basic concepts of statistics and, at the same time, the mathematical language used in the subject: for example, elementary calculus. It is intended for students with no previous calculus or statistics. The treatment throughout is on an abstract level: applications, to psychology or to any other field, are rare. The concepts of power of a test and interval estimation are introduced early in connection with simple artificial examples dealing with finite populations. They are later used in more mature situations. It is a serious criticism that the important concepts of efficiency of an estimate and the likelihood function are not mentioned. There is a long appendix on the calculus including derivations of the common sampling distributions. The book is not likely to please the mathematician: it will probably confuse the practical worker trained in British schools. D. V. L.

Ionized Gases. By A. von Engel. (Clarendon Press.) [Pp. xi+281.] Price 42*s.*

This book fills a wanted place as a text-book for advanced students of the conduction of electricity in gases. It contains a great deal of information well arranged, especially on the individual processes that are the basis of discharge phenomena. Rather over two thirds of the book is concerned with these processes, which are studied in considerable detail. The experimental results are shown in a large number of clear diagrams, experimental methods are dealt with more sketchily. On the theoretical side a rough order-of-magnitude approach is wisely given wherever possible, and the more refined results are usually only quoted. Except in an appendix no attempt is made to deal with methods involving a change in the distribution function of electrons in a gas. Most of this book is concerned with conditions in which mobility is a valid concept, and more might perhaps have been said of the conditions of high fields and low pressures when this is no longer true. Regarded as a text book for the honours student, the balance, apart from this, is about right, but for those interested in research or in practical applications more on the actual discharge and less on the individual processes would have given a more useful book, especially as the latter have been so well dealt with by Massey and Burhop.

The style is rather abrupt, suggesting lecture notes, and at times the statement is a little too compressed, but the author is to be congratulated on his ability to get at the essentials of a physical argument and to put them across concisely.

G.P.T.

Progress in Nuclear Energy, Series 1 : *Physics & Mathematics*, Vol. 1, 1956. Edited by R. A. Charpie, D. J. Hughes, D. J. Littler, and S. Horowitz. With forewords by Sir John Cockcroft and V. F. Weisskopf. Published by Pergamon Press, London. [Pp. x+398.] Price 70*s*.

This is the first volume of one of six series of collected review articles based on the 1955 Geneva Conference on the Peaceful Uses of Atomic Energy, and including the results of much informal discussion made possible by the conference.

A very considerable addition to the literature of neutron physics is made in the present volume, which contains the following reviews :

Summary of Data on the Cross Sections and Neutron Yields of U^{235}, U^{233}, Pu^{239}, by J. A. Harvey and J. E. Sanders.

Resonance Structure of U^{233}, U^{235}, Pu^{239}, by P. A. Egelstaff and D. J. Hughes.

Theoretical Analysis of Neutron Resonances in Fissile Materials by H. A. Bethe.

Techniques for Measuring Elastic and Non-Elastic Neutron Cross Sections, by L. Cranberg, R. B. Day, L. Rosen, R. F. Taschek and M. Walt.

The Cross Section of Xe^{135}, by S. Bernstein and E. C. Smith.

Resonance Capture Integrals, by R. L. Macklin and H. S. Pomerance.

Delayed Neutrons, by G. R. Keepin.

Homogeneous Critical Assemblies, by D. Callihan.

Physics of Fast Reactors, by J. Codd, L. R. Shepherd and J. H. Tait.

Heterogeneous Methods for Calculating Reactors, by S. M. Feinberg.

Highly Enriched Intermediate and Thermal Assemblies, by H. Hurwitz and R. Ehrlich.

This publication is the first to contain a summary in this field of the work of scientists throughout the world, and will do much to spread the spirit of the conference as well as the fruits of the information presented.

G. D.

Physics and Chemistry of the Earth, Vol. 1. (London: Pergamon Press, 1956.) [Pp. viii+317.] Price 55*s*.

This is the first of an annual series, each of which will contain reviews of geophysical and geochemical topics. Volume I includes :—

1. The Origin of the Solar System, by Sir Harold Spencer-Jones.
2. Temperatures within the Earth, by J. Verhoogen.
3. Radioactive Methods of determining Geological Age, by L. H. Ahrens.
4. Seismology and the Broad Structure of the Earth's Interior, by K. E. Bullen.
5. The Hydrodynamics of the Earth's Core, by Raymond Hide.
6. Investigations under Hydrothermal Conditions, by Rustum Roy and O. F. Tuttle.
7. Geochemistry of the Halogens, by Carl W. Correns.
8. Geochemistry in the U.S.S.R., by S. I. Tomkeieff.

and Name and Subject indices.

The series should provide valuable reference books for workers in these fields and will also be useful to other scientists who wish to follow recent developments in the study of the physics and chemistry of the Earth.

B. C. B.

Numerical Mathematical Analysis. By J. B. Scarborough. (Johns Hopkins University Press, London: Cumberlege.) [Pp. xix+554.] Price 48*s*.
Introduction to Numerical Analysis. By F. B. Hildebrand. (London: McGraw-Hill.) [Pp. x+511.] Price 64*s*.

These two books are of a very different character. The first is the third edition of a work which originally appeared in 1930, well before the development of automatic digital computers had given the present impetus to the study of numerical analysis. It was, for a long time, one of the best of the relatively few books on the subject available. The author made substantial revisions for the second edition which was published in 1950. The present edition is largely a corrected reprint of the second edition with a little extra material on errors in the evaluation of determinants and a new chapter on the numerical solution of simultaneous linear equations.

The book by Hildebrand covers interpolation, quadrature, numerical solution of differential equations, least-squares polynomial approximations, the numerical solution of equations, and related topics. Although the book is technically an introduction to the subject in that it starts at the beginning, it is really a textbook for the advanced student. It might, as the author suggests, be put into the hands of beginners to be read in conjunction with a course of lectures, but the treatment is really too detailed for those who are meeting the subject-matter for the first time. But for anyone who has progressed beyond this stage, and has had some practical experience either with a desk calculating machine or with a digital computer, the book is quite excellent. It is perhaps of most value as a source of theoretical results relating to the formulae and methods of numerical analysis, rather than as a source of advice for the practical man faced with a specific problem. As an example showing the level of treatment sustained, I might mention the author's discussion of the convergence with increasing n of the Newton-Cotes n-strip quadrature formula. He shows that if the integrand has a singularity in the complex plain too near the axis of integration a divergent result is obtained, whereas the repeated application of the trapezoidal rule, or of Simpson's rule, to the same number of strips may give a convergent result.

The book is very well printed and edited, but it would be worthy of a more detailed index.

M. V. W.

Progress in Metal Physics. Vol. 6. Edited by Bruce Chalmers and R. King. (London and New York: Permagon Press.) [Pp. viii+354.] Price 70*s*.

The volume for 1956 of this series, though it appears rather late, contains as usual much of interest. There are articles on the effect of pressure on resistance and on filamentary growth, a fashionable subject owing to the high strength of filaments. Mehl contributes an authoritative article on the austenite–pearlite raction and Sully an interesting article on creep which shows how little agreement there is between different investigators on the role of grain-boundary movement and cell formation. Knacke and Stranski have an excellent article on the mechanism of evaporation describing the known facts and with much information about the migration of atoms on a surface. Finally Hirsch provides a thorough and detailed review of our present knowledge of mosaic structure.

N. F. M.

[The Editors do not hold themselves responsible for the views expressed by their correspondents.]

Fig. 1

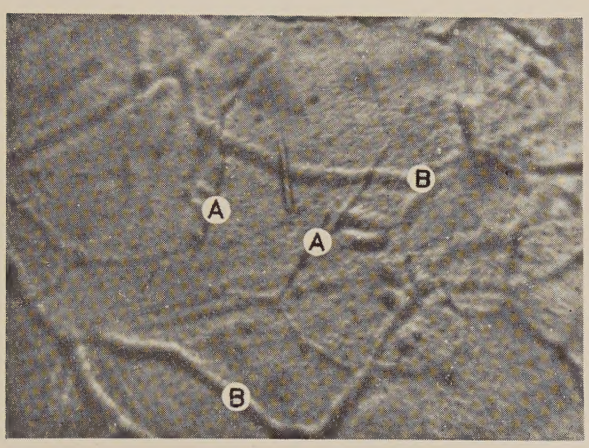

Thermally-etched grain boundaries on the front (A) and back (B) surfaces of a specimen of solid argon. (× 75.)

Fig. 2

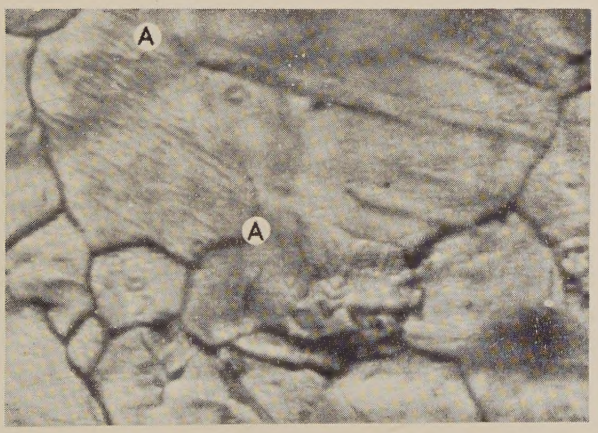

The surface of a solid argon specimen showing thermally-etched detail within the grains, including the boundary AA. (× 90.)

Fig. 2

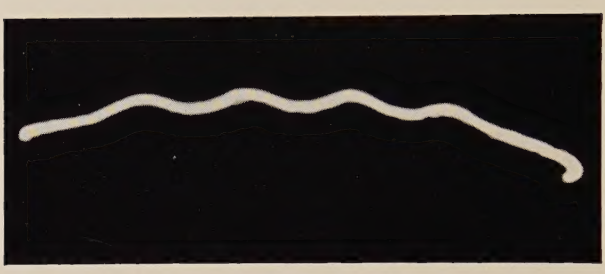

(*a*)

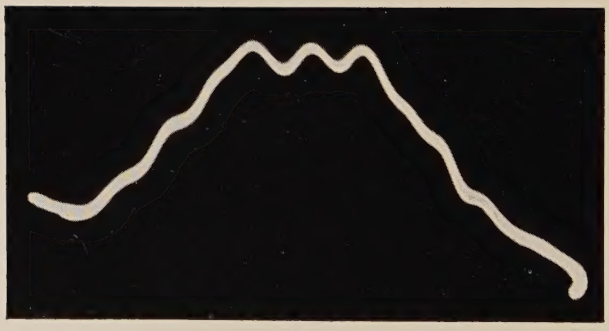

(*b*)

Period 5 mm.

Period 5 mm.

Period 33 mm.